

NanoSpain
Conf  2011
NANOIBERIAN CONFERENCE

NANOSPAIN 2011



INDEX: INVITED CONTRIBUTIONS

	pag
Samuel D. Bader (Argonne National Laboratory, USA) <i>"Spintronics and Beyond"</i>	145
Gianaurelio Cuniberti (TU Dresden, Germany) <i>"From molecular wires to organic semiconductors and back -some "don't ask, don't tell" of soft electronics"</i>	165
Luisa De Cola (Universität Münster, Germany) <i>"Nanocontainers: properties, manipulation and bio-medical applications"</i>	167
Yannick De Wilde (ESPCI, France) <i>"Direct near-field study of generation, coupling, and propagation of surface plasmons in the mid-infrared"</i>	171
Morinobu Endo (Shinshu University, Japan) <i>"Title not available"</i>	-
Christian Joachim (CEMES-CNRS, France) <i>"Molecule logic gate or surface atomic scale circuits"</i>	197
Leo Kouwenhoven (Technical Univ. Delft, Netherlands) <i>"Quantum mechanics in semiconductor nanowires"</i>	201
Francois Leonard (Sandia National Laboratories, USA) <i>"Charge injection and transport in nanowires"</i>	207
Christopher Marrows (University of Leeds, UK) <i>"Artificial Spin Ice"</i>	209
Bill Milne (Cambridge Univ, UK) <i>"Optimisation of CNT Based Nanostructures for Use as Electron Sources"</i>	225
Dirk Sander (Max-Planck-Institut für Mikrostrukturphysik, Germany) <i>"New insights into nanomagnetism by spin-polarized scanning tunneling microscopy and spectroscopy"</i>	239

INDEX: INVITED CONTRIBUTIONS (CNANO GSO SESSION)

	pag
Jean-Marie Devoisselle (Université de Montpellier/ENSCM, France) <i>"Nanostructured materials as drug delivery systems"</i>	177
Benoît Jouault (Univ Montpellier 2, France) <i>"Quantum hall effect in epitaxial graphene on off-axis (000-1) SiC"</i>	199
Brahim Lounis (Université Bordeaux 1, France) <i>"Title not available"</i>	-
Nathan D. McClenaghan (CNRS / Université Bordeaux 1, France) <i>"Communication between molecules via photocontrolled ions"</i>	217
Thomas Plénat (Université Paul Sabatier Toulouse III, France) <i>"A novel DNA chip for single molecule analysis"</i>	231
Bertrand Raquet (Université de Toulouse, France) <i>"Quantum Transport and High Magnetic Field Phenomena in Carbon Nanotubes and Nanoribbons"</i>	233

INDEX: ORALS CONTRIBUTIONS (CNANO GSO SESSION)

	pag
Ashod Aradian (Centre de Recherche Paul Pascal, France) <i>"Plasmonic particles organized in nanostructured polymer matrices"</i>	141
Noemi Barros (Université de Perpignan Via Domitia, France) <i>"Optimal switching of a nanomagnet assisted by a microwave field"</i>	147
D. Brevet (France) <i>"Mannose-targeted mesoporous silica nanoparticles for photodynamic therapy"</i>	151
Daniela Cardinale (INRA, France) <i>"Virus scaffolds as Enzyme Nano-Carriers (ENCs) to organize bio-catalytic enzyme cascades. Design of a scanning electrochemical nanoreactor microscopy device"</i>	157
Noelle Carette (INRA, France) <i>"Plant virus particles as nanoscaffolds for controlled positioning of enzyme cascades on solid supports"</i>	159
Marie-Hélène Delville (ICMBC/CNRS, France) <i>"Internalisation Mechanisms of Modified Titanium Oxide Nanoparticles in Skin Cells and Multicellular Living Specimens : Resulting Toxicity"</i>	173
Illia Guralskyi (Laboratoire de Chimie de Coordination, France) <i>"Spin crossover nanomaterials: towards sensor applications"</i>	187
Renaud Marty (CNRS-UPS, France) <i>"Physics of two photon luminescence imaging in nanoplasmonics"</i>	215
Celia Mercader (CANOE, France) <i>"Novel carbon nanotube multifunctional composite fibers"</i>	223
Fabio Pistolesi (LOMA-Université Bordeaux 1/CNRS, France) <i>"Euler buckling instability and enhanced current blockade in suspended single-electron transistors"</i>	229
Andrey Ryzhikovi (Laboratoire de Chimie de Coordination, France) <i>"Gas sensor for food industry and agriculture based on ZnO nanoparticles and nanorods"</i>	237
Olivier Sandre (LCPO (Univ Bordeaux/CNRS/IPB), France) <i>"Doxorubicin Loaded Magnetic Polymersomes: Theranostic Nanocarriers for MR Imaging and Magneto-Chemotherapy"</i>	241

INDEX: ORALS CONTRIBUTIONS

	pag
Ibon Alonso Villanueva (CIC microGUNE, Spain) <i>"Highly photostable organic distributed feedback lasers fabricated by thermal nanoimprint"</i>	139
Rémi Avriller (DIPC, Spain) <i>"Inelastic Quantum Transport in Nanoscale Junctions: Role of electron-phonon interactions on the current-current noise characteristics"</i>	143
Stéphane Berciaud (IPCMS, Université de Strasbourg & CNRS, France) <i>"Observation of electronic raman scattering in metallic carbon nanotubes"</i>	149
Olga Caballero-Calero (IMM-CSIC, Spain) <i>"Nanowire arrays of Bi₂Te₃ for Thermoelectric Applications"</i>	153
Julio Camarero (UAM/IMDEA Nanoscience, Spain) <i>"Quantifying and imaging magnetization reversal of buried interfaces by soft x-ray spectroscopy and holography"</i>	155
Silvia Cavalli (CIBER-BBN, Institute for Research in Biomedicine (IRB Barcelona) PCB, Spain) <i>"Cell Penetrating Peptide-Superparamagnetic Iron Oxide Nanoparticle Conjugates as Bimodal Imaging Nanoagents"</i>	161
Francesca Cecchet (FUNDP - University of Namur, Belgium) <i>"Vibrational Sum-Frequency Generation Spectroscopy of Self-Assembled and Langmuir-Blodgett films on surfaces: from monolayers to model lipid membranes"</i>	163

Jose M. De Teresa (CSIC-U. Zaragoza, Spain) <i>"Focused electron beam induced deposition and etching of functional materials"</i>	169
Vito Despoja (DIPC, Spain) <i>"Role of the surface electronic structure in the enhancement of quantum friction between parallel silver slabs"</i>	175
Ismael Diez-Perez (IBEC, Spain) <i>"Last advances in single-molecule electric contacts"</i>	179
Dietrich Foerster (University of Bordeaux I, France) <i>"An $O(N^3)$ implementation of Hedin's scheme for molecules in organic semi conductors"</i>	181
Jose Garcia Sole (UAM, Spain) <i>"Nanoparticles for two-photon intracellular thermal sensing."</i>	183
Aran Garcia-Lekue (Donostia International Physics Center (DIPC), Spain) <i>"Surveying Molecular Vibrations in Single Molecule Nanojunctions"</i>	185
Abdou Hassanien (AIST, Japan) <i>"Probing nanoscale superconductivity in organic molecular chains"</i>	189
Beatriz Hernandez Juarez (IMDEA Nanociencia, Spain) <i>"Ultrathin PbS Sheets by Two-Dimensional Oriented Attachment"</i>	191
Olatz Idigoras (CIC nanoGUNE, Spain) <i>"Magnetization reversal of uniaxial Co films with tunable crystallographic order"</i>	193
Ignacio Iglesias (Universidad de Murcia, Spain) <i>"Optical forces on small magnetodielectric particles in the focal volume of high numerical aperture microscopes"</i>	195
Bérengère Lebental (IFSTTAR, France) <i>"Nanosensors for structural monitoring in civil engineering: New insight on promising carbon nanotubes devices"</i>	203
Pierre Legagneux (THALES R&T, France) <i>"Carbon nanotube photocathodes for optically driven multiple X-ray sources"</i>	205
Virginia Martinez-Martinez (Universidad del Pais Vasco, Spain) <i>"Selective Luminescence Switching in Entangled Metal-Organic Frameworks by Inclusion of Aromatic Guests. Molecular Sensor for Substituted-Benzenes"</i>	211
Iñigo Martin-Fernandez (IMB-CNM, CSIC, Spain) <i>"Wafer scale fabrication of passivated carbon nanotube transistors for electrochemical sensing"</i>	213
Javier Méndez (ICMM-CSIC, Spain) <i>"Ordered vacancy network induced by the growth of epitaxial graphene on Pt(111)"</i>	219
David Meneses-Rodriguez (IMM-CNM-CSIC, Spain) <i>"Probing the electromagnetic field distribution within a magnetoplasmonic nanodisk"</i>	221
Rafael Morales (University of the Basque Country, Spain) <i>"Tuning writing magnetic fields in multi-state storage media"</i>	227
Javier Reguera (EPFL, Switzerland) <i>"One-step synthesis of Janus Nanoparticles by self-assembly monolayers"</i>	235
Guillaume Schull (CNRS - Strasbourg, France) <i>"Atomic-scale control of molecular contacts"</i>	243
Clivia Marfa Sotomayor Torres (ICN, Spain) <i>"Effect of phonon confinement on heat dissipation in ridges"</i>	245
Anna K. Suszka (CIC nanoGUNE, Spain) <i>"Origin and evolution of positive exchange bias in epitaxial (hcp)Co/CoO bi-layer structures"</i>	247
Javier Tamayo (CSIC, Spain) <i>"Novel paradigms for biological sensing based on nanomechanical systems: from microcantilevers to nanowires"</i>	249
Gerard Tobias (ICMAB-CSIC, Spain) <i>"Exploring the use of filled carbon nanotubes for biomedical applications"</i>	251
Jaume Veciana (ICMAB-CSIC, Spain) <i>"Non volatile molecular memory devices based on switchable and bistable self-assembled monolayers of electroactive organic radicals"</i>	253
Lucía Vergara (Instituto de Química-Física "Rocasolano" (CSIC), Spain) <i>"STM and LEEM characterization of the interaction between magnesium grown on Ru(0001) and hydrogen"</i>	255

ALPHABETICAL ORDER

I: Invited / IC: Invited CNano GSO Session / O: Oral / OC: Oral CNano GSO Session

		pag
Ibon Alonso Villanueva (CIC microGUNE, Spain) <i>"Highly photostable organic distributed feedback lasers fabricated by thermal nanoimprint"</i>	O	139
Ashod Aradian (Centre de Recherche Paul Pascal, France) <i>"Plasmonic particles organized in nanostructured polymer matrices"</i>	OC	141
Rémi Avriller (DIPC, Spain) <i>"Inelastic Quantum Transport in Nanoscale Junctions: Role of electron-phonon interactions on the current-current noise characteristics"</i>	O	143
Samuel D. Bader (Argonne National Laboratory, USA) <i>"Spintronics and Beyond"</i>	I	145
Noemi Barros (Université de Perpignan Via Domitia, France) <i>"Optimal switching of a nanomagnet assisted by a microwave field"</i>	OC	147
Stéphane Berciaud (IPCMS, Université de Strasbourg & CNRS, France) <i>"Observation of electronic raman scattering in metallic carbon nanotubes"</i>	O	149
D. Brevet (France) <i>"Mannose-targeted mesoporous silica nanoparticles for photodynamic therapy"</i>	OC	151
Olga Caballero-Calero (IMM-CSIC, Spain) <i>"Nanowire arrays of Bi₂Te₃ for Thermoelectric Applications"</i>	O	153
Julio Camarero (UAM/IMDEA Nanoscience, Spain) <i>"Quantifying and imaging magnetization reversal of buried interfaces by soft x-ray spectroscopy and holography"</i>	O	155
Daniela Cardinale (INRA, France) <i>"Virus scaffolds as Enzyme Nano-Carriers (ENCs) to organize bio-catalytic enzyme cascades. Design of a scanning electrochemical nanoreactor microscopy device"</i>	OC	157
Noelle Carette (INRA, France) <i>"Plant virus particles as nanoscaffolds for controlled positioning of enzyme cascades on solid supports"</i>	OC	159
Silvia Cavalli (CIBER-BBN, Institute for Research in Biomedicine (IRB Barcelona) PCB, Spain) <i>"Cell Penetrating Peptide-Superparamagnetic Iron Oxide Nanoparticle Conjugates as Bimodal Imaging Nanoagents"</i>	O	161
Francesca Cecchet (FUNDP - University of Namur, Belgium) <i>"Vibrational Sum-Frequency Generation Spectroscopy of Self-Assembled and Langmuir-Blodgett films on surfaces: from monolayers to model lipid membranes"</i>	O	163
Gianaurelio Cuniberti (TU Dresden, Germany) <i>"From molecular wires to organic semiconductors and back -some "don't ask, don't tell" of soft electronics"</i>	I	165
Luisa De Cola (Universität Münster, Germany) <i>"Nanocontainers: properties, manipulation and bio-medical applications"</i>	I	167
Jose M. De Teresa (CSIC-U. Zaragoza, Spain) <i>"Focused electron beam induced deposition and etching of functional materials"</i>	O	169
Yannick De Wilde (ESPCI, France) <i>"Direct near-field study of generation, coupling, and propagation of surface plasmons in the mid-infrared"</i>	I	171
Marie-Hélène Delville (ICMCB/CNRS, France) <i>"Internalisation Mechanisms of Modified Titanium Oxide Nanoparticles in Skin Cells and Multicellular Living Specimens : Resulting Toxicity"</i>	OC	173
Vito Despoja (DIPC, Spain) <i>"Role of the surface electronic structure in the enhancement of quantum friction between parallel silver slabs"</i>	O	175
Jean-Marie Devoisselle (Université de Montpellier/ENSCM, France) <i>"Nanostructured materials as drug delivery systems"</i>	IC	177

I: Invited / IC: Invited CNano GSO Session / O: Oral / OC: Oral CNano GSO Session

		pag
Ismael Diez-Perez (IBEC, Spain) <i>"Last advances in single-molecule electric contacts"</i>	O	179
Morinobu Endo (Shinshu University, Japan) <i>"Title not available"</i>	I	-
Dietrich Foerster (University of Bordeaux I, France) <i>"An $O(N^3)$ implementation of Hedin's scheme for molecules in organic semi conductors"</i>	O	181
Jose Garcia Sole (UAM, Spain) <i>"Nanoparticles for two-photon intracellular thermal sensing."</i>	O	183
Aran Garcia-Lekue (Donostia International Physics Center (DIPC), Spain) <i>"Surveying Molecular Vibrations in Single Molecule Nanojunctions"</i>	O	185
Illia Guralskyi (Laboratoire de Chimie de Coordination, France) <i>"Spin crossover nanomaterials: towards sensor applications"</i>	OC	187
Abdou Hassanien (AIST, Japan) <i>"Probing nanoscale superconductivity in organic molecular chains"</i>	O	189
Beatriz Hernandez Juarez (IMDEA Nanociencia, Spain) <i>"Ultrathin PbS Sheets by Two-Dimensional Oriented Attachment"</i>	O	191
Olatz Idigoras (CIC nanoGUNE, Spain) <i>"Magnetization reversal of uniaxial Co films with tunable crystallographic order"</i>	O	193
Ignacio Iglesias (Universidad de Murcia, Spain) <i>"Optical forces on small magnetodielectric particles in the focal volume of high numerical aperture microscopes"</i>	O	195
Christian Joachim (CEMES-CNRS, France) <i>"Molecule logic gate or surface atomic scale circuits"</i>	I	197
Benoît Jouault (Univ Montpellier 2, France) <i>"Quantum hall effect in epitaxial graphene on off-axis (000-1) SiC"</i>	IC	199
Leo Kouwenhoven (Technical Univ. Delft, Netherlands) <i>"Quantum mechanics in semiconductor nanowires"</i>	I	201
Bérengère Lebental (IFSTTAR, France) <i>"Nanosensors for structural monitoring in civil engineering: New insight on promising carbon nanotubes devices"</i>	O	203
Pierre Legagneux (THALES R&T, France) <i>"Carbon nanotube photocathodes for optically driven multiple X-ray sources"</i>	O	205
Francois Leonard (Sandia National Laboratories, USA) <i>"Charge injection and transport in nanowires"</i>	I	207
Brahim Lounis (Université Bordeaux 1, France) <i>"Title not available"</i>	IC	-
Christopher Marrows (University of Leeds, UK) <i>"Artificial Spin Ice"</i>	I	209
Virginia Martinez-Martinez (Universidad del Pais Vasco, Spain) <i>"Selective Luminescence Switching in Entangled Metal-Organic Frameworks by Inclusion of Aromatic Guests. Molecular Sensor for Substituted-Benzenes"</i>	O	211
Iñigo Martin-Fernandez (IMB-CNM, CSIC, Spain) <i>"Wafer scale fabrication of passivated carbon nanotube transistors for electrochemical sensing"</i>	O	213
Renaud Marty (CNRS-UPS, France) <i>"Physics of two photon luminescence imaging in nanoplasmonics"</i>	OC	215
Nathan D. McClenaghan (CNRS / Université Bordeaux 1, France) <i>"Communication between molecules via photocontrolled ions"</i>	IC	217
Javier Méndez (ICMM-CSIC, Spain) <i>"Ordered vacancy network induced by the growth of epitaxial graphene on Pt(111)"</i>	O	219
David Meneses-Rodriguez (IMM-CNM-CSIC, Spain) <i>"Probing the electromagnetic field distribution within a magnetoplasmonic nanodisk"</i>	O	221

I: Invited / IC: Invited CNano GSO Session / O: Oral / OC: Oral CNano GSO Session

		pag
Celia Mercader (CANOE, France) <i>"Novel carbon nanotube multifunctional composite fibers"</i>	OC	223
Bill Milne (Cambridge Univ, UK) <i>"Optimisation of CNT Based Nanostructures for Use as Electron Sources"</i>	I	225
Rafael Morales (University of the Basque Country, Spain) <i>"Tuning writing magnetic fields in multi-state storage media"</i>	O	227
Fabio Pistolesi (LOMA-Université Bordeaux 1/CNRS, France) <i>"Euler buckling instability and enhanced current blockade in suspended single-electron transistors"</i>	OC	229
Thomas Plénat (Université Paul Sabatier Toulouse III, France) <i>"A novel DNA chip for single molecule analysis"</i>	IC	231
Bertrand Raquet (Université de Toulouse, France) <i>"Quantum Transport and High Magnetic Field Phenomena in Carbon Nanotubes and Nano-ribbons"</i>	IC	233
Javier Reguera (EPFL, Switzerland) <i>"One-step synthesis of Janus Nanoparticles by self-assembly monolayers"</i>	O	235
Andrey Ryzhikovi (Laboratoire de Chimie de Coordination, France) <i>"Gas sensor for food industry and agriculture based on ZnO nanoparticles and nanorods"</i>	OC	237
Dirk Sander (Max-Planck-Institut für Mikrostrukturphysik, Germany) <i>"New insights into nanomagnetism by spin-polarized scanning tunneling microscopy and spectroscopy"</i>	I	239
Olivier Sandre (LCPO (Univ Bordeaux/CNRS/IPB), France) <i>"Doxorubicin Loaded Magnetic Polymersomes: Theranostic Nanocarriers for MR Imaging and Magneto-Chemotherapy"</i>	OC	241
Guillaume Schull (CNRS - Strasbourg, France) <i>"Atomic-scale control of molecular contacts"</i>	O	243
Clivia Marfa Sotomayor Torres (ICN, Spain) <i>"Effect of phonon confinement on heat dissipation in ridges"</i>	O	245
Anna K. Suszka (CIC nanoGUNE, Spain) <i>"Origin and evolution of positive exchange bias in epitaxial (hcp)Co/CoO bi-layer structures"</i>	O	247
Javier Tamayo (CSIC, Spain) <i>"Novel paradigms for biological sensing based on nanomechanical systems: from microcantilevers to nanowires"</i>	O	249
Gerard Tobias (ICMAB-CSIC, Spain) <i>"Exploring the use of filled carbon nanotubes for biomedical applications"</i>	O	251
Jaume Veciana (ICMAB-CSIC, Spain) <i>"Non volatile molecular memory devices based on switchable and bistable self-assembled monolayers of electroactive organic radicals"</i>	O	253
Lucía Vergara (Instituto de Química-Física "Rocasolano" (CSIC), Spain) <i>"STM and LEEM characterization of the interaction between magnesium grown on Ru(0001) and hydrogen"</i>	O	255

ABSTRACTS
ALPHABETICAL ORDER



HIGHLY PHOTOSTABLE ORGANIC DISTRIBUTED FEEDBACK LASERS FABRICATED BY THERMAL NANOIMPRINT

I. Alonso¹, V. Trabadelo^{1*}, A. Juarros¹, A. Retolaza¹, S. Merino¹, V. Navarro-Fuster², M.G. Ramírez², P.G. Boj², I. Vragovic², J.M. Villalvilla², J.A. Quintana², M.A. Díaz-García²

¹Micro/Nano Engineering Unit, CIC microGUNE, Avda. Otaola 20, 20600 Eibar, Spain

²Instituto Universitario de Materiales de Alicante, Universidad de Alicante, 03080 Alicante, Spain

*Present address: EMPA-Swiss Federal Laboratories for Materials Science and Technology, Advanced Materials Processing, CH-3602 Thun, Switzerland.

ialonsovillanueva@tekniker.es

Nanoimprint lithography (NIL) is a promising technique for the fabrication of surface pattern features down to 20 nm, even for future industrial applications, because of its high throughput, low cost and high fidelity pattern transfer. We have used this technique to make distributed feedback (DFB) resonant cavities for solid-state lasers based on semiconducting polymers, an active field of research in the past few years [1].

In this work we present the last results obtained with two kind of devices. First, DFB gratings in SiO₂ (periodicity of 368 nm and equal line and space) on which polystyrene (PS) films doped with 0.5 wt% of a perylenediimide (PDI) derivative were spin-coated afterwards. Using a master grating fabricated by e-beam lithography and plasma etching, the grating was first imprinted onto an mrl-8030E resist layer spin-coated on a thermally oxidized silicon wafer. The embossing was carried out at 180 °C and the applied force (20000 N) was held for 900 s. The residual layer was removed using an O₂ plasma and the grating was transferred to the SiO₂ by CHF₃/Ar plasma etching. Several grating depths were obtained by varying the etching time.

On the other hand, we also imprinted DFB gratings directly on the active material using the same master stamp. After spin-coating a PS film doped with 0.5 wt% of PDI on a SiO₂ wafer, it was embossed at 155 °C applying 15000 N for 900 s. This way the dry-etching step can be avoided, so the fabrication process for this second kind of devices becomes more cost-effective.

For the optical characterization of the samples, they were pumped with a circular spot (1.3 mm diameter) provided by a pulsed Nd:YAG laser (10 ns, 10 Hz) operating at 532 nm. The emitted light was collected normal to the surface with a fiber spectrometer. For DFB gratings in SiO₂, the laser showed laser emission at between 569 nm and 572 nm, depending on the grating depth. In the case of imprinted DFB gratings, the emitted wavelength is at around 578 nm. Thresholds were drastically reduced compared with the amplified spontaneous emission of a sample without grating [2]. Moreover, the thresholds of the devices with gratings directly embossed on the doped PS film were even lower than for devices with gratings in SiO₂. Furthermore, this combination of low threshold devices and material properties has shown to be very photostable. The half-life, defined as the number of excitation pulses at which the emission intensity decays at half of its maximum value, is longer than 300000 pump pulses (i.e., more than 8 h at 10 Hz), at a pump intensity twice the threshold (see figure below).

Acknowledgements:

This work is funded by the "Ministerio de Ciencia e Innovación" and the European Community (FEDER) through grant MAT2008-06648-C02. It was also partially supported by the ETORTEK Project MIBIO2 funded by the Basque Government. MGR is supported by a CSIC fellowship within the program JAE.

References:

- [1] D.W. Samuel, G.A. Turnbull, Chem. Rev., 107 (2007) 1272.
- [2] V. Navarro-Fuster, E. M. Calzado, P. G. Boj, J. A. Quintana, J. M. Villalvilla, M. A. Díaz-García, V. Trabadelo, A. Juarros, A. Retolaza, S. Merino, Appl. Phys. Lett., 97, (2010) 171104.

Figures:

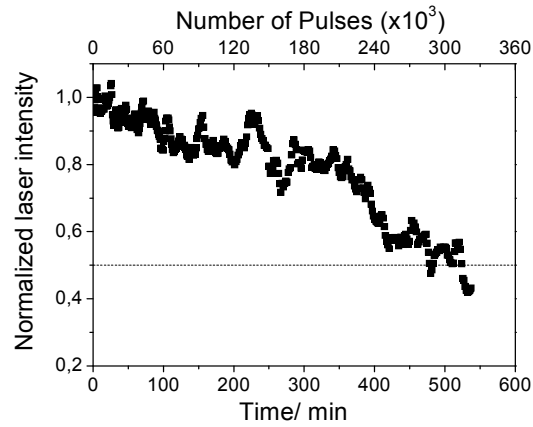


Figure 1: Normalized laser intensity vs irradiation time (bottom axis) and vs the number of pump pulses (10 ns, 10 Hz; top axis) for a DFB device based on a 0.5 wt % PDI- doped PS film and grating depth of 105 nm at 4 $\mu\text{J}/\text{pulse}$ (twice the threshold)

Ashod Aradian, Clémence Tallet, Julien Vieaud, Olivier Merchiers, Anitha Kumar, Frédéric Nallet, Virginie Ponsinet and Philippe Barois

Université Bordeaux 1 – CNRS, Centre de Recherche Paul Pascal UPR 8641,
Avenue Schweitzer, 33600 Pessac, France

aradian@crpp-bordeaux.cnrs.fr

New “bottom-up” fabrication techniques are now effectively explored for the production of nanostructured functional materials, and specifically for nanophotonic devices and metamaterials. Expected benefits from bottom-up approaches include assembling true three-dimensional metamaterials and synthesizing resonators with sizes appropriate for the optical range. Nanochemistry and self-assembly appear as interesting nanofabrication tools. Among the promising self-assembled systems are the diblock copolymers made of two molecular chains of distinct chemical nature linked together, which present solid state spontaneous structures with long-range order and tunable characteristic sizes between 10 and 50 nm. In particular, alternating lamellar and hexagonally-ordered cylindrical structures are described in many systems. These are, however, organic materials exhibiting moderate susceptibilities and low optical constant contrast. Therefore, in their native state, they should be considered essentially as ‘optically neutral’ templates, used to spatially organize ‘active’ entities. Our work focuses on nanoparticles presenting plasmonic resonances as these ‘active’ entities. Recent developments in the wet chemistry synthesis of plasmonic nanoparticles have allowed for significant improvements in terms of control of composition, surface chemistry, properties and size. In our study, gold nanoparticles are incorporated in polymer matrices with different nanostructures. We wish to correlate the nature, density and spatial organization of the nanoparticles with the optical properties of the nanocomposite materials.

Two different experimental systems are studied. In the first system, 15-nm diameter gold spheres are dispersed randomly in poly(vinyl alcohol) thin films deposited on silicon wafers or glass plates. Volume fraction of gold is varied from 1 to 30% and film thickness from a few nanometers to 300 nm. The structure of the films is studied by atomic force microscopy (Fig. 1) and X-ray reflectivity. In the second system, 10-nm diameter gold nanoparticles are incorporated in the 18-nm thick poly(acrylic acid) layers of the ordered lamellar phase of a poly(styrene)-block-poly(acrylic acid) copolymer. Volume fraction of gold is varied in both thin films on silicon wafer and bulk samples. Small-angle scattering and reflectivity of X-rays, atomic force and electron microscopies (Fig. 2) are used to get a detailed structural description of the nanostructured composites and validate the control of the density and organization of the nanoparticles. The optical properties of the nanocomposites are studied using spectrophotometry and spectroscopic ellipsometry.

The refractive index results, in the visible and infra-red spectral regions, are confronted to effective medium models. As shown in Fig. 3, the classical Maxwell-Garnett model shows an important discrepancy with the measured results, and we will show how the situation can be improved taking into account the appropriate dispersion function for the nanoparticles, as well as substrate effects. Similar systems using rod-shape gold nanoparticles, developments towards unusual optical properties at high gold fraction, and search for experimental evidence of anisotropic optical properties will also be described in this presentation. The conclusions will allow discussing the use of self-assembly for fabrication of new nanostructured optical materials.

Acknowledgments:

The support of the Région Aquitaine, the French Agence Nationale de la Recherche (NANODIELLIPSO, ANR-09-NANO-003) and the European Union's Seventh Framework Programme (FP7/2008) under grant agreement n° 228762 (METACHEM) is acknowledged.

Figures:

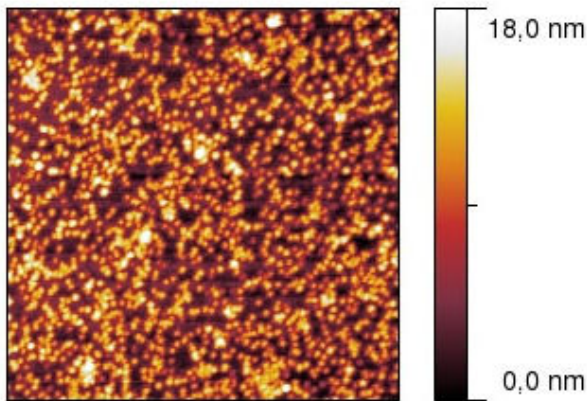


Figure 1: $2 \times 2 \mu\text{m}$ atomic force microscopy topography (upper-view) image obtained on a thin composite film of gold nanoparticles randomly dispersed in poly(vinyl alcohol).

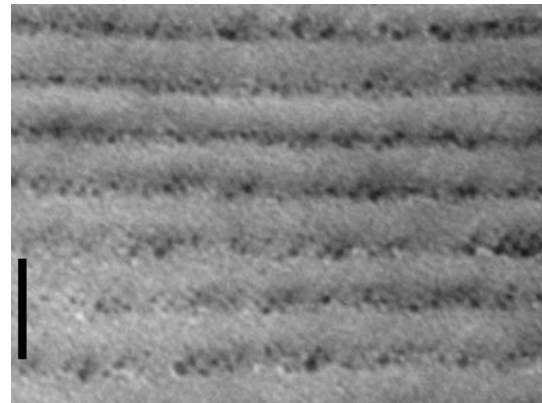


Figure 2: Transmission electron micrograph (side view) of an ordered lamellar composite film of gold nanoparticles and poly(styrene)-*b*-poly(acrylic acid) copolymer. Bar = 50 nm.

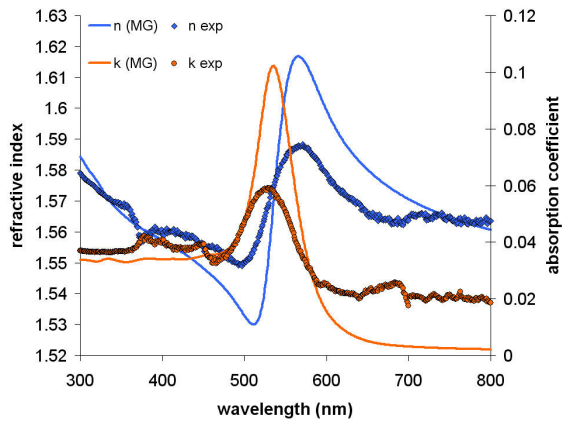


Figure 3: Optical index n and absorption coefficient k , determined by analysis of spectroscopic ellipsometry data, of a 77nm-thick composite film of gold nanoparticles randomly dispersed in poly(vinyl alcohol), as a function of the wavelength. The discrepancy with a simple Maxwell-Garnett model (full lines) is apparent and motivates the inclusion of other effect such as electron confinement and substrate effects.

INELASTIC QUANTUM TRANSPORT IN NANOSCALE JUNCTIONS : ROLE OF ELECTRON-PHONON INTERACTIONS ON THE CURRENT-CURRENT NOISE CHARACTERISTICS

V R. Avriller¹, D.F. Urban² and A. Levy Yeyati³

¹DIPC (Donostia International Physics Center), Paseo Manuel de Lardizabal, 4, 20018 Donostia-San Sebastián, Spain.

²Physikalisches Institut, Albert-Ludwigs-Universität, 79104 Freiburg, Germany

³Departamento de Física Teórica de la Materia Condensada C-V, Facultad de Ciencias, Universidad Autónoma de Madrid, E-28049 Madrid, Spain.

remi_avriller@ehu.es

Recent theoretical advances have unveiled the role of electron-phonon (e-ph) interactions in the current-current fluctuations (shot noise) versus voltage characteristics of molecular nano-devices [1,2,3]. For voltages crossing the inelastic threshold, the correction to the noise induced by e-ph interactions was shown to exhibit a crossover between a positive and negative correction, depending on the parameters describing the junction (position of the molecular level, asymmetry of the coupling to the leads) [1,2,3]. More generally the high-bias properties of the noise versus voltage characteristics were shown to result from both electronic and vibronic dynamics [4], the fluctuations of the later being responsible of a dynamical feedback inducing strong non-linear effects in the transport properties [5].

In this work, we would like to review the state of the art of the literature concerning transport properties of molecular junctions (current, noise and full counting statistics) in presence of such inelastic effects. We also would like to address the description of the remaining open questions, as well as some possible directions for further theoretical works.

The aim of such investigations could be to generate simulation tools for computing noise characteristics as efficient as the one available for computing I-Vs [6], and to provide a new way of characterizing experimentally transport properties of molecular junctions [7].

References:

- [1] T. L. Schmidt and A. Komnik, Phys. Rev. B. 80, 041307(R) (2009).
- [2] R. Avriller and A. Levy Yeyati, Phys. Rev. B. 80, 041309(R) (2009).
- [3] F. Haupt, T. Novotny, and W. Belzig, Phys. Rev. Lett. 103, 136601 (2009).
- [4] R. Avriller, arXiv:1007.4450 (2010).
- [5] D.F. Urban, R. Avriller and A. Levy Yeyati, Phys. Rev. B 82, 121414(R) (2010).
- [6] T. Frederiksen, M. Paulsson, M. Brandbyge, and A.-P. Jauho, Phys. Rev. B 75, 205413 (2007).
- [7] O. Tal, M. Krieger, B. Leerink and J.M. van Ruitenbeek, Phys. Rev. Lett. 100, 196804(2008).

S. D. Bader

Materials Science Division and Center for Nanoscale Materials Argonne National Laboratory,
Argonne, IL 60439, USA
ialonsovillanueva@tekniker.es

Spintronics encompasses the ever-evolving field of magnetic electronics.[1] It offers the possibility to communicate via pure spin currents as opposed to electric charge currents. [2] The talk provides a brief perspective of recent developments to switch magnetic moments by spin-polarized currents, electric fields and photonic fields. Developments to reinvent today's semiconductor electronics depend on the exploration and discovery of novel nanostructured materials and configurations.

The talk highlights select promising areas, featuring recent work at Argonne, [3] including complex-oxide-based Mott-tronics research [4] ferromagneticsuperconducting heterostructural opportunities, [5] and most strikingly, the realm of new cancer treatment approaches.[6]

Work supported by the U.S. Department of Energy, Office of Science, Basic Energy Sciences, under contract No. DE-AC02-06CH11357.

References:

- [1] S. D. Bader and S. S. P. Parkin, "Spintronics," in Annual Reviews of Condensed Matter Physics 1, 71-88 (2010)
- [2] O. Mosendz, J. E. Pearson, F. Y. Fradin, G. E. W. Bauer, S. D. Bader, and A. Hoffmann, Phys. Rev. Lett. 104, 046601 (2010)
- [3] S. D. Bader, Rev. Mod. Phys. 78, 1-15 (2006).
- [4] S. J. May, P. J. Ryan, J. L. Robertson, J.-W. Kim, Tiffany. S. Santos, Elena Karapetrova, J. L. Zarestky, X. Zhai, Suzanne. G. E. te Velthuis, J. N. Eckstein, S. D. Bader, and A. Bhattacharya, Nature Materials 8, 892-897 (2009).
- [5] P. Cadden-Zimansky, Ya. Bazaliy, L.M. Litvak, J.S. Jiang, Jiyeong Y. Gu, C.-Y. You, M.R. Beasley, and S.D. Bader, Phys. Rev. B 77, 184501 (2008)
- [6] Dong-Hyun Kim, Elena A. Rozhkova, Ilya V. Ulasov, S. D. Bader, Tijana Rajh, Maciej S. Lesniak, and V. Novosad, Nature Materials 9, 165-171 (2010).

Noemi Barros, Mhamed Rassam, Hamid Kachkachi

Université de Perpignan Via Domitia - 52, Avenue Paul Alduy - 66860 Perpignan cedex, France
noemi.barros@univ-perp.fr

Magnetic recording is a key technology in the field of high density information storage. In order to increase thermal stability, small nanoparticles with a high anisotropy may be used. However, high fields are then needed to reverse the magnetization but these are difficult to achieve in current devices. In 2003 Thirion et al. [1] showed that the combination of a constant applied field (DC field), well below the switching field, with a microwave (MW) field pulse can reverse the magnetization of a nanoparticle. Further studies on single domain magnetic nanoelements [2] proved that the effect is stronger if the frequency of the MW field matches the ferromagnetic resonance frequency of the nanoelements. Numerical simulations [3] confirm that chirped MW fields are more efficient than monofrequency fields.

The aim of this work is to find the optimal MW field triggering the switching of a nanoparticle under specified constraints. We consider a single-domain nanoparticle, modelled by a macroscopic magnetic moment (macrospin). The shape of the MW field is then sought by minimizing the absorbed energy, following the trajectory of the macrospin, which is a solution of the damped Landau-Lifshitz equation. The boundary conditions are a given initial state and a specified target state that is supposed to be reached after switching. This boundary value problem is reformulated by defining a cost functional that is then minimized using the Lagrange parameter technique [4]. The problem is then solved numerically using the conjugate gradient algorithm coupled to a simulated annealing scheme.

The calculation is carried out for a nanoparticle with a uniaxial anisotropy in an oblique DC magnetic field and a linearly polarized MW field. According to our results, the optimal MW field is modulated both in amplitude and in frequency (see Fig. 1). Its role is to drive the magnetization from the metastable equilibrium position towards the saddle point, then damping induces the relaxation to the stable equilibrium position. A small magnitude of the MW field is sufficient to induce a substantial reduction of the switching field. For the pumping to be efficient, the MW field frequency must match the proper precession frequency of the magnetization, which equals the ferromagnetic resonance frequency at the early stage of the switching process.

The MW field is optimized for various intensities and orientations of the DC field. The switching field curve (Stoner-Wohlfarth astroid) in presence of a given MW field is then computed. The results are in qualitative agreement with experiments on isolated nanoclusters [1] and on single-domain magnetic elements [2]. The effect of damping is also investigated. The strong dependency of the optimal MW field and the switching curve on the damping parameter provides a means of probing experimentally the latter in nanoclusters.

This study is part of a collaboration with the teams of V. Dupuis (LPMCN, Lyon, France) and E. Bonet (Institut Neel, Grenoble, France), within the ANR project DYSC.

References:

- [1] C. Thirion, W. Wernsdorfer, D. Maily, Nat. Mater. 2 (2003) 524
- [2] G. Woltersdorf, C. H. Back, Rhys. Rev. Lett. 99 (2007) 227207
- [3] S. Okamoto, N. Kikuchi, O. Kitakami, Appl. Phys. Lett 93 (2008) 142501
- [4] N. Barros, M. Rassam, H. Jirari, H. Kachkachi, Phys. Rev. B, submitted

Figures:

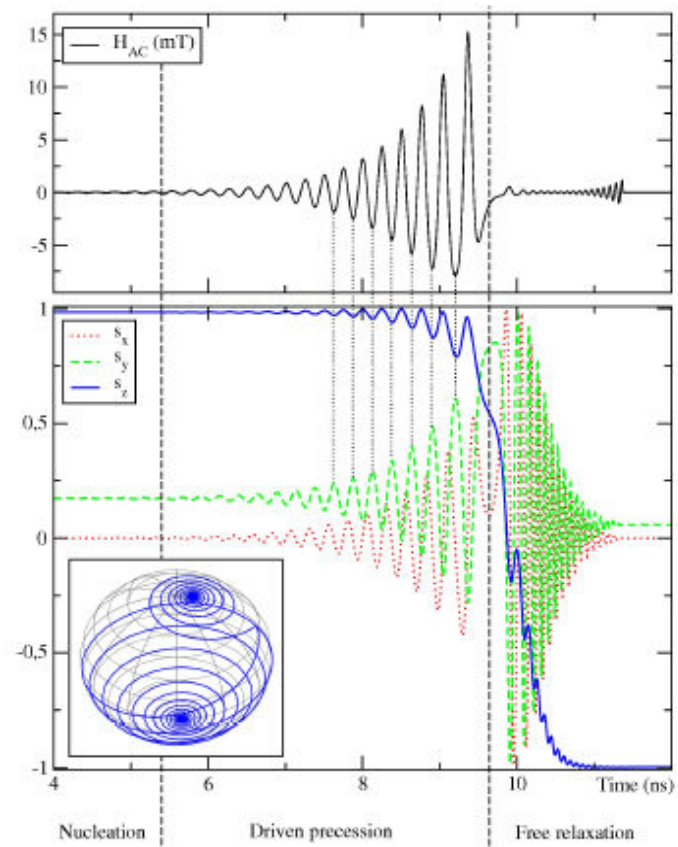


Figure 1: Optimized MW field (upper panel) and the corresponding spin trajectories (lower panel). The DC field is applied in the yz plane making an angle of 170° with respect to the easy axis (z axis), and its magnitude is 150 mT. The inset is a 3D plot of the spin trajectory on the unit sphere.

OBSERVATION OF ELECTRONIC RAMAN SCATTERING IN METALLIC CARBON NANOTUBES

H. Farhat¹, **S. Berciaud**^{2,3}, M. Kalbac¹, R. Saito⁴, T. F. Heinz², M. S. Dresselhaus¹, and J. Kong¹

¹Massachusetts Institute of Technology, Cambridge, MA 02139, USA

²Columbia University, New York, NY 10027, USA

³IPCMS (UMR 7504), Université de Strasbourg and CNRS, F-67034 Strasbourg, France

⁴Tohoku University, Sendai, 980-8578, Japan

berciaud@unistra.fr

Raman scattering spectroscopy, a powerful tool for studying elementary excitations in materials, has been instrumental in the progress of carbon nanotube research. The Raman features that have been studied to date in carbon nanotubes are associated with the phonon modes that scatter light due to electron-phonon coupling [1]. In metallic nanotubes, low energy electron-hole pairs are another important type of excitation [2], but their inelastic scattering of light [3], via the Coulomb interaction, has not been yet observed. Here, we report on a new feature in the Raman spectrum of individual metallic carbon nanotubes, that we attribute to resonant electronic Raman scattering (ERS) from low-energy electron-hole pairs created across the “graphene-like” linear electronic subbands of metallic nanotubes. The ERS spectra exhibit broad peaks that appear at a constant photon energy due to a resonance of the scattered photons with the optical transition energies of the metallic nanotube. Our results are consistent with the picture that the mild asymmetry in the lineshape of the Raman G-mode feature [4] is the result of an interference between the overlapping ERS and vibrational Raman scattering by the longitudinal optical (LO) phonon mode.

References:

- [1] M. S. Dresselhaus et al., *Physics Reports*, 409, 47 (2005).
- [2] V. V. Deshpande et al., *Nature*, 464, 209 (2010).
- [3] A. Pinczuk, and G. Abstreiter, *Light Scattering in Solids V*, Springer-Verlag, Berlin, (1989).
- [4] Y. Wu et al., *Phys. Rev. Lett.* 99, 027402 (2007).
- [5] M. Y. Sfeir et al., *Science*, 312, 554 (2006).
- [6] J. C. Meyer, M. Paillet et al., *Phys. Rev. Lett.* 95, 217401 (2005).
- [7] S. Berciaud, C. Voisin et al., *Phys. Rev. B.* 81, 041414(R) (2010).

Figures:

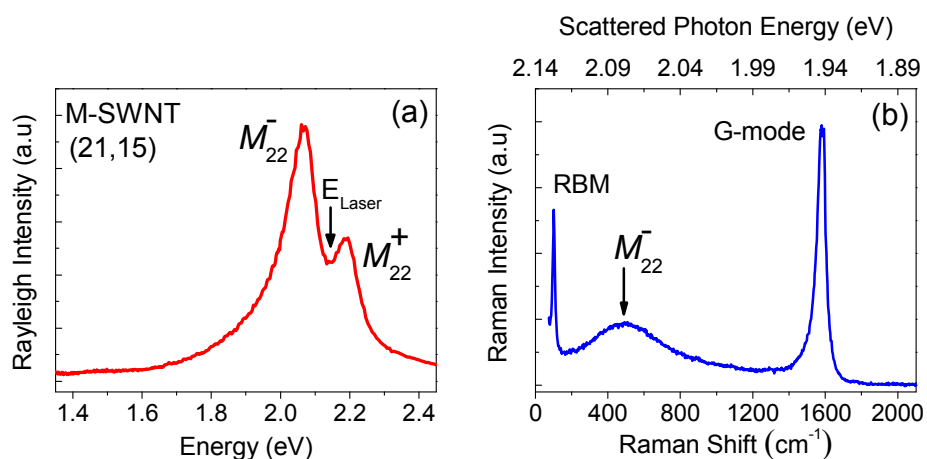


Figure 1: Electronic Raman Scattering in a structure assigned (21,15) metallic carbon nanotube. The Rayleigh (a) and Raman (b) scattering spectra of an individual, freestanding metallic nanotube are used to determine its (n,m) indices [5, 6]. The labels in a indicate the optical transitions, while the laser energy for the Raman measurement is indicated with arrow. Likewise, the arrow in the Raman spectrum indicate the energies of the optical transitions as obtained from fitting the Rayleigh scattering spectra using an excitonic model [7]. The ERS feature is the broad peak at $\sim 500\text{ cm}^{-1}$ in (b). The corresponding scattered photon energy (2.08 eV, see top axis in (b)) match the energy of the M_{22}^{-} transition. No ERS features are found in the Raman spectrum of semiconducting nanotubes.

MANNOSE-TARGETED MESOPOROUS SILICA NANOPARTICLES FOR PHOTODYNAMIC THERAPY

David Brevet,^a Magali Gary-Bobo,^b Ouahiba Hocine,^a Sébastien Richeter,^a Laurence Raehm,^a Jean-Olivier Durand,^a Bernard Loock,^c Philippe Maillard,^c Pierre Couleaud,^d Céline Frochot,^d Alain Morère,^e Marcel Garcia.^b

- a) Institut Charles Gerhardt Montpellier UMR 5253 CNRS-UM2-ENSCM-UM1, laboratoire CMOS, CC 1701, Place Eugène Bataillon, 34095 Montpellier cedex 05, France
b) INSERM, Unité 896, Montpellier, F 34298 France; Université Montpellier1, Montpellier, F 34298 France; CRLC Val d'Aurelle Paul Lamarque, Montpellier, F 34298 France
c) UMR 176 CNRS/Institut Curie, Institut Curie, Bât 110, Université Paris-Sud, F-91405 Orsay, France; Institut Curie, Section de Recherches, Centre Universitaire, Université Paris-Sud, F-91405 Orsay, France.
d) Département de Chimie Physique des Réactions, UMR 7630, CNRS-INPL, ENSIC, 1, rue Grandville BP 20451, 54001 Nancy Cedex, France
e) UMR 5247 CNRS- UM1-UM2 - Institut des Biomolécules Max Mousseron, Ecole Nationale Supérieure de Chimie de Montpellier, 8 rue de l'Ecole Normale, 34296 Montpellier, France
durand@univ-montp2.fr

Covalent attachment of water-soluble photosensitizers (Figure 1) into mesoporous silica nanoparticles (MSN) for photodynamic therapy (PDT) applications is described. Those MSN were monodispersed with a diameter of 100 nm, a specific surface area of 860 m²/g and a pores diameter of 2.2 nm. These MSN were proved to be active on breast cancer cells after endocytosis. Moreover, MSN were functionalized on their surface by mannose using an original pathway with diethyl squarate as the linker. Those mannose-functionalized MSN dramatically improved the efficiency of PDT on breast cancer cells. In addition, the involvement of mannose receptors for the active endocytosis of mannose-functionalized MSN was demonstrated (Figure 2).

Figures:

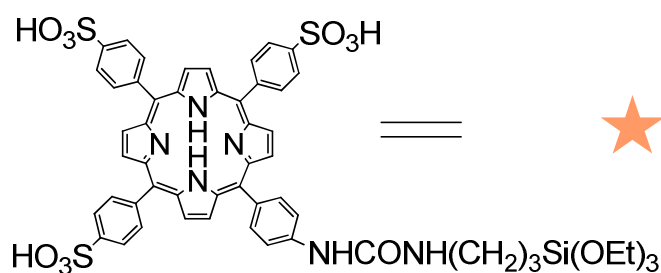


Figure 1

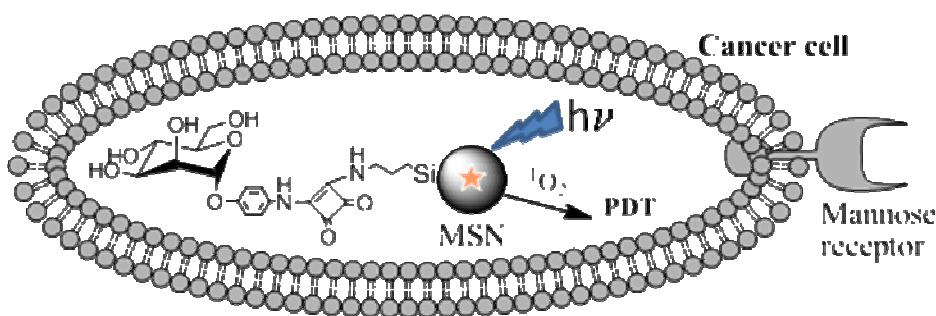


Figure 2

NANOWIRE ARRAYS OF Bi_2Te_3 FOR THERMOELECTRIC APPLICATIONS

O. Caballero-Calero¹, P. Díaz-Chao¹, Deb², Y. Shinohara², M.S. Martín-González¹

¹Thermoelectrics group, IMM-Instituto de Microelectrónica de Madrid (CNM-CSIC), Isaac Newton 8, PTM, E-28760 Tres Cantos, Madrid, Spain

²National Institute for Materials Science 1-2-1 Sengen, Tsukuba, Ibaraki, 305-0047 Japan

olga.caballero@imm.cnm.csic.es

Thermoelectric materials are those which can convert heat into electricity and vice versa. These materials appear as a promising way to recover power from the heating produced in most of the motors and machines, which is usually wasted [1]. Their main disadvantage is their low efficiency, which depends on their figure of merit (ZT), which is defined as $ZT=(S^2 \cdot \sigma \cdot T)/\kappa$, where S stands for the Seebeck coefficient, σ , κ are the electrical and thermal conductivity, respectively, and T is the absolute temperature. Nowadays, the increase of this ZT is the main objective to optimize them for practical device fabrication. In 1993 a theoretical work presented suggested that a way to enhance their efficiency is by quantum confinement of the electron charge carriers [2]. Therefore, a great effort is being made in demonstrating experimentally this prediction.

One way of achieving this quantum confinement is reducing the dimensions of the material, which can be accomplished by fabricating wires of thermoelectric materials with wire diameters within the nanoscale range. Moreover, nanowire array configuration has some advantages over films, mainly due to a higher freedom in the design of morphology and composition. In our case, we have studied the nanowire formation and properties of Bi_2Te_3 , which is a thermoelectric material that has been thoroughly studied in both bulk and film configurations. The fabrication and optimization of these nanowire arrays in order to obtain more efficient thermoelectric devices is the aim of this work.

First of all, Bi_2Te_3 films were grown via electrochemical deposition, following the fabrication procedure described in Martín-González et al. [3,4]. These films were optimized and their morphology (SEM micrographs, see Figure 1), structure (XR-diffraction), and transport properties (Seebeck coefficient and electrical resistivity) were characterized. Finally, films with a well defined crystal orientation (c-axis parallel to the substrate plane, which is the best direction for the thermoelectric performance in this material, see Figure 2) with a homogeneous composition were obtained.

Once this procedure was well established, the method was modified in order to give rise to nanowire arrays in a similar way. To this end, nanoporous anodic aluminium oxide membranes with a nominal pore diameter of 200nm from Whatman® were used. Prior to the growth of the nanowires, all membranes were coated with an evaporated layer of 50 nm Cr and 1500 nm Au. The synthesis of the nanowires was made inside these matrices by electrodeposition. The membrane was placed into electric contact with a Cu plate through the metallic layer, which served as back electrode, forming the working electrode of the electrochemical cell, in a similar arrangement to that described for the growth of Bi_2Te_3 films. Samples grown with different applied potentials between the electrodes and for different time periods were fabricated. SEM micrographs showed that the nanowires have grown along the whole width of the alumina template (Figure 3), giving rise to well oriented wires of Bi_2Te_3 . Novel methods developed for the measurement of the thermoelectric-relevant parameters in these structures, comprising the electrical conductivity and thermal conductivity measurement will be presented.

Acknowledgements:

Authors acknowledge financial support from MICINN (FCCI program) ACI PLAN E -JAPON- Grant number PLE2009-0073 and ERC 2008 Starting Grant 240497.

References:

- [1] D. M. Rowe, G. Ming, S. G. Willieams, G. K. Kuznetsov, Proceedings of the 17th International Conference on Thermoelectrics (2000), 1499 – 1504.
- [2] L. D. Hicks, M. S. Dresselhaus, Phys. Rev. B 47 (1993) 12727 – 12731.
- [3] M. Martín-González, J. Electrochem Society 149 11 (2002) C546 – C554.
- [4] A.L. Prieto, M.S. Sander, M.S. Martín-González, R. Gronsky, T. Sands, and A.M. Stacy J. Am. Chem. Soc. 123 (2001) 7160.

Figures:

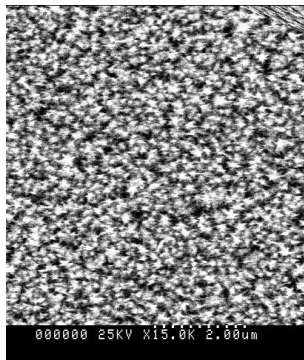


Figure 1: SEM micrograph a Bi_2Te_3 film grown by electrodeposition.

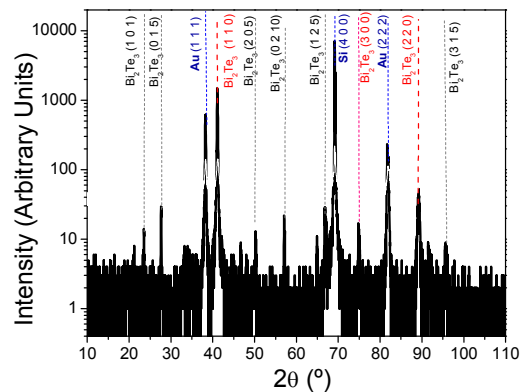


Figure 2: X-Ray Diffraction data from a Bi_2Te_3 film. Apart from the peaks corresponding to the substrate (Au and Si), the most important diffraction occurs for Bi_2Te_3 oriented along (110), (2 2 0) and (3 0 0), that is, the sample is oriented with the c-axis parallel to the substrate plane (Ref. Natl. Bur. Stand. (U.S.) Monogr. 25,3 (1964) 16)

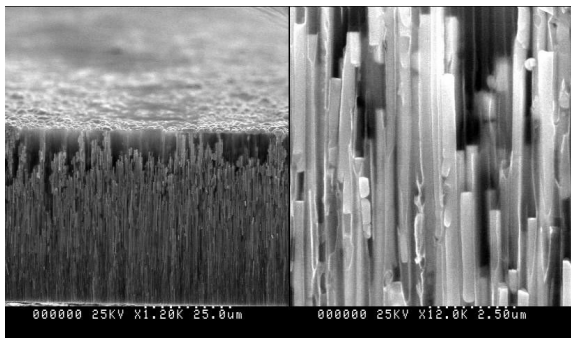


Figure 3: Different micrographs of the cross-section of nanowire arrays of Bi_2Te_3 grown by electro-deposition in an alumina matrix prepared at IMM.

QUANTIFYING AND IMAGING MAGNETIZATION REVERSAL OF BURIED INTERFACES BY SOFT X-RAY SPECTROSCOPY AND HOLOGRAPHY

J. Camarero,^{1,2,*} E. Jiménez,¹ J. Vogel,³ C. Tieg,^{4,5} P. Perna,² A. Bollero,² F. Yakhou-Harris,⁴ C. Arm,⁶ E. Gautier,⁶ S. Auffret,⁶ B. Delaup,⁶ G. Gaudin,⁶ B. Rodmacq,⁶ B. Dieny,⁶ and R. Miranda.^{1,2}

¹Departamento de Física de la Materia Condensada and Instituto de Física de Materiales “Nicolás Cabrera”, Universidad Autónoma de Madrid, 28049 Madrid, Spain

²IMDEA-Nanoscience, Campus de Cantoblanco, 28049 Madrid, Spain

³Institut Néel-CNRS, 38042 Grenoble, France

⁴ESRF, F-38043 Grenoble, France

⁵Laboratory Helmholtz-Zentrum Berlin Albert-Einstein-Strasse 15 D-12489 Berlin Germany

⁶SPINTEC, URA2512 CNRS/CEA, 38054-Grenoble, France

julio.camarero@uam.es

The spin arrangement at the interface in layered magnetic nanomaterials is often crucial for the understanding of their magnetic properties and has profound consequences for practical applications. The most striking feature is the unidirectional coupling between the spins in an antiferromagnet (AFM) and those in an adjacent ferromagnet (FM), referred to as exchange bias [1]. FM/AFM structures are at the heart of today's spintronic devices, stabilizing the direction of FM reference layers, while taking advantage of the interfacial exchange interaction effects [2]. In addition, there are a plethora of other magnetic phenomena associated in exchange-coupled FM/AFM systems, such as coercivity enhancement, magnetization reorientation, modified antiferromagnetic spin structures, and asymmetric magnetization reversal, which are not fully understood. Prospects for control, tailor, and enhancement of desirable effects depend upon a clear understanding of the mechanisms governing exchange bias. However, the lack of techniques capable of providing detailed magnetic information of buried interfacial layers with element selectivity and upon external fields is delaying this understanding.

Only very few experimental techniques can address the microscopic magnetization reversal behavior of the different magnetic layers in a multilayered system with element selectivity. Scattering based techniques, such as soft x-ray magnetic resonant scattering (SXMR) [3] and lensless holographic imaging [4], have been established as a powerful tools for studying magnetic structures in surfaces and thin films on the nanometer length scale. The soft x-ray range hosts the largest magnetic resonances of the magnetically important transition-metal and rare-earth series. Additionally, holographic imaging combines the magnetic sensitivity obtained with x-ray magnetic circular dichroism in transmission geometry with the spatial resolution from a simple Fourier inversion of a reciprocal space soft x-ray interference pattern from an object (sample) and a reference aperture (which defines the final spatial resolution). In addition, the technique can image deeply buried magnetic systems and, as a pure photon-based technique (photon-in/photon-out), can be used in applied magnetic fields. Up to now, soft x-ray holography has focused on [non magnetic/magnetic]_n multilayers with perpendicular magnetic anisotropy for both remanence and field-dependent measurements. However, only relatively large (> 5 nm) effective magnetic thicknesses have been studied, and both element-specificity and quantification-availability has not been yet exploited.

We have recently spread out the capabilities of soft x-ray holography for imaging the magnetization reversal, by adding the quantitative aspects of magnetic spectroscopy [5]. We have implemented a unique experimental set-up at beamline ID08 of the European Synchrotron Radiation Facility (ESRF) combining soft x-ray holography and spectroscopy capabilities. This new set-up allows performing element-selective soft x-ray holography measurements for imaging the domain structure of buried magnetic ultrathin films with perpendicular anisotropy under applied magnetic fields, adding the quantitative aspects of magnetic spectroscopy measurements in both total electron yield (TEY) and transmission detection modes. We have investigated ferromagnetic (FM) [Co/Pt]_n multilayers with perpendicular anisotropy exchange coupled with antiferromagnetic (AFM) FeMn and IrMn films. From the spectroscopy analysis, both spectroscopy and element-selective XMCD hysteresis loops measurements confirm the existence of interfacial uncompensated AFM moments, i.e., ~1 ML (monolayer) thick, which behave differently during FM reversal. We have quantified the unpinned (pinned) uncompensated AFM moments, providing direct evidence of its parallel (antiparallel)

alignment with respect to the FM moments. In addition, the Fe- L_3 hysteresis loop reproduces the Co- L_3 one, i.e., it shows a horizontal shift to negative values (opposite to the field cooling FC) direction, exchange bias field $\mu_0 H_E < 0$) and, it is slightly shifted vertically downwards (see Fig.1.a). This indicates that the majority (90%) of the uncompensated AFM moments rotates during FM reversal (unpinned moments) whereas a small amount (10%) stays aligned antiparallely to the FC direction (pinned moments).

The holography experiments allow to image the magnetization reversal of an exchange-biased FM layer with an equivalent Co thickness below 3 nm in real space (1.8 μm diameter field-of-view FOV with 50 nm spatial resolution) and in external magnetic fields [5]. The field dependence images shows that the reversal mechanism of the FM layer is via nucleation, propagation and annihilation of magnetic domains and, in addition, different nucleation sites were found in both hysteresis branches, pointing out a possible deterministic nature of the reversal. A remarkable highlight is that we could image for the first time the magnetization reversal of the uncompensated AFM moments, which correspond to an equivalent thickness of less than one monolayer only [6], and under applied fields [7]. The images show that the uncompensated AFM moments reproduce the magnetic domain structure of the FM layer during the whole hysteresis loop (see Fig1.b), which prove that the FM moments locally drag the unpinned AFM moments during reversal.

Our results provide new microscopic insights into the exchange coupling phenomena and explore the sensitivity limits of these techniques. Future trends will be also discussed.

References:

- [1] W. H. Meiklejohn and C. P. Bean, Phys. Rev. 102, 1413 (1956).
- [2] J. Nogués and I. K. Schuller, J. Magn. Magn. Mater. 192, 203 (1999).
- [3] J. Miguel, J. Camarero, J. Vogel, J. Peters, N. B. Brookes, and J. Goedkoop, Appl. Surf. Sci. 254, 335 (2007).
- [4] S. Eisebitt, J. Lüning, W. F. Schlotter, M. Lörger, O. Hellwig, W. Eberhardt, and J. Stöhr, Nature 432, 885 (2004).
- [5] C. Tieg, E. Jiménez, J. Camarero, J. Vogel, C. Arm, B. Rodmacq, E. Gautier, S. Auffret, B. Delaup, G. Gaudin, B. Dieny, and R. Miranda, Appl. Phys. Lett. 96, 072503 (2010).
- [6] J. Camarero, E. Jiménez, J. Vogel, C. Tieg, P. Perna, A. Bollero, F. Yakhou-Harris, C. Arm, E. Gautier, S. Auffret, B. Delaup, G. Gaudin, B. Rodmacq, B. Dieny, and R. Miranda, 55th-MMM Conf. invited paper. To appear in J. Appl. Phys. (2011).
- [7] E. Jiménez, et al. submitted

Figures:

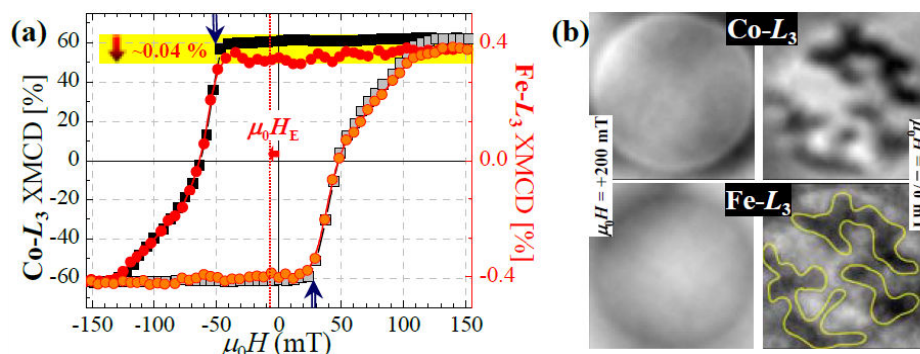


Figure 1: (a) Element-selective XMCD hysteresis loops of a [1.8 nm Pt/0.6 nm Co]/10 nm FeMn system recorded in transmission geometry: XMCD data are normalized to their corresponding absorption L_3 peaks. (b) Magnetic domain images of the FM layer (top) and the uncompensated AFM moments (bottom) at selected applied fields. FOV=1.8 μm . The images are retrieved from the Fourier transform of magnetic holograms acquired at the Co- L_3 and Fe- L_3 absorption edges, respectively.

VIRUS SCAFFOLDS AS ENZYME NANO-CARRIERS (ENCs) TO ORGANIZE BIO-CATALYTIC ENZYME CASCADES. DESIGN OF A SCANNING ELECTROCHEMICAL NANOREACTOR MICROSCOPY DEVICE

Daniela Cardinale¹, Noëlle Carette¹, Amandine Barra¹, Jocelyne Walter¹, Thierry Delaunay¹, Christophe Demaille², Agnès Anne², Olivier Courjean³, Nicolas Mano³, Jean-Paul Salvétat³, Jean-Pierre Aime⁴, Thierry Michon¹

¹INRA, UMR 1090 GDPP, IBVM Virologie, 71 Av. Edouard Bourlaux, B.P. 81, 33883 Villenave d'Ornon, France

²Laboratoire d'Electrochimie Moléculaire, UMR CNRS – P7 7591, Université Paris Diderot – Paris 7, Bâtiment Lavoisier, 15 rue Jean-Antoine de Baïf, 75205 Paris cedex 13, France

³CRPP, Centre de Recherche Paul Pascal, 115 Av. Schweitzer, 33600 Pessac, France

⁴CPMOH, Centre de Physique Moléculaire Optique et Hertzienne, UMR5798, Université Bordeaux 1, 351 Cours de la Libération, 33405 Talence, France

daniela.cardinale@bordeaux.inra.fr

In cellular systems, the association of collaborating enzymes in supramolecular structures enables metabolic processes to be performed more efficiently, accelerating reactions rates and preventing the diffusion of intermediates in the cell medium. The aim of the Cascade project is to create a new experimental tool at the nanoscale level mimicking *in vivo* enzymatic cascade reactions. The set up will also offer the opportunity to study enzymatic processes at the level of one single or few molecules. To this purpose two model enzymes will be used to build artificial redox cascades: the lipase B (CalB) from *Candida antarctica* and the glucose oxidase (GOX) from *Penicillium amagasakiense*. The free electrons generated by enzymatic activities will be detected by electrochemistry. To this purpose a new nanoelectrochemical technique will be used to confine the clustered enzymes and to measure the final activity. The confined reaction medium will be permitted by a “nanocavity” microelectrode fabricated at the tip of an AFM probe; the combination of AFM/SECM (Scanning Electro Chemical Microscopy) will enable to measure the electrochemical current generated by a few enzyme molecules. Varying the diameter of the nanocavity from few hundreds to about ten nanometers should eventually permit to follow a single enzyme activity.

In order to study one-single enzyme kinetics the very faint signal of the enzyme needs to be amplified. After CalB hydrolysis of p-aminophenyl acetate (pAPA) an electro-inactive substrate to p-aminophenol (pAP) the electro-active product the red-ox couple pAPA/pAP will be continuously recycled between two electrodes amplifying the single enzymatic initial event. Kinetics parameters of pAPA hydrolysis by CALB determined spectrophotometrically and electrochemically are in good agreement. This supports the suitability of pAPA for AFM/SECM single enzyme studies.

In order to control the distribution of enzymes on the electrode we will use virus capsids as Enzyme Nano-Carriers (ENCs). To this aim, two plant viruses, Tobacco mosaic virus (TMV) and potato virus A (PVA) will be tested. Three different strategies will be attempted for the virus to enzyme interfacing: the fusion of leucine zipper (LZ) pairs to enzymes and capsomers, bi-specific antibodies and peptides obtained from phage display screening.

Regarding the first strategy, three pairs of LZ having different characteristics in term of length, affinity and orientation have been selected and the cloning at the N- and C- terminus of CalB is in progress. One assembly CalB (LZKg-CalB) was expressed in *Escherichia coli* periplasm and we are currently optimizing its purification.

Monoclonal antibodies for CalB have been produced and fusion with antibodies for TMV and PVA will be attempted.

As third strategy, three peptides were selected that recognize PVA. Cloning at the N-terminus of CalB and GOX is in progress.

PLANT VIRUS PARTICLES AS NANOSCAFFOLDS FOR CONTROLLED POSITIONING OF ENZYME CASCADES ON SOLID SUPPORTS

Noëlle Carette¹, Daniela Cardinale¹, Jane Besong², Thierry Delaunay¹, Agathe Urvoas³, Christophe Thibault⁴, Jocelyne Walter¹, Amandine Barra¹, Philippe Minard³, Christophe Vieu⁴, Kristiina Mäkinen² and Thierry Michon¹

¹INRA, UMR BFP, Laboratoire de virologie végétale, 71, Avenue Edouard Bourlaux 81BP, 33883 Villenave d'Ornon, France

²University of Helsinki, Applied Biochemistry and Molecular Biology, Department of Food and Environmental Sciences, P.O.Box 27 (Street: Latokartanonkaari 11), Finland

³Université Paris Sud, Institut de Biochimie et de Biophysique Moléculaire et Cellulaire, Laboratoire de Modélisation et d'Ingénierie des Protéines, UMR8619, Bât 430, 91405 Orsay, France

⁴LAAS-CNRS, 7, avenue du Colonel Roche, 31077, Toulouse Cedex 4, France

ncarette@bordeaux.inra.fr

In the cell, the close spatial location of enzymes catalyzing consecutive reactions increases the metabolic pathways efficiency, the product of an enzyme becoming substrate of the next enzyme (diffusion limitation or channeling). We intend to design an experimental platform mimicking this enzyme organization to determine the parameters controlling the cascade reactions. If demonstration is made that a precise positioning of enzymes catalyzing consecutive reactions gives a net advantage upon diffusion controlled processes, the project's outcomes will serve the technology of enzymatically assisted catalysis in organic synthesis with potential applications for the technology of microreactors and biosensors.

Our first goal consists in controlling the distribution of active enzymatic systems on solid supports. The systems concerned are constituted of several enzymes catalyzing a cascade of up to 3 consecutive reactions.

Virus particles are precisely defined nanometer-sized objects, well-ordered, formed by a self-association of capsid proteins monomers. These particles will be used as Enzymes Nano -Carriers (ENCs). Subsequently these ENCs can be finely positioned on solid supports using nanolithography techniques. The rod shaped tobacco mosaic virus (TMV) and the flexuous filamentous potato virus A (PVA) were chosen as ENCs.

Candida Antarctica lipase B (CALB), glucose oxidase (GOx) and horseradish peroxidase (HRP) were chosen as demonstrating enzymes. Three strategies are under investigation for enzymes to virus interfacing.

The first strategy consists in introducing complementary leucine zippers (basic and acid) peptides on TMV (or PVA) and enzymes. We are trying to produce engineered TMV *in planta*. The surface of TMV being negative, acidic leucine zipper (LZecoil) was genetically introduced at the C-terminus part of the capsid protein within the virus genome. A weak systemic infection of *Nicotiana benthamiana* plants by TMV-LZecoil was observed (2 plants/24). The virus progeny eliminated the LZecoil insert in inoculated leaves 15 days after inoculation. Engineered PVA like particles will be reconstituted from an N-terminus fusion between acidic leucine zippers and capsid proteins expressed in *Escherichia coli*.

A second approach consists in the selection by M13 phage display of peptides which present an affinity for the virus surface (TMV or PVA). The sequence of these peptides will be genetically introduced at the N-terminus part of the enzymes.

Three peptide sequences were found to have a specific affinity for PVA particles; their genetic fusion to the enzymes is in progress.

In a third approach, bispecific antibodies will be selected to insure the coupling between virus particles and enzymes. A selection of monoclonal antibodies against either the viruses (TMV, PVA) or the enzymes (CALB, HRP) is in progress. Then a fusion of the cells producing each monoclonal antibody will be attempted.

CELL PENETRATING PEPTIDE-SUPERPARAMAGNETIC IRON OXIDE NANOPARTICLE CONJUGATES AS BIMODAL IMAGING NANOAGENTS

Silvia Cavalli, Daniel Carbajo, Miriam Royo, Fernando Albericio

CIBER-BBN, Networking Centre on Bioengineering, Biomaterials, and Nanomedicine. Barcelona Science Park, Institute for Research in Biomedicine, Baldiri Reixac 10, 08028 Barcelona, Spain.

silvia.cavalli@irbbarcelona.org

Molecular imaging has attracted more and more attention in the past decades. There is a strong interest in developing and validating imaging technologies such as fluorescence imaging and magnetic resonance (MR) to image biological target in vivo. Exploiting the intrinsic properties of superparamagnetic iron oxide nanoparticles (SPION) could result in obtaining medical breakthroughs in diagnosis and therapy. SPION can be used as magnetic contrast agents in magnetic resonance imaging (MRI) as well as hyperthermia agents, where the magnetic particles are heated selectively by application of an high frequency magnetic field (i.e. in thermal ablation/hyperthermia of tumors) or as magnetic vectors that can be directed by means of a magnetic field gradient towards a certain location, such as in the case of the targeted drug delivery. [1] Cell penetrating peptides have been used to increase cellular uptake of these nanoparticles. As an example HIV-1 Tat protein-derived peptide sequences, in particular GRKKRRQR48-57, have been extensively used as an efficient way of increasing internalization into cells. [2]

In this project we developed a bioorthogonal chemical approach [3] to functionalize SPION with a new class of cell-penetrating peptide, cis-g-amino-proline derived peptides, previously developed in our group. [4] A schematic representation of the general approach is shown in Figure 1. Commercially available amino-functionalized SPION (SPION-NH₂) were partially modified with a reacting group (blue triangle, SPION-RG). Fluorescent labelled cell penetrating peptides, previously modified with a complementary reacting group (yellow triangle), were subsequently conjugated to SPION-RG exploiting bioorthogonal chemical reactions that occurred in buffer media close to physiological conditions. A Tat sequence, modified as described above, was included in the study as positive control for cellular uptake, while acetylated peptides were used as negative controls for proving the occurrence of the ligation. An advantage of this approach is that crude peptides could be used during the conjugation thanks to the high chemoselectivity of the reaction. Purification occurred during dialysis of the final nanoconjugate samples.

This study comprised of a synthetic part, in which the peptide-nanoparticle conjugates were prepared and characterized, followed by biological studies conduced to evaluate their cellular uptake and toxicity. In Figure 2 confocal laser microscopy confirmed internalization into HeLa cells of the SPION-CCP obtained by the conjugation of a cis-g-amino-proline derived peptide. Currently, we are performing MRI investigations to validate such new nanodevices as novel bimodal contrast agents for optical imaging as well as MRI.

References:

- [1] a) M. J. Kogan, I. Olmedo, L. Hosta, A. R. Guerrero, L. J. Cruz and F. Albericio, *Nanomedicine*, 2 (2007), 287. b) M. Arruebo, R. Fernández-Pacheco, M. R. Ibarra, J. Santamaría, *Nanotoday*, 2 (2007), 22. c) C. Carot, P. Robert, J.-M. Idée, M. Port, *Adv. Drug Delivery Rev.*, 58 (2006), 1471.
- [2] M. Lewin, N. Carlesso, C.-H. Tung, X.-W. Tang, D. Cory, D. T. Scadden, R. Weissleder, *Nature Biotechnology*, 18 (2000), 410.
- [3] E. M. Sletten, C. R. Bertozzi, *Angew. Chem. Int. Ed.*, 48 (2009), 6974.
- [4] J. Farrera-Sinfreu, E. Giralt, S. Castel, F. Albericio, M. Royo, *J. Am. Chem. Soc.* 127 (2005), 9459.

Figures:

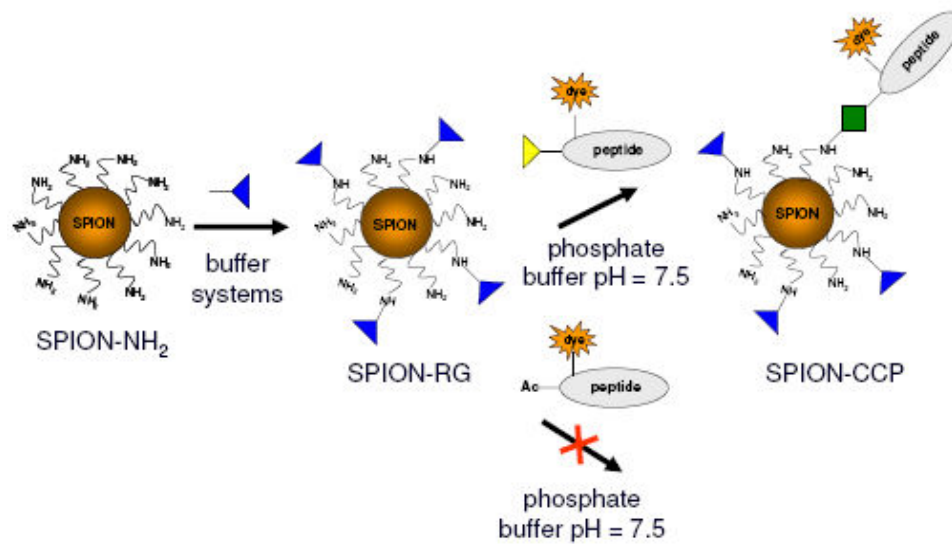


Figure 1: Schematic representation of the general approach.

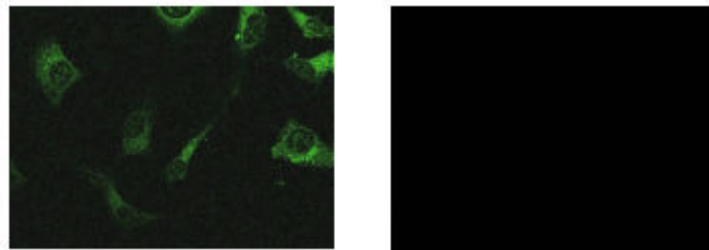


Figure 2: Confocal laser microscopy images of HeLa cells incubated with 1 μ M concentration of SPION-CCP sample (left panel) and negative control with SPION-FG + AcCCP (right panel).

VIBRATIONAL SUM-FREQUENCY GENERATION SPECTROSCOPY OF SELF-ASSEMBLED AND LANGMUIR-BLODGETT FILMS ON SURFACES: FROM MONOLAYERS TO MODEL LIPID MEMBRANES

Francesca Cecchet, Julien Guthmuller, Benoit Champagne, Yves Caudano, André Peremans, and Dan Lis

Laboratory of Lasers and Spectroscopy (LLS), Research Centre in Physics of Matter and Radiation (PMR), Laboratory of Theoretical Chemistry, FUNDP - University of Namur, Belgium
francesca.cecchet@fundp.ac.be

Investigating the structure and the physico-chemical properties of biomimetic lipid membranes on surfaces is a pre-requisite for a detailed investigation of biological processes occurring within such bio-films, and their selective detection. This also represents a platform to build-up reliable bio-devices mimicking the membrane behaviour. Indeed, the structure and the physico-chemical properties of thin films on surfaces are intrinsically linked. Knowing the organization of organic layers on surfaces is therefore a key element to understand, to control and to tailor their physical, chemical, or biological properties. This requires highly surface/interface sensitive techniques which are able to discriminate interfacial responses from those of the surrounding bulk phases.

The analysis of the physico-chemical properties of bio-interfaces can be achieved by probing their vibrational response. Among the vibrational spectroscopies, sum-frequency generation (SFG) has emerged in the characterization of thin organic layers adsorbed on surfaces [1,2,3]. Indeed, being based on a second order nonlinear optical process, SFG spectroscopy is intrinsically specific to surfaces and interfaces [1,2,3], and therefore it represents an ideal tool to probe organic layers confined at solid surfaces.

In this work, the vibrational signature of (bio)-organic films mimicking the membrane structure has been in order to retrieve information about their structural organization and their molecular orientation. In particular, self-assembled monolayers (SAMs) of thiols (Figure 1a), and solid-supported lipid layers, either in the form of monolayers (Figure 1b), or in that of hybrid bilayers (Figure 1c), have been investigated by SFG spectroscopy (Figure 1, top).

Firstly, we have focused on the analysis of self-assembled monolayers (SAMs) of alkane and of aromatic thiols [4,5], which are models for the interpretation of the vibrational nonlinear optical response of more complex architectures mimicking the lipid membranes. Secondly, we have probed the organization of solid-supported lipid films, prepared either by vesicle fusion or by Langmuir-Blodgett and Langmuir-Schaeffer methods on bare or pre-functionalized substrates. Different lipid molecules have been used to build the model membranes, such as the well-known phosphatidylcholine lipid (PC) or the less-known antigenic 2,4-dinitrophenyl lipid (DNP) [6]. Information about the lipid films order and organization has been obtained, and has indicated that the intimate film organization, which is probed through the analysis of the SFG signature of the lipid hydrophobic chains, strongly depends on the molecular composition and on the surface properties. The SFG responses have been interpreted with the support of DFT calculations, and of experimental measurements of the solid-state IR and Raman activities. This has enabled to predict the SFG active modes of the (bio)-organic films, and therefore to attribute, with high accuracy, the detected signals to vibrational motions.

This analysis is performed in the framework of investigating the structural changes and the physico-chemical interactions induced by recognition processes, which take place within such interfacial layers.

In particular, the high interface/surface sensitivity of SFG spectroscopy may open the way to novel solutions for the detection of biological processes occurring within surface-confined (bio)-organic films.

References:

- [1] Shen Y.R., Nature 337 (1989) 519.
- [2] Roke, S. ChemPhysChem 10 (2009) 1380.
- [3] Chen X., Clarke M.L., Wang, J., Chen Z. Intern. J. Mod. Phys. B 19 (2005) 691.
- [4] Cecchet, F., Lis D., Guthmuller J., Champagne B., Caudano Y. Silien, C., Mani A.A., Thiry P., Peremans A. ChemPhysChem 11 (2010) 607.
- [5] Cecchet, F., Lis D., Guthmuller J., Champagne B., Fonder G., Mekhalif Z., Caudano Y., Mani A.A., Thiry P., Peremans A. J. Phys. Chem. C 114 (2010) 4106.
- [6] Lis D., Guthmuller J., Champagne B., Humbert C., Busson B., Tadjeddine A., Peremans A., Cecchet F. Chem. Phys. Lett. 489 (2010) 12.

Figures:

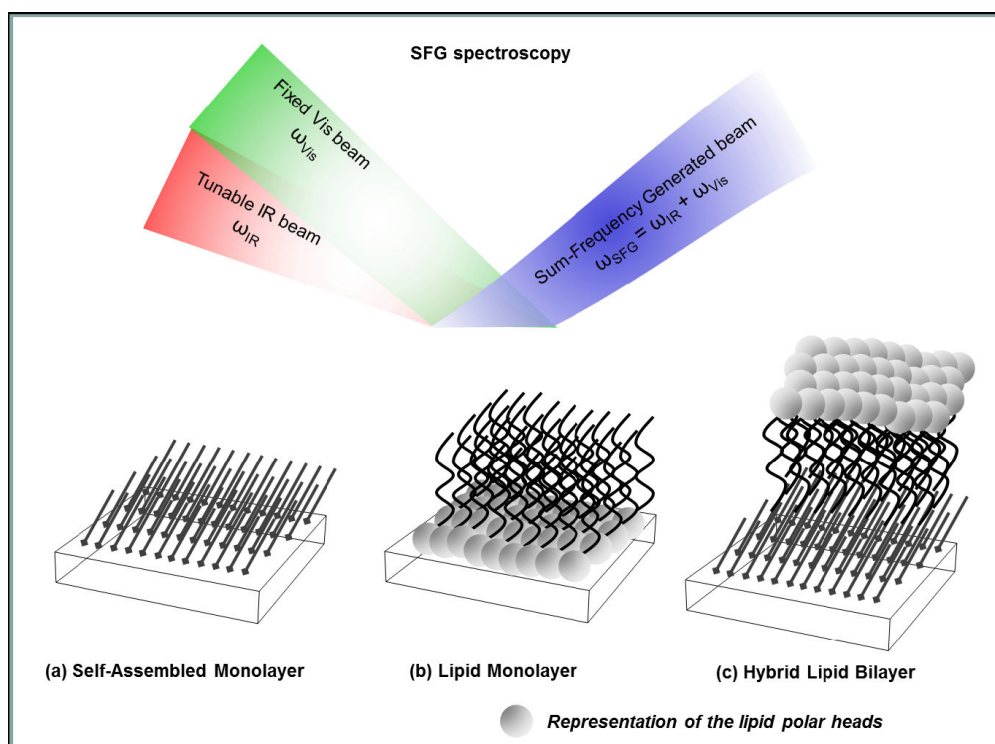


Figure 1: Schematic representation of the SFG spectroscopy (top), and modeling of the (bio)-organic films which are investigated, namely Self-Assembled Monolayers (a), Lipid Monolayers (b), and Hybrid Lipid Bilayers (c).

**FROM MOLECULAR WIRES TO ORGANIC SEMICONDUCTORS AND BACK - SOME
"DON'T ASK, DON'T TELL" OF SOFT ELECTRONICS**

Gianaurelio Cuniberti

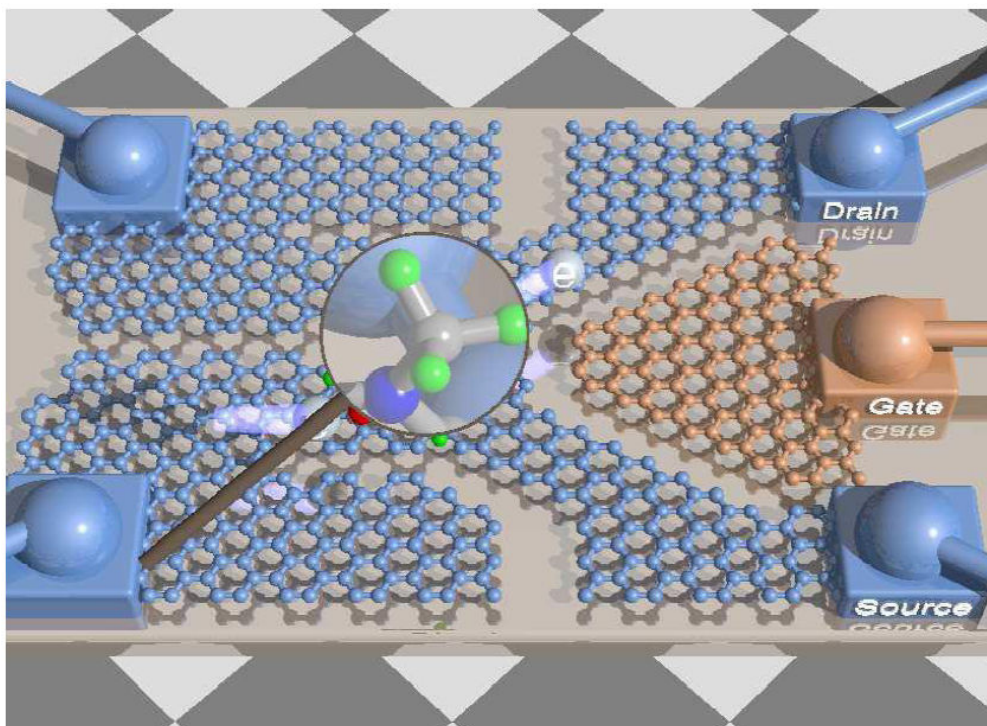
Institute for Materials Science and Max Bergmann Center for Biomaterials,
Dresden University of Technology, 01062 Dresden, Germany

g.cuniberti@tu-dresden.de

Charge migration is a ubiquitous phenomenon with profound implications throughout many areas of chemistry, physics, biology and materials science. The long-term vision of designing functional materials with pre-defined molecular scale properties has triggered an increasing quest to identify prototypical systems where truly inter-molecular conduction pathways play a fundamental role. Such pathways can be formed due to molecular organization of various organic materials and are widely used to discuss electronic properties at the nanometer scale. Many of the mechanisms of charge migration in soft matter nanosystems are common to single molecule electronics and organic electronics. In this talk I will illustrate how recent important contributions of unimolecular electronics research can crossfertilize the field of organic electronics and vice versa how the recent breakthrough in engineering molecular materials in organic semiconductor could inspire new developments in molecular electronics.

References:

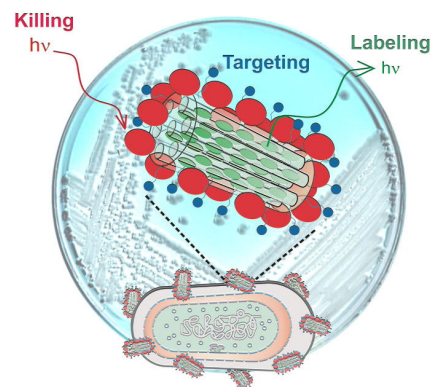
- [1] C. Gollub et al., Charge migration in organic materials: Can propagating charges affect the physical quantities controlling their motion?, preprint
- [2] T. Kawai et al., Mechanically-induced transport switching effect in graphene-based nanojunctions, preprint
- [3] H. Kleemann et al., Organic Zener Diodes: Tunneling across the gap in organic semiconductor materials, *Nano Letters*, 2010, 10, 4929.
- [4] R. Gutierrez et al., *Physical Review Letters* 2009, 102, 208102.
- [5] D. Dulic et al., *Angewandte Chemie International Edition* 2009, 48, 8152.



Luisa De Cola

Westfälische Wilhelms-Universität, and CeNTech, Mendelstr. 7, 48149 Münster, Germany
decola@uni-muenster.de

The creation of molecular (nano)containers: crystalline or amorphous, rigid or soft is a very fascinating field at the cross point of different disciplines. Our effort, in this talk, focuses on the synthesis and use of crystalline materials, zeolites L, which are transparent, stiff, nanocontainers. They are made of hundreds of parallel aligned unidimensional channels, which can be filled with molecular dyes or other responsive molecules. The selective and spatial resolved functionalization of these nanocontainers can lead to multifunctional systems [1]. Furthermore the selective functionalization of the channel entrances, lead to the self-assembly of the zeolites, and the assembly process can be extended to living organism such as bacteria [2]. The use of appropriate light responsive components in combination with the smallest zeolites (30 nm) has been very successfully applied for the labeling targeting and killing of antibiotic resistant bacteria (see figure) [3].



Finally we have realized hierarchical supramolecular organization by optical control of nano-containers that contain highly ordered molecules. Holographic optical tweezers allow for precise, exible, and dynamic 3D position and orientation control of arbitrary shaped multiple container particles. [4].

References:

- [1] M. Busby, H. Kerschbaumer, G. Calzaferri, L. De Cola *Adv. Mat.* 2008, 20, 1614
- [2] Z. Popovic, M. Otter, G. Calzaferri, L. De Cola, *Angew. Chem. Ind.Ed.*, 2007, 46, 6188. Z. Popovic, L. De Cola et al. *Angew. Chem., Ind. Ed.* 2007, 46, 8898.
- [3] C. Strassert, M. Otter, R. Albuquerque, A. Höne, Y. Vida, B. Maier, L. De Cola *Angew. Chem. Int. Ed.* 2009, 48, 7928.
- [4] M. Woerdemann, S. Gläsener, F. Hörner, A. Devaux, L. De Cola, C. Denz *Adv. Mat.*, 2010, 22, 4176; *OPN Optics & Photonics News*, 2010, 21, 40.

J.M. De Teresa^{1,2}, R. Córdoba^{2,3}, A. Fernández-Pacheco^{1,2,3}, L. Serrano^{1,2}, F. Schoenaker¹,
M.R. Ibarra^{1,2,3}

¹Inst de Ciencia de Materiales de Aragón, Universidad de Zaragoza-CSIC, Zaragoza, 50009, Spain

²Departamento de Física de la Materia Condensada, Universidad de Zaragoza, 50009, Spain

³Instituto de Nanociencia de Aragon, Universidad de Zaragoza, Zaragoza, 50018, Spain

deteresa@unizar.es

Many working devices in the field of nanotechnology rely on the top-down approach for their creation. This implies the use of thin-film growth techniques in tight cooperation with micro- and nanolithography techniques. The method of choice should address crucial aspects such as resolution, roughness, shape, materials involved, cost, etc. Optical lithography is normally preferred down to the micron scale and electron-beam lithography below the micron scale. However, some of the involved steps are critical and the final sample nanometric features can be far from ideal. In order to circumvent the annoying use of resists, direct patterning by focused-ion-beam is not rare, but this technique can strongly modify the properties of the materials, restricting its use. It is in this context that focused electron-beam-induced-deposition (FEBID) and focused-electron-beam-induced-etching (FEBIE) techniques are becoming promising routes for the direct growth or patterning of functional nanostructures in a single step. These techniques do not involve the painful use of resists, etching or lift-off processes, whereas maintaining the high lateral resolution down to the nanometric scale. In the present contribution, we will show successful examples of the use of FEBID and FEBIE for the creation of functional nanostructures. The deposition or etching experiments have been carried out by means of a field-emission-gun scanning electron microscopy (SEM) and gas injectors which permit to deliver precursor gas to the area of interest.

Cobalt-based nanostructures have been grown by FEBID using $\text{Co}_2(\text{CO})_8$ as the precursor gas on Si substrates or insulating Si//SiO₂ substrates. Our previous work has shown that Co by FEBID can be grown with high purity, showing remarkable properties for applications in magnetic sensing, storage and logic [1-4]. In the present contribution we show the successful growth of cobalt nanowires with lateral size down to 30 nm, which could be used for highly-integrated domain-wall manipulation. Besides, for the application in Hall sensing, we have grown Co squares with lateral size around 100 nm plus narrower contact lines to permit injection of current from opposite edges of the square and measurement of voltage from the remaining two contacts.

Titanium is a relevant technological material due to its extraordinary mechanical and biocompatible properties, its nanopatterning being an increasingly important requirement in many applications. We report the successful nanopatterning of titanium by means of Focused Electron Beam Induced Etching using XeF_2 as a precursor gas [5]. Etch rates up to $1.25 \times 10^{-3} \mu\text{m}^3 \text{s}^{-1}$ and minimum pattern sizes of 80 nm were obtained. Different etching parameters as beam current, beam energy, dwell time and pixel spacing are systematically investigated, the etching process being optimized by decreasing both beam current and beam energy.

References:

- [1] A. Fernández-Pacheco et al, J. Phys. D : Appl. Phys. 42, 055005 (2009).
- [2] A. Fernández-Pacheco et al, Appl. Phys. Lett. 94, 192509 (2009).
- [3] A. Fernández-Pacheco et al, Nanotechnology 20, 475704 (2009).
- [4] S. Sangiao et al, Solid State Communications 151, 37 (2011).
- [5] F. Schoenaker et al, submitted to Nanotechnology (2011).

Figures:

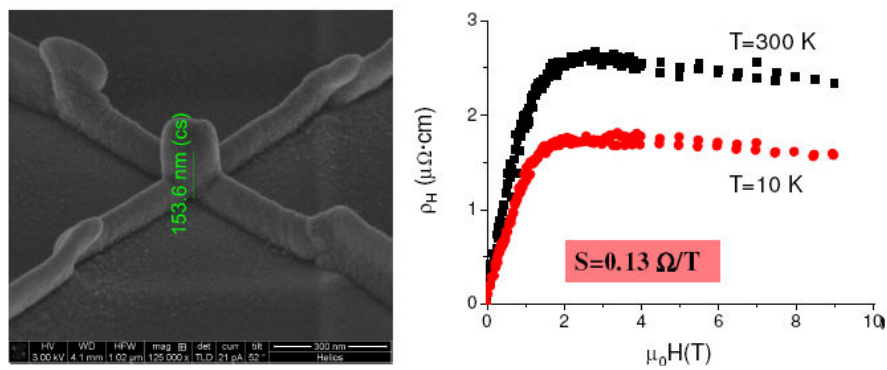


Figure 1: One of the grown Hall devices based on Co by FEBID and its Hall characterization.

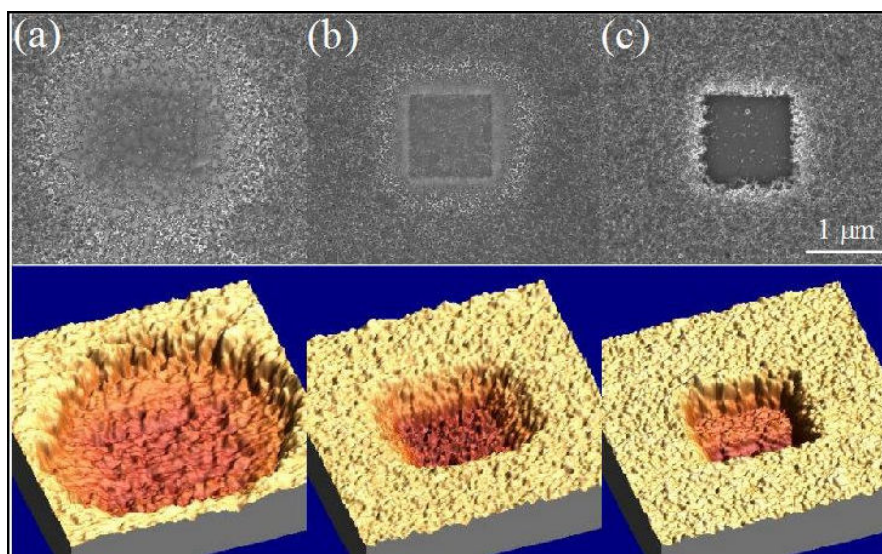


Figure 2: SEM (top) and AFM (bottom) images of Ti etchings made with 2 kV electron beam energy and different beam currents and etching times. (a) Beam current of 1.35 nA and a 30 s etching time. (b) Beam current of 318 pA and a 105 s etching time. (c) Beam current of 5.4 pA and a 600 s etching time.

DIRECT NEAR-FIELD STUDY OF GENERATION, COUPLING, PROPAGATION AND DESIGN OF SURFACE PLASMONS POLARITONS IN THE MID-INFRARED

Y. De Wilde¹, A. Babuty¹, I. Moldovan-Doyen¹, L. Greusard¹, R. Rungswang¹, J.-P. Tetienne², D. Costantini², A. Bousseksou², R. Colombelli², G. Beaudoin³ and I. Sagnes³

¹Institut Langevin, ESPCI ParisTech, CNRS, 10 rue Vauquelin, 75231 Paris Cedex 05, France

²Institut d'Electronique Fondamentale, Université Paris Sud and CNRS, 91405 Orsay, France

³CNRS/LPN, Laboratoire de Photonique et de Nanostructures, 91460 Marcoussis, France

yannick.dewilde@espci.fr

Scattering-type near-field optical microscopy (sNSOM) uses the tip of an atomic force microscope to scatter the electromagnetic near-field towards a detector located in the far-field. Recording the scattered near-field as a function of the position of the tip while it is scanned over the sample surface, allows one to obtain an optical image of the scanned area with subwavelength resolution, at the same time as its topography is recorded. As the scattered light propagates in free space, sNSOM can be applied at any wavelength. Application of sNSOMs at low photon energies such as mid-infrared and terahertz wavelengths is the nanoscale observation of the dielectric contrast between materials [1], or the mapping of the spatial distribution of evanescent waves at the surface of waveguides or devices [2].

Surface plasmons polaritons (SPPs) are propagating electromagnetic modes bound at the interface between a metal and a dielectric, which originate from electron oscillation in the metal. These electromagnetic waves are evanescent in the direction perpendicular to the interface, while they can propagate in a direction parallel to it. sNSOM is a unique tool to perform direct imaging with subwavelength resolution of SPPs propagating on metal surfaces. In this talk, we will give an overview of our recent sNSOM investigations of various types of plasmonic devices which are active, in the sense that they use a mid infrared (midIR) quantum cascade laser (QCL) as an electrical generator of SPPs [3,4].

Due to their dispersion relation, the generation of SPPs generally requires the use of a prism or a grating combined with an external laser source. In situ generation is clearly required to produce compact integrated SPPs devices. We have achieved this goal in a device operating at $\lambda \approx 7.5 \mu\text{m}$ which includes all the building blocks required for a fully integrated plasmonic active source: an electrical generator of SPPs based on a 1st order distributed feed-back (DFB) metal grating at the surface of the laser cavity, a grating coupler, and a passive metallic waveguide. We have demonstrated the operation of the device by reproducing the analogue in the near-field of the slit-doublet experiment, using the sNSOM to observe directly the standing wave pattern which is formed in the near-field on the passive section of the device, due to the interference of two counter-propagating SPPs [3]. An alternative method to inject SPPs on a passive waveguide is end-fire coupling, which we have used to generate SPPs on a flat metallic strip from the end facet of a QCL at $\lambda \approx 7.5 \mu\text{m}$. We demonstrate the propagation of SPPs at distances of several hundreds of micrometers from the end facet of the laser via both far-field and near-field imaging techniques [4]. At midIR wavelength, SPPs propagating on a flat gold surface have a decay-length (perpendicular to the gold surface) of tens of micrometers [4]. The “designer’s” or spoof SPPs allow one to dramatically change this behavior by artificially designing the dispersion relation using structured surfaces [5]. The idea is to mimic at IR wavelengths features which in principle are observed at shorter wavelength, and which result in an enhanced confinement of the SPPs at the surface [5,6]. We have achieved this by replacing the flat surface of the SPPs waveguide by a properly designed sub-wavelength metallic groove grating. Increasing the groove depth results in an increased in-plane wavevector and, therefore, long wavelength spoof SPPs have a shorter decay-length and can be manipulated just as their short wavelength counterpart. Based on sNSOM imaging, we demonstrate curved spoof SPPs trajectories and we present our progress towards the realization of a sub-wavelength-sized “hot spot” where local field enhancement occurs (7).

We acknowledge financial support from the French National Research Agency (ANR-07-NANO-039 “NanoFtir” and ANR-09-NANO-020 “Gospel”) and from the Centre de compétences NanoSciences Ile-de-France (Project PSTS).

References:

- [1] B. Knoll and F. Keilmann, "Near-field probing of vibrational absorption for chemical microscopy", *Nature* 399, (1999) 134.
- [2] V. Moreau, M. Bahriz, R. Colombelli, P-A. Lemoine, Y. De Wilde, L.R. Wilson, and A.B. Krysa, "Direct imaging of a laser mode via mid-infrared near-field spectroscopy", *Appl. Phys. Lett.* 90, (2007) 201114.
- [3] A. Babuty, A. Bousseksou, J-P. Tetienne, I. Moldovan Doyen, C. Sirtori, G. Beaudoin, I. Sagnes, Y. De Wilde, R. Colombelli, "Semiconductor Surface Plasmon Sources", 104, (2010) 226806.
- [4] J.-P. Tetienne, A. Bousseksou, D. Costantini, R. Colombelli, A. Babuty, I. Moldovan-Doyen, Y. De Wilde, C. Sirtori, G. Beaudoin, L. Largeau, O. Mauguin, and I. Sagnes, "Injection of midinfrared surface plasmon polaritons with an integrated device", *Appl. Phys. Lett.* 97, (2010).211110.
- [5] J. B. Pendry, L. Martín-Moreno, and F. J. García-Vidal, "Mimicking Surface Plasmons with Structured Surfaces", *Science* 305, (2004) 847.
- [6] A. I. Fernandez-Dominguez, C. R. Williams, F. J. García-Vidal, L. Martín-Moreno, S. R. Andrews and S. A. Maier, "Terahertz surface plasmon polaritons on a helically grooved wire", *Appl. Phys. Lett.* 93, (2008).141109.
- [7] M. I. Stockman, "Nanofocusing of Optical Energy in Tapered Plasmonic Waveguides", *Phys. Rev. Lett.* 93, (2004) 137404.

Figures:

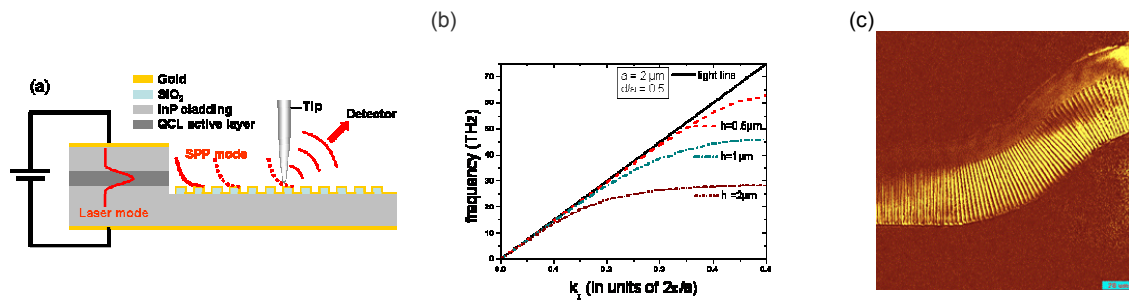


Figure 1: (a) Schematic cross section of a spoof SPPs device using a mid IR QCL as generator, and schematic view of the sNSOM detection; (b) Dispersion relation of spoof SPPs corresponding to a metal grating with a pitch of $2 \mu\text{m}$, duty cycle 0.5, and depth h ; (c) sNSOM image measured on a curved spoof SPPs waveguide.

INTERNALISATION MECHANISMS OF MODIFIED TITANIUM OXIDE NANOPARTICLES IN SKIN CELLS AND MULTICELLULAR LIVING SPECIMENS: RESULTING TOXICITY

M.H. Delville¹, M. Simon², A. Girard^{1,2}, P. Barberet², P. Moretto²,
H. Seznec², D. Dupuy³

¹CNRS, Université de Bordeaux, ICMCB, 87 avenue du Dr. A. Schweitzer,
Pessac, F-33608 Cedex, France

²Université Bordeaux, CNRS/IN2P3, Centre d'Etudes Nucléaires de Bordeaux

³Gradignan, CENBG, Chemin du Solarium, BP120, 33175 Gradignan, France

Institut Européen de Chimie et Biologie, Univ Bordeaux 1, 2 rue R. Escarpit, 33607 Pessac, France
delville@icmcb-bordeaux.cnrs.fr

Nanotechnologies are of great interest from both academic and industrial points of view, with numerous applications in domains such as medicine, catalysis and material sciences. However, their nanotoxicology has also attracted the attention of public and governments' worldwide and established methods of chemical safety assessments have to be modified to address the special characteristics of nanoparticles and more especially to assess the biological effects of these highly reactive materials.

Most of these manufactured nanoparticles have been produced for several decades on an industrial scale. There is an urgent need to evaluate the risks of these particles to ensure their safe production, handling, use, and disposal. Moreover, a comprehensive study is clearly needed to fully explore the toxicity of manufactured nanoparticles, which may help to better understand their deleterious health effects and create environmentally friendly and biologically relevant nanoparticles. In particular, the behavior of nanoparticles inside living cells is still an enigma, and no metabolic responses induced by these particles are understood so far.

This presentation concerns the potential toxicity due to exposure of TiO₂ NPs used in sunscreens and cosmetics. We propose to apply an original imaging methodology (Ion Beam Analysis, TEM, and Confocal microscopy) to in vitro studies, combining technologies for on one hand, the detection, tracking, and quantification of TiO₂ nanoparticles and on the other one, the use of indicators for ion homeostasis, cell metabolism, or cell fate.

The main goal is to precisely identify the molecular and cellular mechanisms involved in the nanotoxicity of TiO₂ nanoparticles in eukaryotic cells and in multi-cellular organisms such as *Caenorhabditis elegans* (*C. elegans*). This study addresses the current knowledge gap of human cells and *C. elegans* responses to TiO₂ nanoparticles exposure. Since the nematodes feed on bacteria and are considered as particle-ingesting organisms, the present study will offer new perspectives in nanoparticles-related risk assessment and food web accumulation modelling.

References:

- [1] Marina Simon, Philippe Barberet, Marie-Hélène Delville, Philippe Moretto, Hervé Seznec Nanotoxicology on line 07/15/2010.

ROLE OF THE SURFACE ELECTRONIC STRUCTURE IN THE ENHANCEMENT OF QUANTUM FRICTION BETWEEN PARALLEL SILVER SLABS

Vito Despoja^{1,2}, Pedro M. Echenique¹, Marijan Sunjic^{1,2}, and V. M. Silkin¹

¹Donostia International Physics Center (DIPC), P. Manuel de Lardizabal,
20018 San Sebastian, Basque Country, Spain and

²Department of Physics, University of Zagreb, Bijenicka 32, HR-10000 Zagreb, Croatia

In the framework of the recent debate [1, 7] about the existence and formulation of quantum friction between two moving metallic slabs, we provided a new, more efficient formulation and applied it to the investigation of the role of realistic electronic structure to friction between two silver slabs in relative motion. The results are compared with those of the Drude and jellium models. We show that low energy electronic excitations play a dominant role in the description of quantum friction, i.e. that the Drude model, because of the absence of low energy electronic excitations, is a completely inappropriate model in the description of friction phenomena. On the other hand, the jellium model, because of the absence of surface states (which reduce low energy electron hole intensity), and absence of low energy surface plasmons [9], gives a significant reduction of the frictional force. We show that in the range $0 < v < v_F$, the friction force shows an v^α dependence whereas in the jellium model $\alpha = 3$ and for a realistic model potential [10] $\alpha = 4$. Because quantum size effects strongly modified low energy electronic excitations [8], we provided an analysis of quantum friction as function of slab thicknesses.

References:

- [1] J. B. Pendry, J. Phys.: Condens. Matter 9 10301 (1997)
- [2] B. N. J. Persson, Phys. Rev. B 57, 7327 (1997)
- [3] A. I. Volokitin, B. N. J. Persson, Phys. Rev. B 78, 155437 (2008)
- [4] J. B. Pendry, New J. Phys. 12, 033028 (2010)
- [5] T. G. Philbin, U. Leonhardt, New J. Phys. 11 033035 (2009)
- [6] U. Leonhardt, New J. Phys. 12, 068001 (2010)
- [7] J. B. Pendry, New J. Phys. 12, 068002 (2010)
- [8] V. M. Silkin, M. Alducin, J. I. Juaristi, E. V. Chulkov and P. M. Echenique, J. Phys.: Condens. Matter 20 (2008) 304209
- [9] B. Diaconescu, et al, Nature 448, 57-59 (2007)
- [10] E. V. Chulkov, V. M. Silkin and P. M. Echenique, Surf. Sci. 437, 330 (1999)

Jean-Marie Devoisselle, Syvie Bégu, Anne Aubert-Pouessel, Corine Tourné-Péteilh,
Philippe Legrand, D. Tichit, Bruno Alonso, Lydie Viau, A. Vioux

Institut Charles Gerhardt Montpellier, UMR CNRS/UM2/ENSCM/UM1 5253
U.F.R. des Sciences Pharmaceutiques et Biologiques
15 ave Ch. Flahault, BP14491, 34093 Montpellier, France
jm.devoisselle@univ-montp1.fr

Nanotechnology represents a new field of research and includes a wide range of technologies and potential applications. One approach consists on creating new materials which are structured at the nanoscale using sol-gel chemistry. Such materials could be of different pore size or morphology. Nanostructured silicas such as Micelle-Templated Silicas (MTS) materials feature unique textural properties owing to their uniform distribution of mesopores with tunable sizes. Since 2002, we have developed a synthesis strategy to control the particle morphology of MTS at the micro- to millimeter scale. Concerning drug delivery systems, we have evaluated the ability of such mesoporous materials for hosting a non-steroidal anti-inflammatory drug (ibuprofen). Different procedures were evaluated: impregnation of calcined mesoporous materials[1], direct synthesis and drug grafting[2]. We show that it is possible to incorporate ibuprofen in MTS in a range compatible with poorly soluble drugs. The release depends on the way ibuprofen is incorporated. Fast release is observed for the “impregnation” and the “direct synthesis” methods that may indicate that ibuprofen is in a molecular state[3]. We have chosen a second direction that allows in fully investigating the potentialities of sol-gel, self-assembly and spray-drying processes in order to form directly new textured materials acting as DDS with tuneable properties. Spray-drying bears also the advantage of being a scalable process and reducing the number of steps. Furthermore we consider a one-pot synthesis in which organometallic oligomers, drug and surfactant molecules are mixed together in solution. During spray-drying of the solutions, these chemicals interact together, eventually phase-separate inside the droplets and form the final microspheres. Here, we particularly show how a simple tuning of the drug and the surfactant contents can lead to very different drug dispersions at the nanometre scale, and consequently to very different drug release profiles[4]. Finally, we proposed a novel approach to confine drugs in mesoporous silica materials. We first prepared a new ionic liquid ([BMIm][Ibu]) where the drug (Ibuprofenate) is the anion and used this new IL to prepare ionogels. Their silica walls could be functionalized to control the drug release[5].

Another example of nanostructured silica materials as DDS is given by the preparation and release property of hybrid lipid/silica materials. First, we have adapted a typical two-step room-temperature MTS (micelle-templated silica) preparation in which the colloidal solution of amphiphiles is replaced by small unilamellar liposomes[6]. The result is the formation of silica shell nanospheres with non-porous walls and a narrow size distribution. We show that kinetic releases of a hydrophilic fluorescent probes depend on the lipid composition of liposomes. The use of zwitterionic phospholipids (non toxic) as templates requires a modified approach since the liposome structure is sensitive to low pH, high ionic strength. The silica growth is directed by the receptiveness of the quaternary ammonium surface of the phospholipid to the silica. We have also advanced this original report in a number of ways. We have reduced the cluster-like particle aggregation into chain-like aggregates of particles by the use of PEGylated phospholipid. We extended the liposil's shell nature to include hydrophobic modifications. We showed the feasibility of the triggered release of the encapsulated content with two types of remote energy sources[7]. Finally, a new supra-organized hybrid material obtained in “green” conditions via anionic exchange of self-assembled unilamellar anionic liposomes with the nitrate ions present in the interlayers of layered double hydroxides (LDH), is fully characterized[8]. This material presents original properties linked to the simultaneous presence of a phospholipid bilayer derived from liposomes, still used as vectors for lipophilic drugs, and LDH which protects the bilayer and brings about a pH-sensitivity. The exchange rate is controlled via the added amount of liposomes. TGA, XRD and TEM confirm the organisation of the trapped phospholipids as a bilayer. The presence of the latter allows the material to load lipophilic and neutral drugs which represent the largest fraction of those newly synthesized. Furthermore, in physiological conditions, preliminary tests show a sustained release of phospholipids (1.5% for 7 days and 6% for 14 days) while a fluorescent lipophilic drug-mimic reveals the reorganisation of the phospholipids into liposomes in the release medium. In the

field of biocompatible materials these new hybrid particles have a strong potential for the storage and sustained release of neutral or lipophilic drugs.

References:

- [1] C. Charnay, S. Bégu, C. Tourne-Peteilh, L. Nicole, D.A. Lerner, J-M. Devoisselle., *European Journal of Pharmaceutics and Biopharmaceutics*, (2004) 57, 533-540.
- [2] C. Tourné-Péteilh, D. Brunel, S. Bégu, B. Chiche, F. Fajula, D.A. Lerner, J.-M. Devoisselle *New Journal of Chemistry* (2003) 27, 1415 – 1418.
- [3] T. Azais, T. Tourné-Péteilh, F. Aussenac, N. Baccile, C. Coelho, J-M Devoisselle, F. Babonneau, *Chemistry of Materials* (2006) 18, 6382-6390.
- [4] M. Fatnassi, C. Tourné-Péteilh, T. Cacciaguerra, J-M. Devoisselle, B. Alonso, *New. J. Chem* (2010) 34, 607–610.
- [5] L. Viau, C. Tourné-Péteilh, J-M. Devoisselle, A. Vioux. *Chem. Comm.*, 2010, 46, 2, 228-230.
- [6] S. Begu, A. Aubert-Pouessel, D.A. Lerner, C. Tourné-Péteilh, J-M Devoisselle. *Journal of Controlled Release* (2007) 118, 1, 1-6.
- [7] Y. Steinberg, A. Schroeder, Y. Talmon, J. Schmidt, R.L. Khalfin, Y. Cohen, y, J-M. Devoisselle, S. Bégu, D. Avnir *Langmuir* (2007), 23(24), 12024-12031.
- [8] S. Bégu, A. Aubert, R. Polexe, E. Leitmanova, D-A. Lerner, C. Tourné-Peteilh, J-M. Devoisselle, D. Tichit. *Chem. Mater* (2009) 21, 13, 2679–2687.

Ismael Díez-Pérez, Josh Hihath, Thomas Hines, Zhihai Li, Nongjian Tao

Institute for Bioengineering of Catalonia, Baldri Reixac 1-5, Barcelona 08028, Spain
Biodesign Institute at Arizona State University, 1001 S. McAllister Ave., Tempe, AZ85287, USA
idiezper@asu.edu, idiez@ibebarcelona.eu

During the last decade, the first experimental demonstrations of the feasibility to build single-molecule electric contacts [1,2] have led to a huge revolution in the field of Molecular Electronics. The possibility to study charge transport through a single molecule bridged between two macroscopic metal beads has placed this field in an unbeatable position to directly address fundamental questions on the relation between the molecular structure and the charge transport behavior. For example, it has already been described the impact that the presence of certain chemical groups in the single-molecule contact, such as saturated linear chains [3], conjugated blocks [4], electron donor/acceptor groups [5] or redox centers, has in the dominating charge transport mechanism.

In this contribution, we describe our latest advances toward the fundamental understanding of the main parameters dominating the charge transport through organic scaffolds and we demonstrate how the chemical structure can be tailored to achieve a desired electron transport profile in the single-molecule device. In the first part, we will describe the last implemented technical methodologies to univocally identify when a single-molecule contact is formed between two metal electrodes. The methodologies are based on the introduction of small AC perturbations within the electrode-electrode gap separation and the corresponding AC current response detection in the frequency space [6,7]. Together with the AC methods, long pulling programs applied to the molecular contact are also performed at the end of the experiment as a method to evidence the single-molecule nature of the junction. After this technical description, two examples showing how to tailor the single-molecule electron transport through the molecular design will be presented. The first case presents one of the first examples of rectification behavior (diode effect) in a single-molecule device [8]. Here we demonstrate that it is possible to go from a perfectly symmetric to a highly rectifying charge transport behavior by introducing small chemical modifications within the molecular architecture (see Figure 1).

The second case explores the feasibility to design single-molecule field effect transistors (FET) by using a graphene-like molecular structure (coronene derivatives) through the exploitation of the previously introduced electrochemical gate [9] (see Figure 2) in order to modulate the conductance of the single-molecule contact and control the ON-OFF behavior as in conventional FET setups [10]. This last example opens up a bottom-up approach for the future design of functional FET based on graphene materials. The final part of this paper will describe another example of how to modulate the single-molecule conductance in this case by using a mechanical perturbation. This last presented device constitutes the first demonstration of single-molecule electromechanical effect [7].

References:

- [1] M. A. Reed, C. Zhou, C. J. Muller, T. P. Burgin, J. M. Tour Science 278 (1997) 252.
- [2] B. Q. Xu and N.J. Tao Science 301 (2003) 1221.
- [3] X. Li, J. He, J. Hihath, B. Xu, S. M. Lindsay, N.J. Tao JACS 128 (2006) 2135.
- [4] L. Venkataraman, J. Klare, C. Nuckols, M. S. Hybertsen, M. Steigerwald Nature 442 (2006) 904.
- [5] L. Venkataraman, Y. S. Park, A. C. Whalley, C. Nuckolls, M. S. Hybertsen, M. Steigerwald Nano Letters 7 (2007) 502.
- [6] J. Xia, I. Díez-Pérez, N.J. Tao Nano Letters 8 (2008) 1960.
- [7] I. Díez-Pérez, T. Hines, J. Hihath, Z.-S. Wang, G. Zhou, K. Müllen, N.J. Tao Nature Nanotechnology, accepted 2011.
- [8] I. Díez-Pérez, J. Hihath, Y. Lee, L. Yu, L. Adamska, M. A. Kozhushner, I. Oleynik, N.J. Tao. Nature Chemistry 1 (2009) 635.
- [9] B. Q. Xu, X. Y. Xiao, X. M. Yang, L. Zang, N.J. Tao JACS 127 (2005) 2386.
- [10] I. Díez-Pérez, Z. Li, J. Hihath, J. Li, C. Zhang, X. Yang, L. Zang, Y. Dai, X. Feng, K. Müllen, N.J. Tao Nature Communication 1 (2010) 31.

Figures:

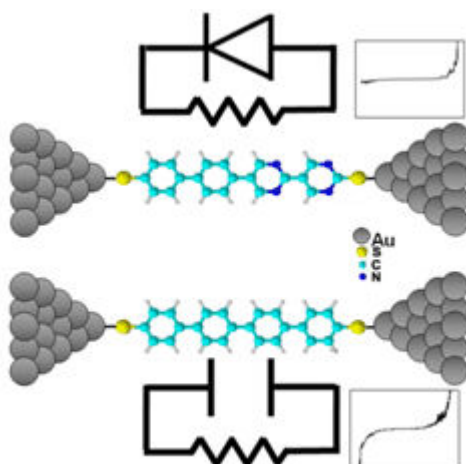


Figure 1: Representation of two single-molecule devices with similar polyphenyl molecular blocks displaying symmetric (bottom) and diode (top) charge transport behaviors.

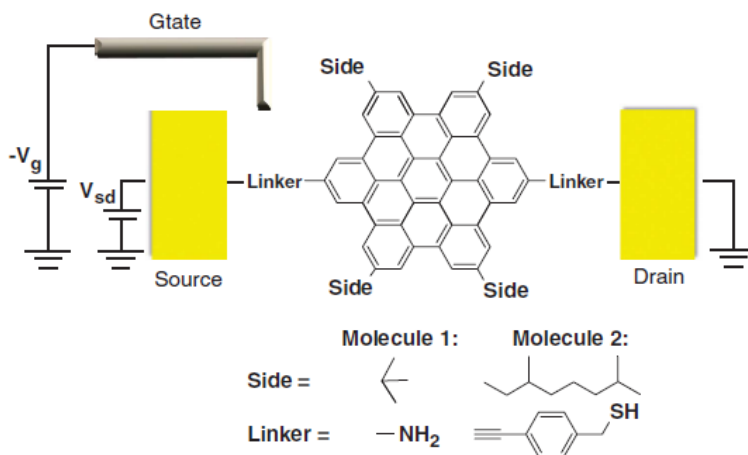


Figure 2: Representation of a single-molecule FET built with coronene derivatives and gated with a reference electrode in an electrochemical configuration.

AN $O(N^3)$ IMPLEMENTATION OF HEDIN'S SCHEME FOR MOLECULES IN ORGANIC SEMI CONDUCTORS

D. Foerster¹, P. Koval² and D. Sanchez-Portal²

¹CPMOH/LOMA, Bordeaux

²CFM/DIPC, San Sebastian

d.foerster@cpmoh.u-bordeaux1.fr

The improved scaling of our method with respect to most published methods is a step forward towards the goal of predicting, prior to their synthesis, the ionization energies and electron affinities of the large molecules that serve as constituents of organic semiconductors.

Here we focus on the principle of locality that previously lead to an efficient solution of the Petersilka-Gossmann-Gross equations of TDDFT and which gives rise to N^3 scaling with the number of atoms N in Hedin's approach for molecules.

For more details on our results, see the contribution by P. Koval on " $O(N^3)$ GW" at the session on HPC.

References:

D. Foerster J. Chem. Phys. 128, 34108 (2008).

P. Koval, D. Foerster and O. Coulaud, J. Chem. Theory Comput. 6, 2654 (2010).

D. Foerster, P. Koval and D. Sanchez-Portal, arXiv:1101.2065v1, submitted to J.Chem.Phys.

Daniel Jaque^{1*}, Martínez Maestro¹, E. Martín Rodríguez¹, F. Sanz Rodríguez², M.C. Iglesias de la Cruz², A. Juaranz², F. Vetrone³, R. Naccache³, J. A. Capobianco³ and **José García Solé**¹

¹ Fluorescence Imaging Group, Departamento de Física de Materiales, C-IV, Universidad Autónoma de Madrid, C/Francisco Tomás y Valiente 7, 28049 Madrid, Spain,

² Departamento de Biología, Universidad Autónoma de Madrid, Madrid 28049, Spain

³ Department of Chemistry and Biochemistry, Concordia University, 7141 Sherbrooke St. W., Montreal, QC H4B 1R6, Canada

daniel.jaque@uam.es

Thermal sensing at the micro and nano scales is one of the most challenging tasks that nanotechnology is nowadays facing. It is required to get a full understanding and characterization of photonic and electrical devices under real operation conditions where relevant local thermal loadings can take place as a consequence of either Joule dissipation or optical activation of non-radiative processes. In biological systems (such as tissues and individual cells) the exact knowledge of the local temperature is essential since it is known that temperature is one of the most important parameter determining the dynamics of the system. During the last years different approaches have been used to achieve thermal sensing with high spatial resolution while ensuring enough temperature sensitivity. Several techniques (such as thermal scanning and molecular fluorescence microscopies) have been already shown to satisfy both requisites simultaneously. Nevertheless, these techniques have limited applications in which, for example, three dimensional thermal imaging or in depth measurements is required.

Very recently a new approach to the thermal imaging at the nanoscale has come into sight. This is based on the incorporation of fluorescent nano-thermometers into the system to be thermally scanned. Fluorescent nano-thermometers are fluorescent nano-particles whose luminescence properties are strongly determined by the local temperature of the environment in which they are hosted. Any luminescent nano-particle whose luminescent properties (in terms of intensity, spectral position, spectral shape or decay time) are strongly dependent on temperature can be considered as a nano-thermometer. Nevertheless, the real application for thermal imaging and sensing in photonic, electrical and biological systems requires additional features such as possibility of multi-photon excitation (for high spatial resolution experiments), possibility of being dispersible in water (for easy incorporation into cells), good thermal stability and, finally, high fluorescence quantum efficiencies for high contrast imaging.

In this work the fluorescence properties of two-photon emitting nano-particles have been systematically investigated as a function of temperature in the 20-70 °C range. We have focused our attention in two different types of two-photon emitting nano-particles: Semiconductor Quantum Dots and double doped Erbium and Ytterbium doped nano-crystals. From the obtained results the potential thermal sensitivity of these two types of nano-particles has been discussed and the mechanisms at the basis of this thermal sensitivity elucidated. We have concluded that in the case of rare earth doped nano-crystals, thermal sensitivity is based on temperature induced changes in the population of excited states. On the other hand, in the case of Semiconductor Quantum Dots, thermal sensitivity is caused by a complex competition between different mechanism including temperature induced changes in the energy gap of bulk material, thermal induced dilatation and changes in the confinement energy. Although complexes, all these process give the opportunity of improvement and tailoring of the potential thermal sensitivity.

We also include in this work experimental evidence of the potential application of these systems for real intracellular thermal sensing by optical methods. Figure 1 shows a simple experiment designed to test the ability of CdSe Quantum Dots for direct measuring in intracellular thermal loading induced in cancer cells by external air fluxes.

Figures:

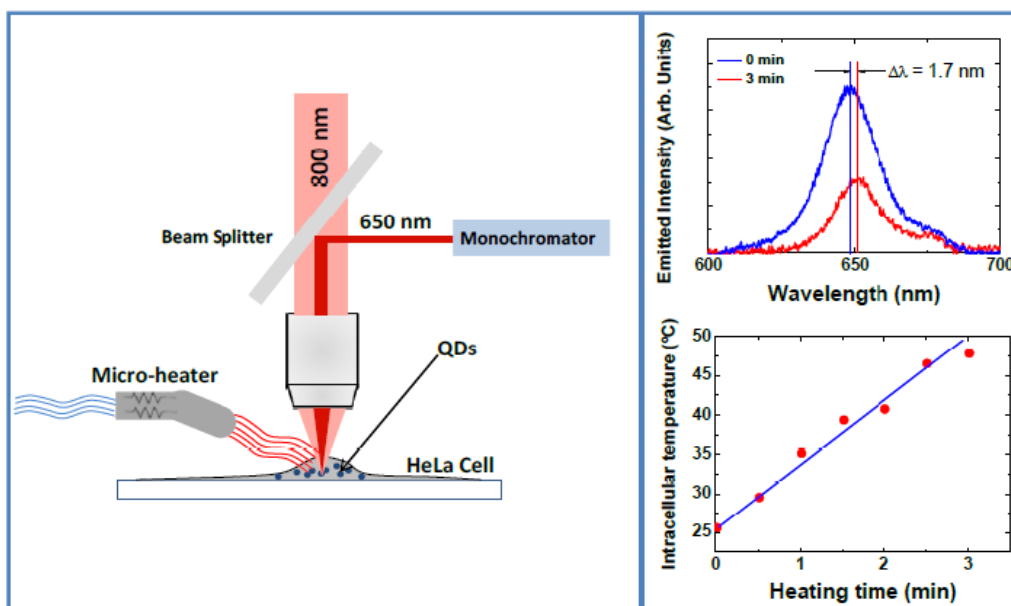


Figure 1: Experimental set-up and experimental results on the intracellular thermal sensing using two-photon emitting QDs.

A. Garcia-Lekue

Donostia International Physics Center (DIPC), Donostia, Spain

Charge transport through metal-molecule junctions is a major subject of study in a rapidly growing interdisciplinary research field. It deals with fundamental and applied aspects of science at the nanoscale aiming to control the electron conductance at the molecular level and the uprising of nanotechnology. One of the major results of this research is that the atomistic arrangement at the junction and the coupling between the molecule and the metal electrodes can significantly alter the electronic and structural properties of the molecule. It is therefore relevant to characterize the influence of the metal contact formation in the electron transport process through a single molecule.

With this aim, we have combined spectroscopic techniques based on scanning tunneling microscopy (STM) with first-principles calculations to achieve a precise characterization of the metal-molecule interaction during the formation of a nanocontact.[1] We use the inelastic tunneling spectroscopy (IETS) signal measured at various molecule-metal distances by approaching the tip of an STM to the CO molecule adsorbed on a Cu(111) metal surface. The vibration modes and inelastic transport have been modeled using density functional theory (DFT) combined with nonequilibrium Green's function methods (NEGF). Both the measured data and the calculations show characteristic shifts of the vibration modes. In particular, we observe a continuous but nonlinear blue shift of the frustrated rotation mode in tunneling with decreasing distance followed by an abrupt softening upon contact formation. This indicates that the presence of the metal electrode sensibly alters the structural and conductive properties of the junction even without the formation of a strong chemical bond.

We have shown that by combining high resolution IETS data and first-principles calculations it is possible to monitor the structural and electronic properties of a molecular nanocontact during its formation. As the tip of the STM can be more widely understood as the presence of any metallic electrode, we believe that these results have a general validity to the measurements of conductance through molecular junctions.

Finally, we report simulated vibrational spectra for CO using chemically functionalized STM tips. Our results indicate that functionalized tips can increase the resolving power of IETS and can yield inelastic signals not observed with a Cu-atom tip. Such effects are originated by changes in the symmetry of the orbitals involved in the inelastic scattering, and reveal that single-molecule IETS can be optimized by selecting the appropriate tip orbital symmetry.[2]

References:

- [1] L. Vitali, R. Ohmann, K. Kern, A. Garcia-Lekue, T. Frederiksen, D. Sánchez-Portal, A. Arnau, *NanoLetters* 10, 657 (2010).
- [2] Garcia-Lekue, D. Sanchez-Portal, A. Arnau, and T. Frederiksen, manuscript in preparation.

Illia Guralskyi, Carlos Quintero, Gabor Molnár, Lionel Salmon, Igor Fritsky, Azzedine Bousseksou

Laboratoire de Chimie de Coordination, 205, route de Narbonne, 31077 Toulouse, France
illia.guralskyi@lcc-toulouse.fr

The phenomenon of spin crossover between high-spin (HS) and low-spin (LS) states of $3d^4$ - $3d^7$ transition metal ions represents an important area of coordination chemistry. Beside its interesting fundamental aspects, the potential applications of this phenomenon draw much attention but can not be readily exploited in bulk materials. Therefore, we have developed various methods for fabricating spin crossover nanoparticles using polymers[1] or reverse micelles[2] as nanoreactors. We will show their size-dependent spin crossover properties, their patterning using soft lithographic techniques[3] and applications of these novel materials. In particular, we will discuss different strategies for signal transduction in chemical and physical sensors based on spin crossover complexes (see figure for an example of fluorescent transduction)[4].

References:

- [1] J. Larionova, L. Salmon, Y. Guari, A. Tokarev, K. Molvinger, G. Molnar and A. Bousseksou, *Angew. Chem. Int. Ed.*, 47 (2008) 8236
- [2] A. Tokarev, L. Salmon, Y. Guari, W. Nicolazzi, G. Molnár, A. Bousseksou, *Chem. Commun.*, 46 (2010) 8011
- [3] C. Thibault, G. Molnár, L. Salmon, A. Bousseksou, C. Vieu, *Langmuir*, 26 (2010) 1557
- [4] L. Salmon, G. Molnár, D. Zitouni, C. Quintero, C. Bergaud, J.-C. Micheau, A. Bousseksou, *J. Mat. Chem.*, 20 (2010) 5499

Figures:

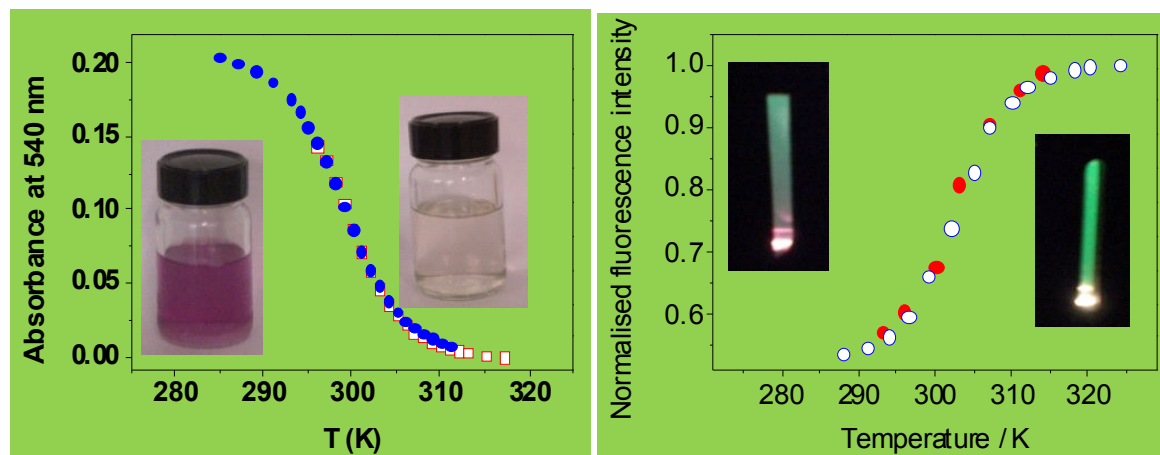


Figure 1: (Left panel) Temperature dependence of the optical absorbance (recorded at 540 nm) of the $\text{Fe}(\text{NH}_2\text{Trz})_3(\text{OTs})_2$ spin crossover nanoparticles (3 nm) suspension in the heating (open symbols) and cooling (closed symbols) modes. The inserts show the photographs of the sample at 295 K (violet) and 320 K (transparent). (Right panel) Temperature dependence of the fluorescence intensity (recorded at 540 nm) of the nanoparticle system doped by Rhodamine-110. The inserts show the luminescence of the sample (at 0.001% doping level) under white light excitation at 295 K and 320 K.

Abdou Hassanien

Nanosystem Research Institute, AIST, 1-1-1 Umezono, Tsukuba, Ibaraki 8568, Japan.
National Institute of Chemistry, Hajdrihova 19, SI-1001 Ljubljana, Slovenia
Abdou.Hassanien@aist.go.jp

The BSC theory has provided a general framework for understanding the microscopic origin of superconductivity in simple metals. With the emergence of new materials, especially high T_c and organic superconductors, clear deviations from the standard theory are reported. Several theories have been proposed to provide microscopic pairing mechanisms and thereby elucidating the macroscopic properties for these unconventional superconductors.

In order to unravel details on the mechanism and test theories one needs to investigate the local nanoscale properties on clean systems. For this purpose we have synthesized high quality single crystals of $(\text{BETS})_2\text{GaCl}_4$, where BETS is (ethylenedithio)tetraselenafulvalene, as source materials for engineering sub-monolayers and chain like structure on Ag(111) surface. In bulk $(\text{BETS})_2\text{GaCl}_4$ has a superconducting transition temperature T_c of ~ 8 K and a two-dimensional layered structure that is reminiscent of the high- T_c cuprate superconductor.

We present low temperature scanning tunneling microscopy and spectroscopy to study directly the nanoscale electronic properties of $(\text{BETS})_2\text{GaCl}_4$. We show that superconductivity still robust down to a single layer islands and chain like structures. A single chain of $(\text{BETS})_2\text{GaCl}_4$ molecules displays a superconducting gap that increases exponentially with the length of the chain. Moreover, we show that a superconducting gap can still be detected for just four of $(\text{BETS})_2\text{GaCl}_4$ molecules. Real-space spectroscopic images directly visualize the chains of BETS molecules as the origin of the superconductivity. These findings not only pave the way to study nanoscale superconductivity on other nanosystems, especially high T_c cuprates, but also to investigate pairing mechanism versus structural parameters and molecular manipulations.

References:

- [1] K. Clark, A. Hassanien, S. Khan, K.-F. Braun, H. Tanaka and S.-W. Hla, "Superconductivity in just four pairs of $(\text{BETS})_2\text{GaCl}_4$ molecules", *Nature Nanotechnology* 5, (2010).261.

Figures:

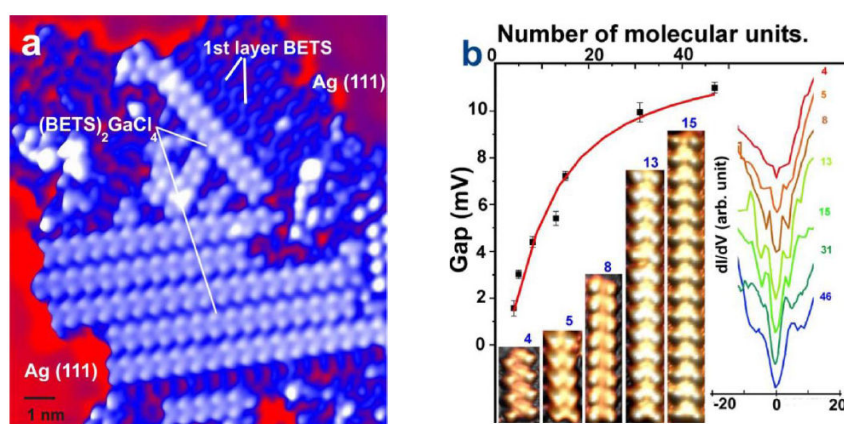


Figure 1: Size dependent molecular superconductivity. *a*, An STM image revealing shorter molecular chains at the centre. Light blue are doubled stacked BETS while darker features are the first layer BETS, The superconducting gap as a function of molecular units. The inset shows the molecular chains with 4, 5, 8, 13, and 15 units. The right inset illustrates corresponding dI/dV curves that reveal superconducting gaps of these chains.

ULTRATHIN PBS SHEETS BY TWO-DIMENSIONAL ORIENTED ATTACHMENT

Beatriz H. Juárez¹, C. Schliehe², C. Klinke², H. Weller²

¹IMDEA Nanoscience, Fco. Tomás y Valiente 7. 28049. Cantoblanco, Madrid, Spain.

²University of Hamburg. Grindelallee 117. Hamburg, Germany

beatriz.hernandez@imdea.org

Nanostructured materials offer a huge range of possibilities for the development of new devices with fascinating optical, magnetic, or electronic properties. The synthesis of colloidal semiconductor nanoparticles has been vastly improved in the last decades. In this work, a novel procedure developed to organize dot-like semiconducting nanocrystals into 2D nano-sheets will be presented. By means of this procedure the nanoparticles initially covered by randomly oriented organic molecules (see illustration on the right) assemble like “lego” bricks to form small aggregates that evolve into crystalline sheets. During this process, the organic molecules densely pack and organize on the surface of the new crystal. This ordered arrangement of the organic molecules allows the formation of these two dimensional crystals.

The work shows the formation mechanism of two-dimensional crystalline structures, based on the interaction among nanocrystals with defined orientations and the self-assembly and packing of the organic molecules on their surface. The results have special relevance to understand and control the shape of colloidal nanostructures, key for the generation of advanced functional materials at the nanoscale. These ordered 2D structures with just 2 nm thicknesses have been integrated in photodetectors. The results may be relevant to generate more efficient devices.

References:

[1] Constanze Schliehe et al. Science, 329, 5991, 2010, 550-553

Figures:

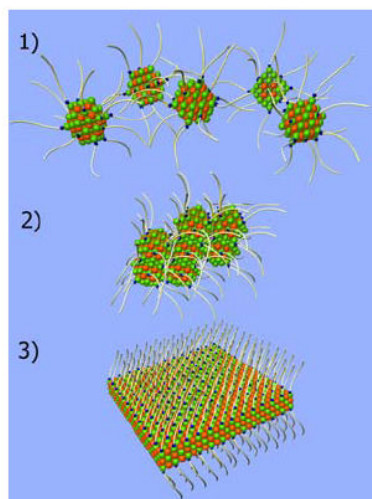


Figure 1: Scheme of the fusion of nanocrystals to form 2D crystals in three steps: Initially, nanocrystals stabilized by organic molecules in solution (1) form small aggregates by fusing in certain crystallographic directions (2). These aggregates evolve to form the crystalline sheets (3). During this process, the organic molecules self-assemble and densely pack on both sides of the crystal.

O. Idigoras, A. K. Suszka, P. Vavassori and A. Berger

CIC nanoGUNE Consolider, Tolosa Hiribidea 76, E-20018 Donostia-San Sebastian, Spain
oidigoras@nanogune.eu

It is well established that crystallographic order has a very pronounced relevance for the magnetic properties of materials due to the quantum mechanical spin-orbit coupling, which is responsible for magneto-crystalline anisotropy [1]. The control of magnetic properties and in particular the tuning of magneto-crystalline anisotropy is also essential for technological applications, such as hard disk drive media [2] or magnetic random access memories (MRAMs) [3]. However, most magnetic materials characterization studies have been focused either on nearly perfect crystallographic samples or highly disordered samples in the past, and there are only very few studies, in which the region in between perfect crystalline samples and disordered materials has been explored.

Here, we have studied the influence of crystallographic order onto the magnetization reversal process in granular Co films. In order to allow for a well-defined variation of the crystallographic order a reproducible processing sequence was developed that enables the continuous modification of epitaxial growth for (10 $\bar{1}$ 0) Co films by partially interrupting the epitaxial growth sequence. Specifically, we used the epitaxial growth sequence Ag(1 $\bar{1}$ 0)/Cr(211)/Co(10 $\bar{1}$ 0) onto HF-etched Si (110) substrates, which enables the fabrication of high-quality epitaxial Co-films with an in-plane easy axis of magnetization by means of ultra high vacuum (UHV) sputter deposition [4]. In order to disturb or interrupt the epitaxy in a well defined manner we have deposited an ultrathin SiO₂ film of the order of one monolayer thickness on top of the Si substrate prior to the Ag layer deposition. By using different deposition times for this Si oxide layer (t_{ox}), we managed to fabricate Co (10 $\bar{1}$ 0) samples with different crystallographic order level.

Figure 1 shows an X-ray θ - 2θ measurement for a fully epitaxial grown sample and a sample with $t_{ox}=12$ s, corresponding to partial epitaxy interruption. While we only observe the Si (220), Ag (220), Cr (211), Co (10 $\bar{1}$ 0) and Co (20 $\bar{2}$ 0) peaks for the fully epitaxial sample, we find multiple Ag peaks that correspond to different crystallographic orientations for the sample with partial epitaxy interruption. Nonetheless, this sample still has a high degree of Ag (220) and Co (10 $\bar{1}$ 0) texture, if one does a quantitative analysis of the X-ray data. The degree of Co (10 $\bar{1}$ 0) texture decreases further in a systematic fashion as t_{ox} is increased.

We have studied the magnetization reversal process in these samples by means of macroscopically and microscopically magneto-optical Kerr effect measurements. Figure 2 shows single domain (SD) vs. multi domain (MD) magnetization state maps, determined from quantitative Kerr microscopy [5], for three samples with different degrees of disorder (fig. 2a $t_{ox}=0$ s, fig. 2b $t_{ox}=12$ s and fig. 2c $t_{ox}=15$ s) as a function of the applied field angle β with respect to the easy axis (EA) and the applied field strength. Here, the blue color indicates a single domain state while other colors reveal the existence of multi-domain structures. We find that while in crystallographically well ordered films no static domain states exist in the entire field size and orientation range, magnetization reversal by means of non-uniform intermediate stable or meta-stable states exists for partially epitaxial samples with sufficient inter-granular misalignment. We also observe that these non-uniform states are more common for intermediate field orientations in between the macroscopic EA and hard axis (HA) directions.

Furthermore, we also observed an anomaly in samples with partial crystallographic alignment, for which conventional HA behavior disappears. When the magnetic field is applied along the nominal HA in such samples, a frustrated magnetic state occurs, which arises from the competition between ferromagnetic exchange and the uniaxial anisotropies of misaligned adjacent grains. The existence of such a frustrated state is related to a non-uniform magnetization reversal in the nominal HA and produces considerably high values of remanent magnetization and coercive field (figs. 3 (b)), while only 2° away from the nominal HA, the magnetization reversal is dominated by coherent rotation, as it is expected for highly uniaxial samples along or near the HA (figs. 3 (a) and (c)). The anomaly has been theoretically explained by means of a two-grain coupled Stoner Wohlfarth model and has been corroborated experimentally by microscopic imaging.

We acknowledge funding from the ETORTEK Program, Project No. IE06-172, the Spanish Consolider-Ingenio 2010 Program, Project No. CSD2006-53 and the Basque Government fellowships No. BFI09.284.

References:

- [1] D. Weller et al., Phys. Rev. Lett. 75, 3752 (1995)
- [2] B. D. Terris and T. Thomson, J. Phys. D: Appl. Phys. 38, R199 (2005)
- [3] A. Chung, J. Deen, J. S. Lee, et al., Nanotechnology 21, 412001 (2010)
- [4] W. Yang, D. N. Lambeth, and D. E. Laughlin, J. Appl. Phys. 85, 4723 (1999)
- [5] O. Idigoras, P. Vavassori, J. M. Porro, and A. Berger, J. Magn. Magn. Mater., L57-L60 (2010)

Figures:

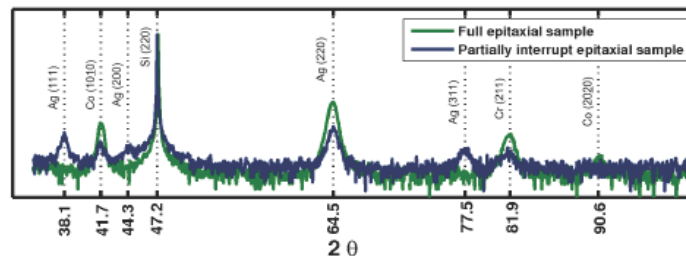


Figure 1: X-ray diffraction spectra in θ - 2θ configuration for a fully epitaxial sample $t_{ox}=0s$ (green) and for a partially epitaxial sample with $t_{ox}=12s$ (blue).

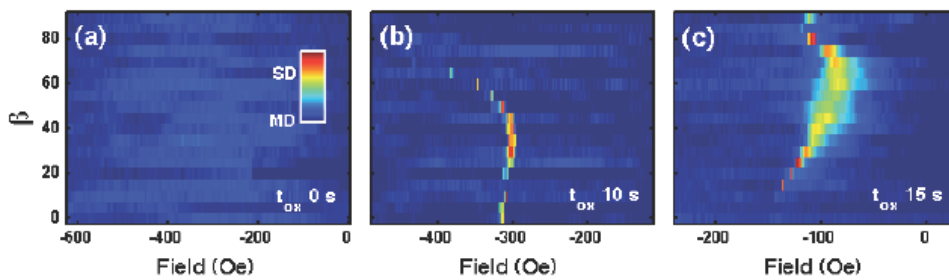


Figure 2: Single-domain/multi-domain existence map for samples with different degrees of crystallographic order as a function of applied field angle and strength: (a) fully epitaxial (1010) Co sample, and partially epitaxial samples, generated by SiO_2 underlayer deposition of (b) 12s and (c) 15s duration.

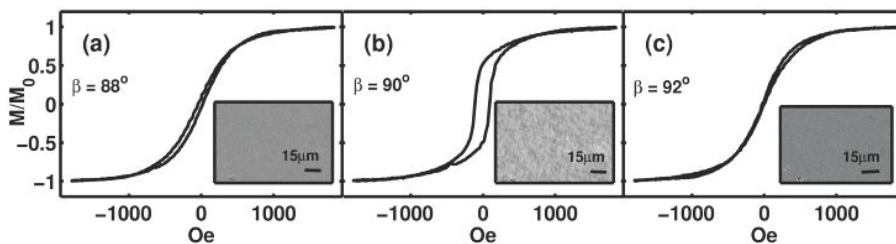


Figure 3: Hysteresis loop for a partially epitaxial sample, grown with $t_{ox}=12 s$, for magnetic field orientations $\pm 2^\circ$ away from the HA (a) and (c) respectively, and along the nominal HA (b). The inset figures show the remanent magnetization states taken by Kerr microscopy after applying a magnetic field along the corresponding field angle.

OPTICAL FORCES ON SMALL MAGNETODIELECTRIC PARTICLES IN THE FOCAL VOLUME OF HIGH NUMERICAL APERTURE MICROSCOPES

Ignacio Iglesias¹ and Juan José Sáenz^{2,3}

¹Dpto de Física, Universidad de Murcia, Campus de Espinardo (CIOyN Bldg.), E-30100, Murcia, Spain

²Dpto de Física de la Materia Condensada, Universidad Autónoma de Madrid, E-28049 Madrid, Spain

³Donostia International Physics Center (DIPC), Paseo Manuel Lardizabal 4, 20018 Donostia-San Sebastian, Spain

iic@um.es

A small dielectric particle experiences an optical field gradient and scattering forces caused by the electric-dipolar response. The scattering forces can be modeled as radiation pressure and a nonconservative force term that emerges from the spin curl [1]. In the focal region field generated by a microscope objective, the curl term is a fundamental contribution to the total force when using high numerical apertures [2]. Its presence explains the asymmetry of the trapping potential, which, for linear polarization, has been observed using focused beams (see Fig.1). Additionally, when other polarization structures in the microscope pupil plane are considered, the curl term becomes fundamental for explaining the force field the particle experiences even for moderate numerical apertures.

Recently it has been shown [3] that there are additional force terms when magnetodielectric particles are considered. These correspond to the magnetic-dipolar response, a counterpart to the aforementioned forces, together with additional components emerging from the electric-magnetic dipolar interaction. These new forces should also apply to pure dielectric particles like submicron silicon spheres which present strong magnetic and electric dipolar response in the near infrared [4,5].

Centered on these particles, this presentation will show the characteristics of the force field in the important particular case of tight focused beams generated by microscope objectives, which are frequently used in optical trapping and manipulation experiments.

References:

- [1] S. Albaladejo, M. I. Marques, M. Laroche, and J. J. Saenz, "Scattering Forces from the Curl of the Spin Angular Momentum of a Light Field," *Phys. Rev. Lett.* 102, 113602-113604 (2009).
- [2] I. Iglesias and J. J. Saenz, "Non conservative scattering forces in the focal volume of high numerical aperture microscope objectives," *Opt. Comm.* (in press)(2010).
- [3] M. Nieto-Vesperinas, J. J. Sáenz, R. Gómez-Medina, and L. Chantada, "Optical forces on small magnetodielectric particles," *Opt. Express* 18, 11428-11443 (2010).
- [4] A. García-Etxarri, R. Gómez-Medina, L. S. Froufe-Perez, C. Lopez, L. Chantada, F. Scheffold, J. Aizpurua, M. Nieto-Vesperinas, and J. J. Saenz, "Strong magnetic response of silicon nanoparticles in the infrared," *ArXiv:1005.5446v1* (submitted 2010).
- [5] M Nieto-Vesperinas, R. Gómez-Medina, and J.J. Sáenz, "Angle-suppressed scattering and optical forces on submicrometer dielectric particles," *J. Opt. Soc. A* 2011 28, 54-60 (2011).

Figures:

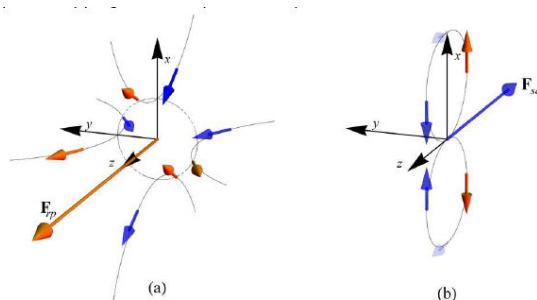


Figure 1: Scattering forces that a small dielectric particle can experience in the focal region of a high numerical aperture microscope objective. In panel (a) the radiation pressure, in panel (b) the force of the curl term for a linear polarized light beam along the x-axis.

C. Joachim

Nanoscience Group & MANA Satellite
CEMES-CNRS Toulouse, France
ICT/FET AtMol
VIP Atom Tech, IMRE Singapore

At the atomic scale, there are 2 ways of implementing a complex logic gate: atom by atom at the surface of a material or in a molecule also interconnected at the surface of a material. Quantum designs are leading to gates with a large calculating power and a short calculation time as compared to a classical design. In a quantum design, the complexity increase is based on the manipulation of states in a dual space with no correlation with the expansion in space of the final gate. In a classical design, it is based on the accumulation in space of independent devices following for example Shannon like design rules. We will compare classical and quantum design from the point of view of their intrinsic performances but also from a more practical point of view: how a quantum design resists the interconnection when constructing the calculator.

QUANTUM HALL EFFECT IN EPITAXIAL GRAPHENE ON OFF-AXIS (000-1) SiC

N. Camara^{1,2}, **B. Jouault**², A. Caboni¹, B. Jabakhanji², W. Desrat², E. Pausas¹, C. Consejo²,
N. Mestres³, P. Godignon¹ and J. Camassel²

¹CNM-IMB-CSIC, Campus UAB, Bellaterra, 08193 Barcelona, Spain

²GES, UMR 5650, Université Montpellier 2/CNRS, 34095 Montpellier Cedex 5, France

³ICMAB-CSIC, Campus UAB, Bellaterra, 08193 Barcelona, Spain

In this presentation, we will discuss on different methods we have used in order to obtain good epitaxial graphene monolayers grown on SiC. Then, we will focus on one of the method, which gives promising results: using high temperature annealing conditions with a graphite cap covering the C-face of an 8° off-axis SiC sample, large and homogeneous single epitaxial graphene layers can be grown. Raman spectroscopy shows evidence of the almost free-standing character of these monolayer graphene sheets. Magnetotransport measurements confirm these results. We find moderate p-type dopings, high carrier mobilities, and half integer quantum Hall effect typical of high quality graphene samples. This opens the way to a fully compatible integration of graphene with SiC devices on wafers that constitute the standard in today's SiC industry. This is also promising for quantum metrology.

References:

[1] N. Camara et al., Applied Physics Letters 97, 093107 (2010).

Leo Kouwenhoven

Kavli Institute of NanoScience, Delft University of Technology,
POB 5046, 2600GA Delft, The Netherlands

We are experimentalists studying quantum phenomena in nanostructures. By carefully shaping the nanostructures and choosing optimal material properties we design the system in such a way that we obtain desirable electronic and optical properties, i.e. quantum engineering. Particularly, the quantum phenomena of superposition and entanglement are interesting to control at the level of individual electrons and photons. Applications of this control are foreseen in the field of quantum information science. In this field superposition and entanglement are used for encoding information in quantum mechanical bits; the qubits.

Various systems are being investigated for realizing quantum hardware. Our favourite systems consists of nanowires (~40 nm in diameter and micrometers long) made out of various semiconducting materials, such as InAs, InSb, Si, etc. See the figure for nanowire examples.

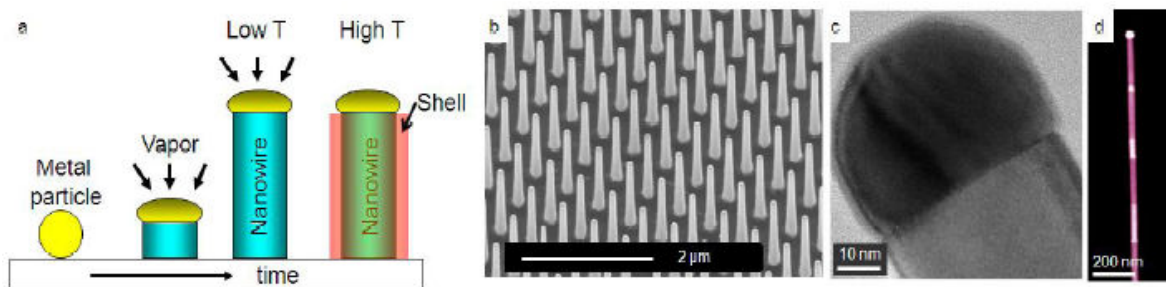


Figure 1: a) Illustration of the growth mechanism of nanowires. The Au particle catalyses the nanowire growth. After axial growth, radial growth can be initiated covering the wire with a shell of different material. b) SEM image of an array of nanowires grown from a pattern of Au particles. c) TEM image of a nanowire with the Au-particle on top. d) dark field TEM image of a GaP-GaAs heterostructured nanowire.

For the quantum transport studies we fabricate electronic devices in such a way that we can trap individual electrons. These electrostatic traps, called quantum dots, are highly stable and flexible such we can deplete all mobile electrons except for the last one. We then study the spin properties of this last electron. The spin-up or spin-down states are our qubit states, so quantum control over the spin states provides the qubit control. See figure below.

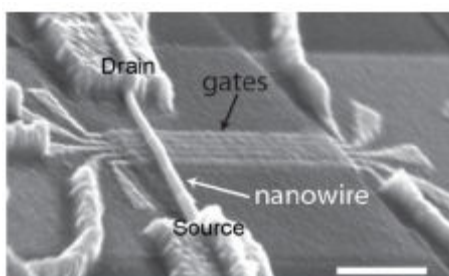


Figure 2: An InAs nanowire crossing 5 gates (horizontal strips made of Au) with electrical source and drain contacts. This device allows to define two quantum dots each containing one electron. The device has been used to operate qubits based on the spin-orbit interaction in InAs.

For optical studies we incorporate different materials in the nanowire. For instance in the first figure the GaP sections are optically inactive, whereas the GaAs sections show luminescence. When the GaAs sections are made small enough, the optical transitions are determined by the quantum confined states. Such quantum optical transition we have investigated in particular in InAsP quantum dots. In these experiments we have shown that we can control the spin of the electron and holes that determine the polarization of the out coming light. This light, importantly, is demonstrated to be a one-by-one emission of individual photons, each photon polarization determined by the spin of the electron and hole.

We are currently pushing two new directions. First of all we wish to convert electron spin superpositions into photon polarization superpositions. This would demonstrate a transfer of the quantum state from an electron-particle to a photon-particle. Quantum state transfer is important for quantum information.

The second new direction is a hunt for a new particle: Majorana Fermion. In solid state systems one can not only engineer a quantum state, one may also be able to engineer particles. A Majorana Fermion is a fundamental particle but never observed. Now theoretical schemes exist that propose using semiconductor nanowires with strong spin-orbit interaction in order to create states that accommodate Majorana Fermions.

References:

- [1] Spin-orbit qubit in a semiconductor nanowire, S. Nadj-Perge, S.M. Frolov, E.P.A.M. Bakkes, L.P. Kouwenhoven, Nature 468, 1084 (2010)
- [2] Selective excitation and detection of spin states in a single nanowire quantum dot, M.H.M. van Weert, N. Akopian, U. Perinetti, M.P. van Kouwen, R.E. Algra, M.A. Verheijen, E.P.A.M. Bakkers, L.P. Kouwenhoven and V. Zwiller Nano Letters 9, 1989 (2009)

NANOSENSORS FOR STRUCTURAL MONITORING IN CIVIL ENGINEERING: NEW INSIGHT ON PROMISING CARBON NANOTUBES DEVICES

B. Lebental¹, E. Norman³, L. Gorintin⁴, P. Renaux², P. Bondavalli⁴, C. S. Cojocaru³ and A. Ghis²

¹Université Paris-EST, IFSTTAR, Paris, 75015, France

²CEA-LETI, Minatec Campus, Grenoble, 38000, France

³LPICM, Ecole Polytechnique, Palaiseau, 91128, France

⁴Nanocarb Laboratory, Thales Research and Technology, Palaiseau, 91767, France

berengere.lebental@ifsttar.fr

In recent years, requirements in terms of service-life of civil engineering structures have become more and more stringent, so that the focus of designers and owners is now set on structural durability. Foreseeing structural failures and repairing damaged structures at an early stage has become a major stake. This approach calls for an accurate knowledge of the state of the structure at any point in its lifetime. This is the incentive for the world-wide development of various *in-situ* monitoring techniques for structural materials. However, by measuring global structural quantities only, the existing monitoring techniques provide only indirect information on the structural health of the structure.

To this day, no existing sensor features the resolution required to investigate in-situ structural materials at the micro- and nanoscale. This is a major lack, as micro and nanoscale features play a significant role in the durability of cementitious materials. From this perspective, IFSTTAR working with CEA-LETI and LPICM has set itself the long-term goal to devise innovative nanoscale structural health monitoring solutions based on nanosensors. Two types of single-walled carbon nanotubes (SWNT) devices are currently being studied with highly promising results: ultrasonic nanotransducers for microporosity assessment [1] and field-effect transistors for humidity monitoring [2].

The SWNT-based ultrasonic nanotransducer developed at the CEA-LETI consists in a metallic membrane of aligned nanotubes suspended above an actuation electrode (fig. 1). It vibrates by capacitive effect upon application of a varying voltage on the actuation electrode. Devices were fabricated by SWNT dielectrophoresis, e-beam patterning of anchoring electrodes and HF wet etching release (fig. 2) [3]. Thanks to a breakthrough laser vibrometry experiment, we observed up-to-5 nm amplitude vibrations of the SWNT membrane in air at ultrasonic (3.7 MHz) frequencies (fig. 3).

These high amplitudes of vibration is explained by the very low thickness of the membrane (fig. 4), obtained as a result of an extensive parametric study of SWNT dielectrophoresis. Our detailed numerical model shows that low membrane thickness is essential to the proposed sensing application. The model also indicates that the proposed devices embedded in a cementitious material could determine the volume and content of the microporosity in their vicinity [1]. Such microscale information would be invaluable in the evaluation of structural durability [4].

Structural durability specialists also know that not only size and content, but also humidity and chemical compositions are important for durability assessment [5]. With LPICM, we are focusing on relative humidity measurements based on field-effect transistors devices made with low density singlewalled carbon-nanotubes networks (fig. 5). The CNTFET devices were fabricated on a silicon substrate with silicon oxide layer. A conventional photolithographic process was used to create the electrodes. Mostly semiconducting CNTs were sprayed to form the gate channel [6].

Although the sensitivity of such devices to water vapor has been very often considered a drawback [7], our electrical characterizations (fig. 6) suggest that it could be exploited as a robust, high sensitivity means to probe high relative humidity environment (>60 %) such as concrete. The sensitivity of the devices to water vapor appears even stronger than that of other gases. It might be due to the strong polar nature of water and its affinity to both the metallic and dielectric parts of the CNTFET. This interpretation could lead us to various original device optimizations to improve the sensing features of the CNTFET devices.

With their very promising outputs, these two studies open up the path toward in-situ morphology and composition monitoring of the microporosity of cementitious materials by nanosensors. This

nanosensors-based microscale knowledge is the key to detect and prevent degradations of cementbased structures. As such, it will significantly contribute to an improved sustainability in civil engineering.

References:

[1] B. Lebental et al., Eur. J. Env. Civil. Eng. 2011, accepted
 [2] P. Bondavalli et al., Sensors and Actuators B: Chemical, 140(1):304-318, 2009
 [3] B. Lebental, PhD Thesis, 2010, University Paris-Est
 [4] O. Coussy and S. Brisard, Journal of Mechanics of Materials and Structures, 2009, 4, 263–279
 [5] O. Coussy, and P. J. M. Monteiro, Cement and Concrete Research, 2008, 38, 40-48
 [6] P. Na et al., Appl. Phys. Lett. 87 (2005) 093101

Figures:

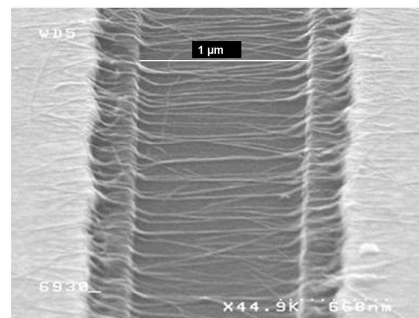
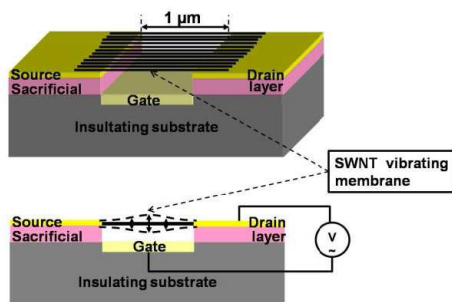


Figure 1: Schematic view of SWNT-based capacitive ultrasonic nanotransducer

Figure 2: SEM picture of a thin membrane of aligned SWNT obtained by AC dielectrophoresis

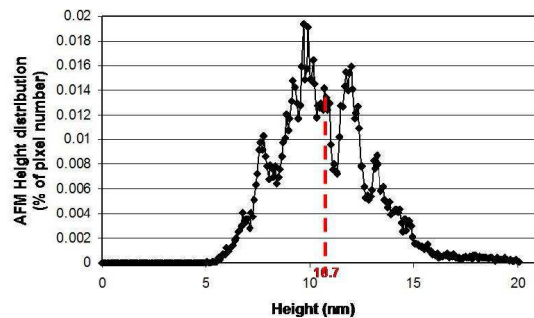
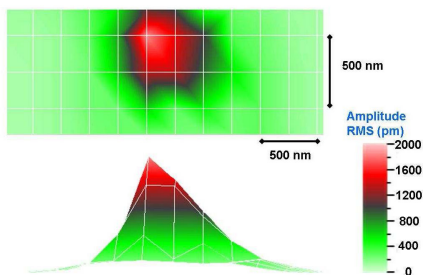


Figure 3: Topview and sideview of the vibration amplitudes of a 2 μm-large SWNT membrane at 3.7 MHz, as measured by scanning laser vibrometry. Peak to peak amplitude of vibration is 5 nm.

Figure 4: AFM measured height distribution of a SWNT based membrane before suspension. Membrane thickness is 10.7 nm.

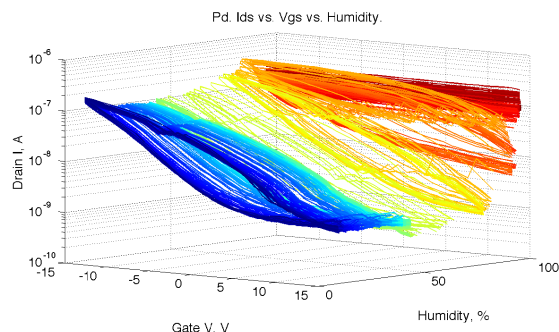
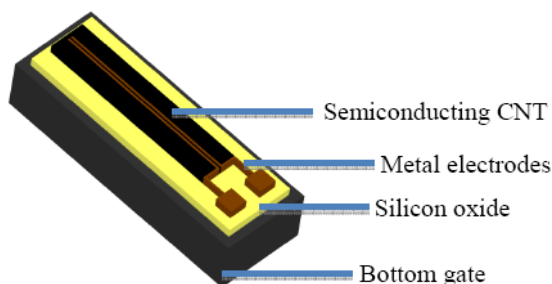


Figure 5: Schematic view of a field-effect transistor using a low density SWNT network as channel material.

Figure 6: IV characteristics of a CNTFET device with Pt electrodes: $V_{ds}=3V$; dual sweep of V_{gs} from -15 V to +15 V

CARBON NANOTUBE PHOTOCATHODES FOR OPTICALLY DRIVEN MULTIPLE X-RAY SOURCES

P. Legagneux¹, P. Ponard², L. Gangloff¹, S. Xavier¹, C. Bourat², J. Martinez², C.S. Cojocar¹,
A. Gohier¹, JP Mazellier¹, JP Schnell¹, D. Pribat¹, K.B.K. Teo³

¹Nanocarb, Thales-Ecole Polytechnique, Palaiseau, France

²Thales Electron Devices, Thonon, France

³Aixtron, Cambridge, UK

Pierre.legagneux@thalesgroup.com

We have demonstrated the first optically driven X-ray source based on carbon nanotube (CNT) photocathodes. It is a compact dual X-ray source and the two sources are accurately and independently controlled with two laser diodes illuminating the photocathodes. Thanks to the emission stability, high quality images have been obtained. This dual source provides two images from two different viewing angles. This concept can be easily extended to multiple X-ray sources. Associated with linear or 2D X-ray detectors, low cost, compact/mobile, efficient and stationary (gantry free) tomosynthesis scanners could be realized. Such systems which provide 3D imaging can be used for security applications, nondestructive inspection in the industry and for medical applications. The innovation is the use of CNT photocathodes [1]. X-ray sources based on these photocathodes exhibit the following features: galvanic insulation for current control, fast switching and accurate control of X-ray emission.

The CNT photocathode is an array of vertically aligned multiwalled CNTs (electron emitters) associated with individual p-i-n photodiodes. These photodiodes act as optically-driven current sources. The emitted current varies linearly with the optical power delivered by the laser diode located under the photocathode.

Figure 1 shows a schematic description and SEM pictures of the fabricated photocathodes which are based on silicon photodiodes. CNTs are grown on n+ doped areas defined by ion implantation in a 5 µm thick intrinsic layer. The p+ doped silicon wafer is thinned to obtain a 7 µm thick membrane and to enable backside illumination of the photocathode. In order to demonstrate the proof of concept of this new system, we have fabricated a dual X-ray source based on two CNT photocathodes (see figures 2-4). The distance between the two sources is 10 cm. Due to the galvanic insulation (optical control), we can use a simple diode configuration with a high voltage applied to the photocathode and with a grounded anode. Compared to the power supply used in a conventional X-ray tube, no high voltage filament transformer is required. Thus our high voltage power supply is compact (see Figure 4). Being grounded, the anode is a tungsten film directly deposited on the X-ray window. The anode cooling is then simply performed by air convection. To obtain X-ray images, we have used a 2D X-ray detector and positioned different objects between the source and the detector. With this dual source, 2 views in parallel are obtained (see Figure 5). Figure 6 shows an image of an animal obtained with one single CNT photocathode.

This work was funded by the ANR project SPIDERS. Through the ANR project NANOSCANNER, we are currently studying the fabrication of CNT photocathodes based on low temperature grown GaAs photoswitches that should exhibit very large ON/OFF ratio (a few hundreds).

References:

- [1] L. Hudanski, E. Minoux, L. Gangloff, K.B.K. Teo, J.-P. Schnell, S. Xavier, W.I. Milne, D. Pribat, J. Robertson, P. Legagneux, "Carbon nanotube based photocathode", *Nanotechnology* 19 105201 (2008).

Figures:

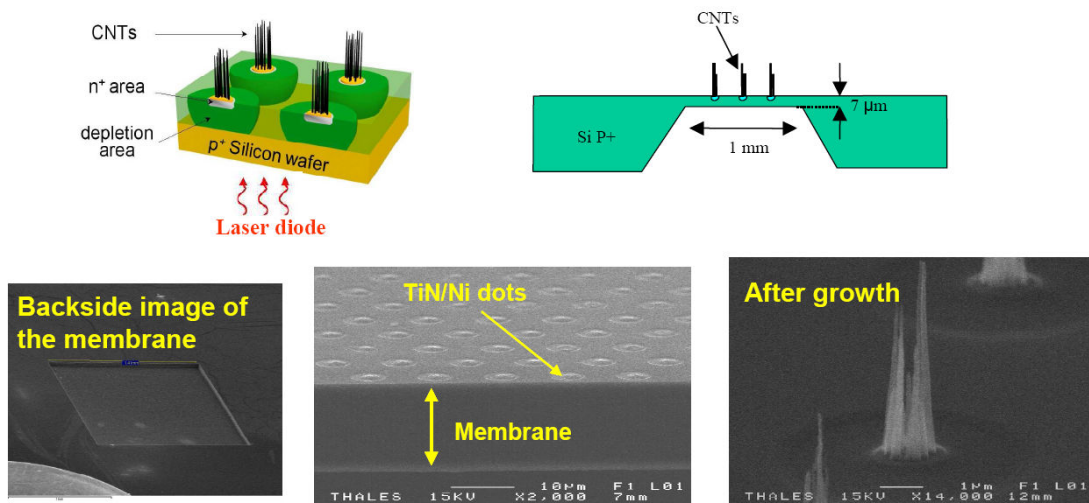


Figure 1: Schematic description and SEM pictures of the CNT photocathode. The photocathode uses multiwalled CNTs as electron emitters and silicon p-i-n photodiodes to control the emission. CNTs are grown on n+ doped areas defined by ion implantation in a 5 μm thick intrinsic layer. The p+ doped silicon wafer is thinned to obtain a 7 μm thick membrane. This enables backside illumination of the photocathode.



Figure 2: Picture showing the two "satellites" holding the CNT photocathodes. The backside of the upper left photocathode is illuminated.

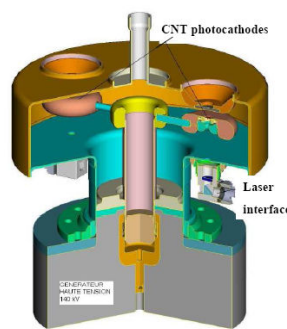


Figure 3: Schematic description of the optically driven dual X-ray source

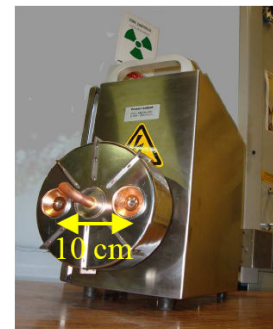


Figure 4: Picture of the dual X-ray source associated with the power supply.

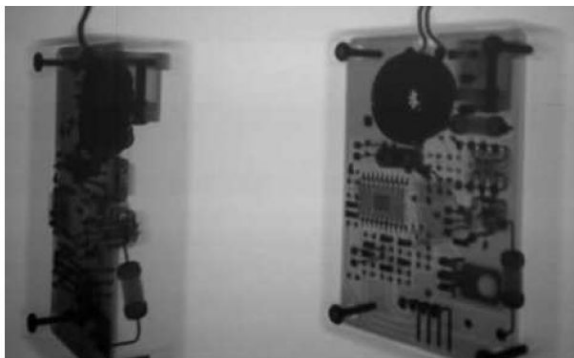


Figure 5: Images of a printed circuit board obtained on the 2D X-ray detector with the dual source (2 views in parallel)



Figure 6: Image of a bird realised with a single CNT source.

François Léonard

Sandia National Laboratories, Livermore, CA, USA

fleonar@sandia.gov

Semiconductor nanowires show promise in electronic, optoelectronic, and sensing devices. To realize this promise, a fundamental understanding of charge injection and electronic transport in these novel nanomaterials is necessary. In this presentation, I will discuss recent work that couples experiment and theory to address this topic. For example, in GaN and InAs nanowires, we achieve efficient charge injection and find that space-charge-limited currents are unusually strong [1,2]. In contrast, charge transport across individual Au-nanoparticle/Ge-nanowire interfaces is injection-limited, and surprisingly, the conductance increases with decreasing nanowire diameter due to a dominance of electron-hole recombination [3]. Furthermore, we find that transport in GaAs nanowires is governed by charge traps, which can be activated to reveal the nature of the charge injection at the contacts [4]. More generally, our results indicate that a broad range of electronic transport regimes can be observed in semiconducting nanowires depending on the particular material system and growth process.

References:

- [1] AA Talin, F Léonard, B Swartzentruber, X Wang, S Hersee. *Physical Review Letters* 101 (2008) 076802.
- [2] A M Katzenmeyer, F Léonard, AA Talin, ME Toimil-Molares, JG Cederberg, JY Huang, and J Lensch-Falk. *IEEE Transactions in Nanotechnology* 10 (2011) 92.
- [3] F Léonard, AA Talin, B Swartzentruber, T Picraux. *Physical Review Letters* 102 (2009)106805.
- [4] AA Katzenmeyer, F Léonard, AA Talin, P-S Wong, and DL Huffaker. *Nano Letters* 10 (2010) 4935.

Figures:

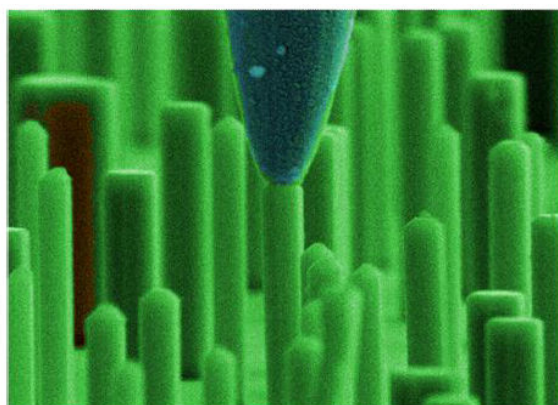


Figure 1: A conducting tip retrofitted inside of a scanning electron microscope measures the electronic properties of individual nanowires.

ARTIFICIAL SPIN ICE

J. P. Morgan¹, A. Stein², J. Akerman^{1,3}, C. Sanchez-Hanke⁴, D. A. Arena⁴, C. J. Kinane⁵, R. Fan⁵, S. Langridge⁵, and C. H. Marrows¹

¹School of Physics & Astronomy, University of Leeds, Leeds LS2 9JT, United Kingdom

²Center for Functional Nanomaterials, Brookhaven National Laboratory, Upton, NY 11973, USA

³Instituto de Sistemas Optoelectrónicos y Microtecnología (ISOM), Universidad Politécnica de Madrid, Avda. Complutense s/n, 28040 Madrid, Spain

⁴National Synchrotron Light Source, Brookhaven National Laboratory, Upton, NY 11972m USA

⁵ISIS, STFC Rutherford Appleton Laboratory, Harwell Science and Innovation Campus, Didcot, Oxon. OX11 0QX, United Kingdom

Spin ices are rare earth pyrochlores where the crystal geometry leads to frustration of the rare earth moments [1], which meet at tetrahedra in the lattice. Like water ice, they violate the third law of thermodynamics, and have been extensively studied by neutron scattering. Recently it has been realised that excitations of this system can be described as deconfined emergent monopoles and associated Dirac strings [2]. Nanotechnology allows many of the essential features of this physical system can be reproduced in arrays of patterned nanomagnets where moments meet at the vertices of a square grid [3]. This approach offers the opportunity to continuously tune the various parameters controlling the magnetic microstate, and also to inspect that microstate using advanced magnetic microscopy [4,5]. A significant difference with the naturally occurring spin-ices is that the change in symmetry gives rise to a true long-range ordered ground state, although the frustrated interactions in these athermal systems mean that its observation is extremely difficult [6].

Here I will describe our recent work on such a system, an array of 250 nm × 80 nm Permalloy islands in the square ice geometry (shown in Figure 1), including the achievement of a thermalised ground state during fabrication and the observation of the effects of fractionalised monopoles on excitations out of it (shown in Figure 2) [7], and athermal achievement of the ground state using a suitable field protocol, both observed using magnetic force microscopy. I will also describe some preliminary data from soft x-ray scattering measurements, the effects of dc field reversal, and also the application of an effective temperature formalism [8] to the frozen microstates we observe.

This work was supported financially by EPSRC and the STFC Centre for Materials Physics and Chemistry. Parts of this research were carried out at the Center for Functional Nanomaterials and at the National Synchrotron Light Source, Brookhaven National Laboratory, which are supported by the U.S. Department of Energy, Office of Basic Energy Sciences, under Contract No. DE-AC02-98CH10886.

References:

- [1] S. T. Bramwell and M. J. P. Gingras, *Science* 294, 1495 (2001).
- [2] C. Castelnovo, R. Moessner, and S. L. Sondhi, *Nature* 451, 42 (2008).
- [3] R. F. Wang et al., *Nature* 439, 303 (2006).
- [4] S. Ladak et al., *Nature Physics* 6, 359 (2010).
- [5] E. Mengotti et al., *Nature Physics* 7, 69 (2011).
- [6] X. Ke et al., *Phys. Rev. Lett.* 101, 037205 (2008).
- [7] J. P. Morgan, A. Stein, S. Langridge, and C. H. Marrows, *Nature Physics* 7, 75 (2011).
- [8] C. Nisoli et al., *Phys. Rev. Lett.* 105, 047205 (2010).

Figures:

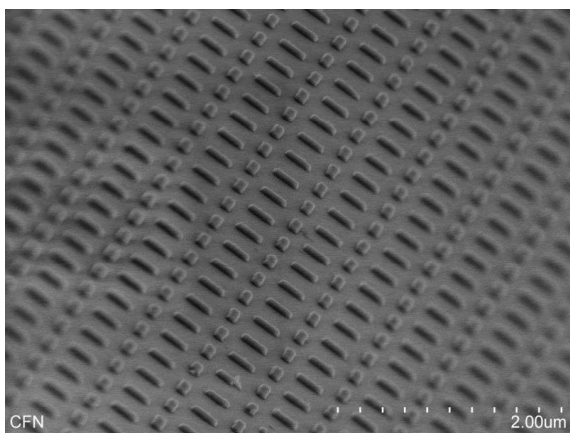


Figure 1: Scanning electron micrograph of a array of Permalloy nanomagnets, prepared using electron beam lithography, that form a frustrated square ice lattice.

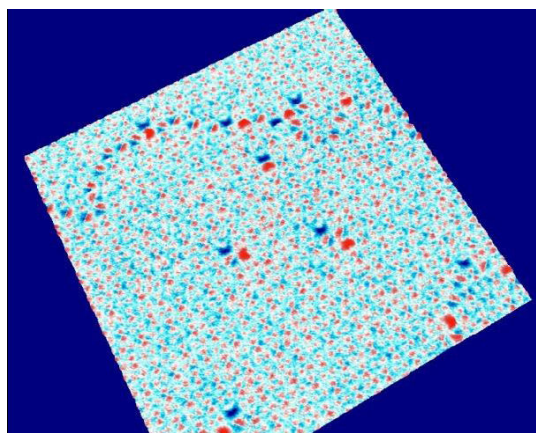


Figure 2: Rendering of a magnetic force micrograph showing the smeared magnetic charge density: monopole defects in the periodic ground state are clearly visible.

SELECTIVE LUMINESCENCE SWITCHING IN ENTANGLED METAL-ORGANIC FRAMEWORKS BY INCLUSION OF AROMATIC GUESTS. MOLECULAR SENSOR FOR SUBSTITUTED-BENZENES

Virginia Martínez-Martínez¹, Yohei Takashima^{2,3}, Shuhei Furukawa^{2,4}, Susumi Kitagawa^{2,3,4} and Iñigo López Arbeloa¹.

¹Dpto de Química Física, Universidad del País Vasco UPV-EHU, Apdo. 644, 48080-Bilbao, Spain

²ERATO Kitagawa Integrated Pores Project, Japan Science and Technology Agency (JST), Kyoto Research Park Bldg#3, Shimogyo-ku, Kyoto 600-8815, Japan

³Department of Synthetic Chemistry and Biological Chemistry, Graduate School of Engineering, Kyoto University, Katsura, Nishikyo-ku, Kyoto 615-8510, Japan

⁴Inst. for Integrated Cell-Material Sciences, Kyoto Univ., Yoshida, Sakyo-ku, Kyoto 615-8510, Japan
virginia.martinez@ehu.es

Porous coordination polymers (PCPs) or metal–organic framework (MOFs) are recently considered as a functional class of porous materials. The designability by varying the nature of the coordination metals and the organic linkers, the crystallinity in their structures resulting in nanometer-size confined spaces and the flexibility by the entanglement of their frameworks are unique properties for the development of multiple applications such as gas storage and gas separation, heterogeneous catalysts and molecular sensors.

The design of a PCP with photoactive entities as part of the structure and whose luminescent properties are highly sensitive to guests can offer potential application as luminescent sensors.

In this work [1], a new interpenetrated porous coordination polymer with naphthalenediimide (NDI) incorporated as fluorophore linker exhibits an unpredicted turn-on emission upon the incorporation of a class of aromatic compounds (substituted-benzenes). The unexpected luminescent properties are as consequence of the induced-fit structural transformation (framework displacement), checked by single-crystal x-ray diffraction, triggered by the guests incorporation to maximize the interaction with NDI. Non-interpenetrated analog. PCP (frameworks are impossible to slide) shows no luminescence, indicating the importance of the dynamic confined space for the luminescence.

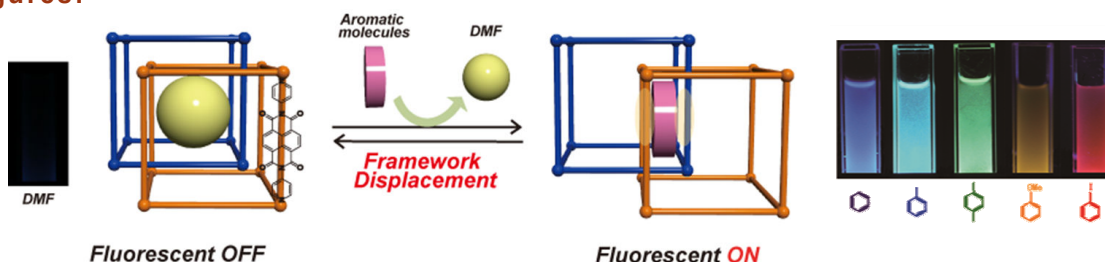
The entangled PCP exhibits different luminescent colour depending on the substitution of the benzene ring as guests. For instance, from strong electron withdrawing (cyano) to electron donating capacity of the substituents (methoxy), the fluorescence can be tuned in the whole visible region (from 400 to 700 nm) or even stabilized radical-ion species (N,N-dimethyl). On the other hand, when halogen atoms are included in the benzene ring, a switching from fluorescence to phosphorescence emission is observed.

In this way, this new PCP can be used as a molecular sensor for benzene derivatives which can recognize tiny differences in the substitution of aromatic ring and converted into a detectable signal (even by eye).

References:

- [1] Y. Takashima, V. Martínez-Martínez, S. Furukawa, M. Kondo, S. Shimomura, H. Uehara, M. Nakahama, K. Sugimoto and S. Kitagawa. Nature Communications (accepted)

Figures:



WAFER SCALE FABRICATION OF PASSIVATED CARBON NANOTUBE TRANSISTORS FOR ELECTROCHEMICAL SENSING

I. Martin-Fernandez¹, X. Borrísé^{1,2}, P. Godignon¹, E. Lora-Tamayo¹, F. Perez-Murano¹

¹Instituto de Microelectrónica de Barcelona (IMB-CNM, CSIC), Campus UAB, E-08193 Cerdanyola del Vallès, Spain

²Institut Català de Nanotecnologia (ICN), Campus UAB, E-08193 Cerdanyola del Vallès, Spain
inigo.martin@imb-cnm.csic.es

Since the operation of carbon nanotube transistors (CNT-FETs) was demonstrated [1], much progress has been achieved on the knowledge about electronic transport on SWCNTs and on their application for sensing [3]. However, there is still no standard high yield technology to fabricate single CNT-FETs.

In this contribution we present a technological process for the batch fabrication of CNT-FET based chips for electrochemical sensing applications (Figure 1) [2]. The fabrication of the CNT-FET structures is performed by using standard microelectronic steps at wafer level. Optical lithography is the only patterning technique to be used. The overall process can be divided in three main steps: the substrate preparation, the selective synthesis of the single-walled (SW) CNTs and the definition of the metallic contacts, stripes and pads. Recently, we have reported the fabrication of 10,000 functional CNT-FET devices on a 4 inch wafer by this technology [4].

An important requirement for the operation of the CNT-FETs in an electrochemical environment is the electrical contacts to be isolated from the electrochemical solution. With this purpose, we have developed a passivation procedure consisting in a PMMA coating of the CNT-FET and an electron beam lithography (EBL) process to locally remove the PMMA from the top of the CNTs and from the liquid polarization electrodes. The EBL process is programmed for the pattern to be automatically aligned on each device and it is performed at low electron beam energy to avoid any damage to the devices [5].

Figure 2(a-c) shows results on the fabrication of the CNT-FET based sensors. Figure 2(a) shows a 4 inch wafer after the fabrication of the CNT-FET structures. The wafer contains 5,616 CNT-FET structures. Almost 30% of the devices on this wafer were identified as operative and one third of those devices showed a semiconducting characteristic. Figure 2(b) shows an optical image of a sensor-platform into which the CNT-FET structures on the wafer are arranged. Each sensor-platform is composed of 24 CNT-FET structures that are located at the center of the chip for an electrochemical cell to be installed. The SEM image in Figure 2(c) shows a CNT-FET structure which channel length is 1.5 μm and where the width of the trench in the PMMA is 800 nm. Two SWCNTs had been contacted in this case by the metal contacts. The typical IV characteristics of a functional CNT-FET are shown in Figure 2(d). The transistors are p-type, their ON current is $\sim 1 \mu\text{A}$ and the $I_{\text{ON}}/I_{\text{OFF}}$ ratio is ~ 105 .

The passivated CNT-FET devices are currently being tested in electrochemical environment.

Acknowledgements:

This work was partially founded by NANOFUN and SENSONAT projects. I.M.F acknowledges financial support through the I3P program.

References:

- [1] R. Martel et al., Applied Physics Letters 73 (1998), 2447; S.J.Tans et al., Nature, 393 (1998), 49.
- [2] I. Martin-Fernandez et al., J. of Vacuum Science and Technology B 28 (2010), C6P1.
- [3] A. Jorio et al., Carbon Nanotubes: Synthesis, Structure, Properties, and Applications (2008), Springer.
- [4] I. Martin-Fernandez et al., Microelectronic Engineering 87 (2010), 1554.
- [5] G. Rius et al., Microelectronic Engineering 84 (2007), 1596.

Figures:

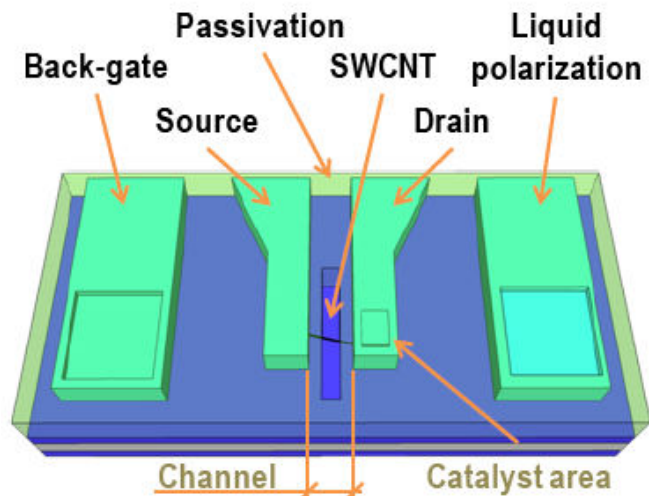


Figure 1: Schematic of the passivated, back-gated CNT-FET sensor. The sensor consists of one (or more than one) SWCNT that is contacted by two metal electrodes, a back-gate that is actuated through a top metal electrode and a top liquid polarization electrode. The sensor is completely passivated by PMMA except for the channel of the CNT-FET, for part of the liquid polarization electrode and for the contact pads.

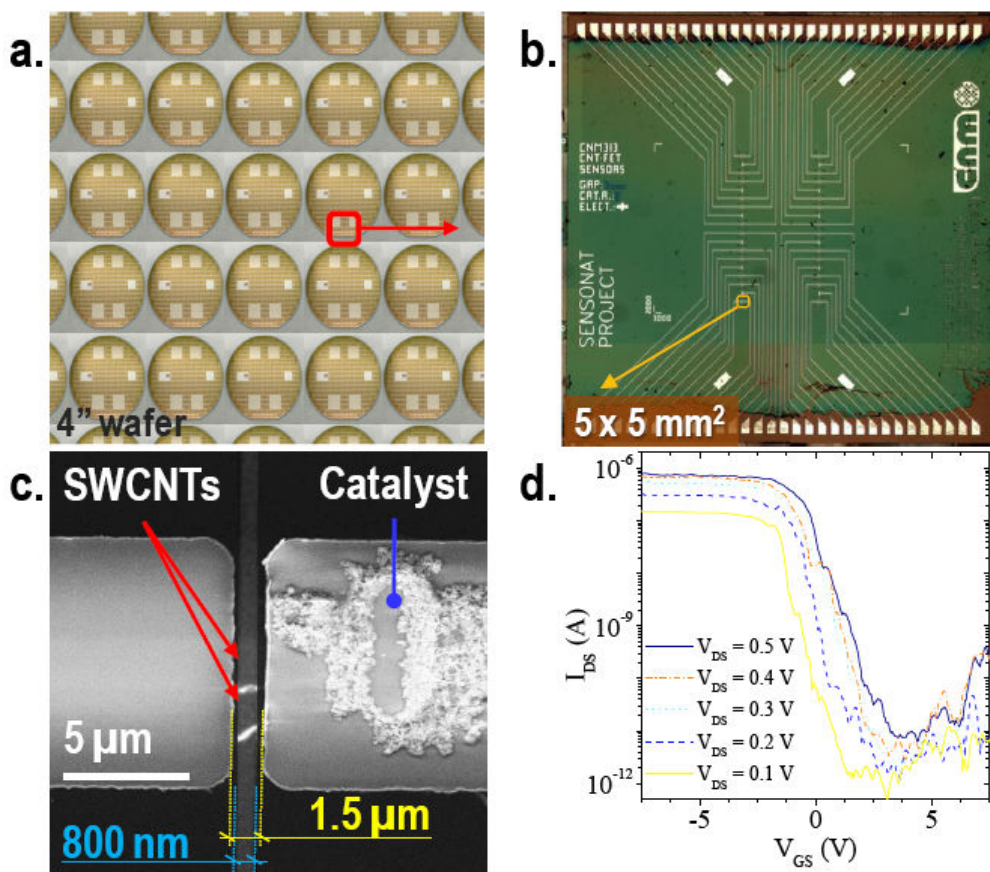


Figure 2: Images on the fabrication and IV characteristics of the CNT-FETs. (a) Photograph of a batch fabricated 4 inch wafer. (b) Optical image of a sensor chip after the passivation procedure. The sensor is 5 x 5 mm². (c) SEM image of a passivated CNT-FET device. (d) Typical IDS vs. VGS characteristics of a CNT-FET formed of a single semiconducting SWCNT.

R. Marty¹, G. Baffou², A. Arbouet¹, V. Paillard¹, R. Quidant^{3,4} and C. Girard¹

¹CEMES, UPR 8011, CNRS-Université de Toulouse, 29 rue Jeanne Marvig, BP 94347, F-31055 Toulouse, France

²Institut Fresnel-Domaine Universitaire de Saint-Jérôme, Avenue Escadrille Normandie-Niémén, F-13397 Marseille, France

³ICFO-The Institute of Photonic Sciences, Mediterranean Technology Park Av. del Canal Olímpic, 08860 Castelldefels (Barcelona), Spain

⁴ICREA-Institucio Catalana de Recerca i Estudis Avançats, 08010 Barcelona, Spain
renaud.marty@cemes.fr

Since the eighties, a tremendous interest has been devoted to the original near-field optical properties of nano-objects (either dielectric or metallic) deposited on surfaces [1]. To investigate these properties, near-field experimental methods such as PSTM and SNOM were initially developed [2]. They however need to accurately locate a near-field detector (tip) in the vicinity of the sample, making the system difficult to describe theoretically since the detector has an influence on the system itself. Recently, an alternative method based on two photon luminescence (TPL) has been developed to give access to near field informations through a far field measurement [3-4]. This technique can be advantageously coupled to optical absorption measurements of isolated nano-objects [5,6].

We investigate here lithographically fabricated gold nanoprisms. Both TPL and scattering by dark-field microspectroscopy were performed on isolated nanoprisms. The signals provided by these experiments are then compared and investigated theoretically.

In a first step, the nanostructure is represented by a single gold nanosphere deposited on a glass substrate and excited by an incident electric field. By using the field susceptibility theory, a simple analytical expression of the scattering signal generated by this nanoparticle is extracted as a function of the experimental parameters (incident wavelength and power, numerical aperture). In a second step, we describe the two photon luminescence signal in this simple configuration. This allows to discuss the origin of the spectral shift of the surface plasmon resonance during the propagation towards the far-field.

Finally we generalize this analytical scheme to realistic gold nanoparticles to simulate our experimental results. This comparison enables us to extract the order of magnitude of the non-linear response function of the nano-object as function of the incident wavelength.

References:

- [1] C. Girard, and A. Dereux, Rep. Prog Phys. 59 (1996) 657
- [2] P. Dawson, F. de Fornel, and J-P. Goudonnet, Phys. Rev. Lett. 72 (1994) 2927
- [3] P. Ghenuche, S. Cherukulappurath, T. H. Taminiau, N. F. van Hulst, and R. Quidant, Phys. Rev. Lett. 101 (2008) 116805
- [4] K. Imura, T. Nagahara, and H. Okamoto, J. Phys. Chem. B 109 (2005) 13214
- [5] A. Arbouet, D. Christofilos, N. Del Fatti, F. Vallee, J. R. Huntzinger, L. Arnaud, P. Billaud, and M. Broyer, Phys. Rev. Lett. 93 (2004) 127401
- [6] M. W. Knight, J. Fan, F. Capasso, and N. J. Halas, Optics Express 18 (2010) 2580.

Figures:

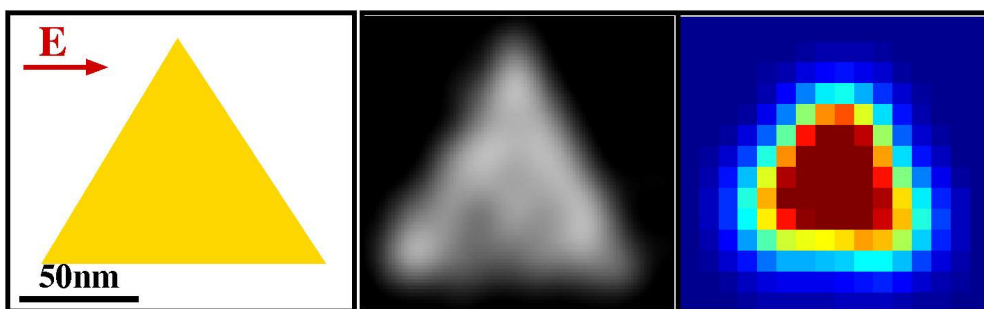


Figure 1: (a) Investigated configuration: the electric field is parallel to the side of the nanoprism and the propagation of the beam is perpendicular to the triangle (and to the substrate). (b) SEM image of the considered gold nanoprism. The length of its side is 120nm. (c) TPL map of the nanotriangle performed at $\lambda=822\text{nm}$.

COMMUNICATION BETWEEN MOLECULES VIA PHOTOCONTROLED IONS

Nathan D. McClenaghan¹, Guillaume Sevez¹, Aurélien Ducrot¹, Robin Bofinger¹, Pinar Bata^{1,2}, Ren-Wei Chang^{1,3}, Gediminas Jonusauskas², Laura Jonusauskaite¹, Jean-Luc Pozzo¹, Reiko Oda³

¹Institut des Sciences Moléculaires, CNRS/Université Bordeaux I (UMR 5255),
351 cours de la Libération, 33405 Talence Cedex, France

²Laboratoire Ondes et Matière d'Aquitaine, CNRS/Université Bordeaux I (UMR 5798),
351 cours de la Libération, 33405 Talence Cedex, France

³Institut Européen de Chimie et Biologie, CNRS/Université Bordeaux I (UMR 5248),
2, rue Robert Escarpit, 33607 Pessac Cedex, France

n.mc-clenaghan@ism.u-bordeaux1.fr

Despite intense research, no single strategy has been shown to satisfactorily connect artificial molecular components in networks. This is perhaps the greatest hurdle to overcome if implementation of artificial molecular devices and sophisticated molecule-based arrays are to become a reality. One major goal of our work is to establish a strategy whereby functional molecular devices (e.g. photo-/electroactive) can communicate with one another in solution and in organized, self-assembled media (biotic and abiotic).[1]

Natural systems use chemical communication with small molecules and ions to promote transfer of information in different processes, including vision and neural transmission. In the current case artificial biomimetic systems are being developed integrating photonic and ionic processes, where remote control of ion release from synthetic molecular receptors, and thus the information transfer, is governed by a photonic stimulus in a bottom-up strategy. Ultimately this is anticipated to lead to coded information transfer through ion movement, which when combined with suitable receptors is signalled by fluorescent reporter groups and induced by photomodulated receptor groups in small photoactive molecules.

A range of artificial nanoobjects are presented with have been synthesized where different ion and molecule messengers are considered and are under study using ultrarapid transient absorption spectroscopy and dynamic fluorescence. Fast processes of photoejection and migration of ions are particularly well-suited to studies in real-time (using time-resolved photophysical techniques) with high spatial resolution (using fluorescence confocal microscopy techniques) allowing evaluation of the versatility of this strategy in the treatment and transfer of information and incorporation into devices.

As well as studies in solution, communication between distant sites / molecules considers the use of photoejected ions in nanocapsules and organized media including membranes, thin films, nanostructured hosts. Proof-of-principle of compartmental effects in dynamic micellar nanodomains has recently been demonstrated, see figure 1.[2]

References:

[1] <http://mcclenaghan.ism.u-bordeaux1.fr/>

[2] M. Cantuel, C. Lincheneau, T. Buffeteau, L. Jonusauskaite, T. Gunnlaugsson, G. Jonusauskas, N. D. McClenaghan, Chem. Commun., (2010) 2468.

Figures:

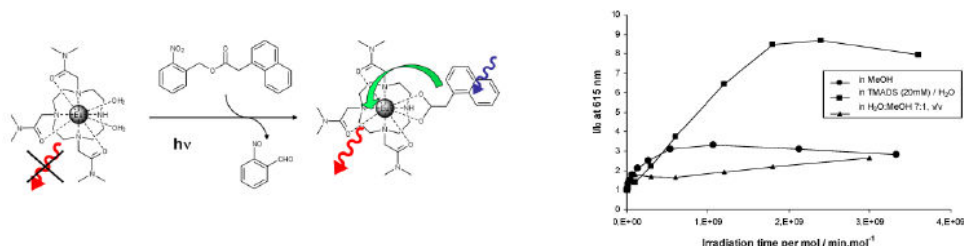


Figure 1: Rudimentary photocontrolled chemical communication between molecules (left) and enhanced chemical communication in self-assembled surfactant (TMADS) nanodomains (right) as denoted by luminescence.

ORDERED VACANCY NETWORK INDUCED BY THE GROWTH OF EPITAXIAL GRAPHENE ON Pt(111)

G. Otero¹, C. Gonzalez¹, A.L. Pinardi¹, P. Merino², S. Gardonio³, S. Lizzit³, M. Blanco-Rey⁴, K. Van de Ruit⁵, C.F.J. Flipse⁵, **J. Méndez**¹, P.L. de Andres¹ and J.A. Martin-Gago^{1,2}

¹Inst Ciencia de Materiales de Madrid (CSIC), C. Sor Juana Ines de la Cruz 3, 28049-Madrid, Spain

²Centro de Astrobiología, INTA-CSIC, Torrejon de Ardoz, 28850 Madrid. Spain

³Sincrotrone Trieste SCpA, Strada Statale 14, Km. 163.5, 34149 Trieste, Italy

⁴Department of Chemistry, University of Cambridge, Cambridge CB2 1EW, United Kingdom

⁵Department of Applied Physics, Eindhoven University of Technology, P.O. box 513, 5600 MB Eindhoven, The Netherlands

jmendez@icmm.csic.es

We have studied large areas of $\sqrt{3}\times\sqrt{3}R30^\circ$ graphene commensurate with a Pt(111) substrate. A combination of experimental techniques with ab initio density functional theory indicates that this structure is related to a reconstruction at the Pt surface, consisting of an ordered vacancy network formed in the outermost Pt layer and a graphene layer covalently bound to the Pt substrate. The formation of this reconstruction is enhanced if low temperatures and polycyclic aromatic hydrocarbons are used as molecular precursors for epitaxial growth of the graphene layers.

References:

[1] G. Otero et al., Physical Review Letters, 105 (2010) 216102.

Figures:

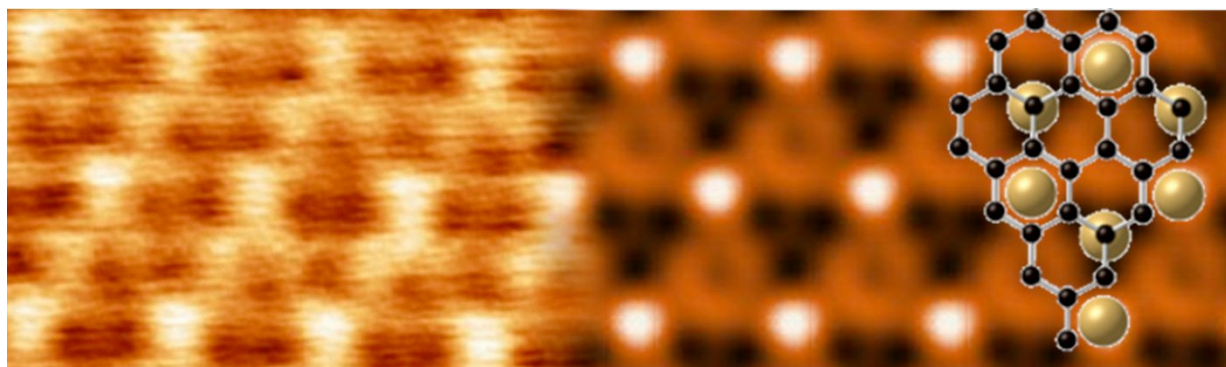


Figure 1: STM image (left) and DFT simulation (right) of the proposed vacancy model (overlaid).

D. Meneses-Rodríguez, E. Ferreiro-Vila, P. Prieto, J. Anguita, A. García-Martín, M. U. González, J. M. García-Martín, A. Cebollada, and G. Armelles

IMM-Instituto de Microelectrónica de Madrid (CNM-CSIC)
Isaac Newton 8, PTM, E-28760 Tres Cantos (Madrid), Spain
david.meneses@imm.cnm.csic.es

It is well known that localized surface plasmon resonances (LSPRs) greatly influence the optical [1, 2] and magneto-optical [3] properties of metallic nanostructures. It has been reported an enhancement of the magneto-optical (MO) activity when these LSPRs are excited. The key factor for this phenomenon is the high intensity of the electromagnetic (EM) field inside the global nanostructure when a LSPR occurs [4, 5]. In this work we show how the EM profile related to the LSPR can be probed locally inside the nanostructure.

We have studied the MO activity upon plasmon excitation in magnetoplasmonic nanodisk arrays. Such arrays have been fabricated in large area onto glass substrates by combining colloidal lithography with deposition under UHV and lift-off techniques. Each nanodisk is a Au (45nm-X)/Co(7nm)/Au (X)/Cr(2nm) multilayer with height=54nm and diameter=140nm, and for the sake of comparison, continuous thin films with identical composition have been also prepared (see Fig. 1(a) left and right, respectively).

The MO activity has been obtained by measuring the MO Kerr effect in polar configuration upon normal incidence illumination. With the help of extinction spectra, it has been checked that the maximum MO activity is in the same spectral range than the LSPR excitation. Fig. 1(b) shows the maximum MO activity as a function of the Co position for the nanodisk arrays as well as for the continuous films. The MO activity in the nanodisks depends on the position of the Co layers. It exhibits maximum values when the Co layer is located near the top or the bottom of the disks and minimum values in-between due to the LSPR excitation. This behavior is in contrast with the MO activity exhibited by the continuous films, which increases monotonously as the Co layer becomes closer to the top surface. This indicates that the EM field inside the nanodisks exhibits a nonuniform distribution in plasmon resonance conditions. In fact, the Co layer acts as a probe sensing the EM field within the nanodisk, since the MO activity depends on the intensity of such field.

This information could be very relevant for the design of magnetoplasmonic systems offering optimum MO enhancement, for instance for sensing applications where maximum sensitivity is expected in the areas with higher EM field.

References:

- [1] S. A. Maier, *Plasmonics: Fundamentals and Applications* (Springer, Berlin, 2007).
- [2] S. A. Maier and H. A. Atwater, *J. Appl. Phys.* 98, (2005) 011101.
- [3] G. A. Wurtz, W. Hendren, R. Pollard, R. Atkinson, L. Le Guyader, A. Kirilyuk, Th. Rasing, I. I. Smolyaninov and A. V. Zayats, *New J. of Phys.* 10 (2008) 105012.
- [4] J. B. González-Díaz, A. García-Martín, J. M. García-Martín, A. Cebollada, G. Armelles, B. Sepúlveda, Y. Alaverdyan and M. Käll, *Small* 4 (2008) 202.
- [5] G. Armelles, A. Cebollada, A. García-Martín, J. M. García-Martín, M. U. González, J. B. González-Díaz, E. Ferreiro-Vila and J. F. Torrado, *J. Opt. A: Pure Appl. Opt.* 11 (2009) 114023.

Figures:

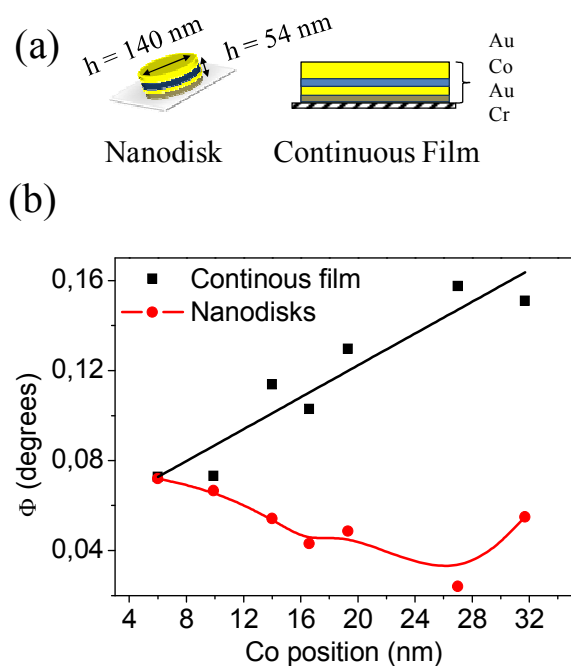


Figure 1: (a) Schemes of the Au/Co/Au/Cr magneto-plasmonic systems here studied: nanodisks and continuous films, respectively. (b) Maximum magneto-optical activity as a function of the Co position for both kinds of structures.

Célia Mercader¹, P. Poulin², P. Gaillard¹

¹CANOE (Consortium Aquitain en Nanomatériaux et électronique Organique),
16 avenue Pey Berland, 33600 Pessac, France

²Centre de Recherche Paul Pascal,
115 avenue Albert Schweitzer, 33600 Pessac, France

cmercader@enscbp.fr

Fibers and yarns are among the most promising forms for using carbon nanotubes (CNTs) on a macroscopic scale [1-8]. In analogy with high performance polymer, fiber spinning allows nanotubes to be preferentially oriented along the main axis of the fiber and then weaved into textile structures or used as cables.

We developed a new spinning method to produce fibers with a nanocomposite structure and with a high nanotube fraction. We spin continuous CNT fibers by a coagulation process which consists in injecting an aqueous dispersion of CNTs, polyvinyl alcohol (PVA) and surfactant in a static coagulation bath containing sodium sulphate. The used surfactant plays a critical role as the quality of the dispersion of the carbon nanotubes in the polymer is the key factor for a spinnable mixture. The surfactant leads to a good dispersion of the nanotubes and prevents from their coagulation in the presence of PVA in the dope material. In addition, it can be easily desorbed. The dope exhibits a homogeneous and aggregate free texture when observed with an optical microscope. This reflects the absence of aggregates larger than a micrometer typically. In the coagulation bath, all the nanotubes remain trapped in the coagulated PVA. The fiber is then washed, dried and collected as shown in figure 1. A 300 meters long fiber collected onto a winder is shown in figure 2. The fibers obtained by this continuous and robust process have a composite structure with large fraction of oriented CNTs, which can reach 50%, bound by the polymer, as shown in figure 3.

The diameter of the fibers can be varied from 10 to 100 μ m by changing the spinning conditions. The nanotubes are homogeneously distributed in the PVA matrix and their orientation along the fiber axis is about $\pm 10^\circ$. These fibers are electro conductive fibers with a resistivity of 10 Ω .cm and can be used for antistatic applications. CNT fibers exhibit also piezo-resistivity properties. This means that the resistivity of the fiber is sensitive to the mechanical loading. The electrical resistivity strongly increases with strain. This property makes CNT fibers good candidates for sensor applications. In addition, the mechanical properties are promising with a Young's modulus of 40GPa and a high toughness.

In order to validate these different applications, a large quantity of fibers is required but scaling up the process is very challenging. In this way, we are now building a multifilaments fiber spinning pilot unit on CANOE, a platform of technological innovation based in Pessac, near Bordeaux, focused on nanostructured materials. The objectives of the platform are to promote the emergence of an integrated value chain (from raw material to finished product) in the field of nanomaterials and more particularly of carbon nanotubes.

References:

- [1] H. Gommans et al., 2000, Journal of Applied Physics, 88, 2509.
- [2] B. Vigolo et al., 2000, Science, 290, 1331.
- [3] H. Zhu et al., 2002, Science, 296, 884.
- [4] K. Jiang et al., 2002, Nature, 419, 801.
- [5] Y. Li et al., 2004, Science, 304, 276.
- [6] L. Ericson et al., 2004, Science, 305, 1447.
- [7] M. Zhang et al., 2005, Science, 306, 1358-1361.
- [8] A. B. Dalton et al., 2003, Nature, 423, 703.

Figures:

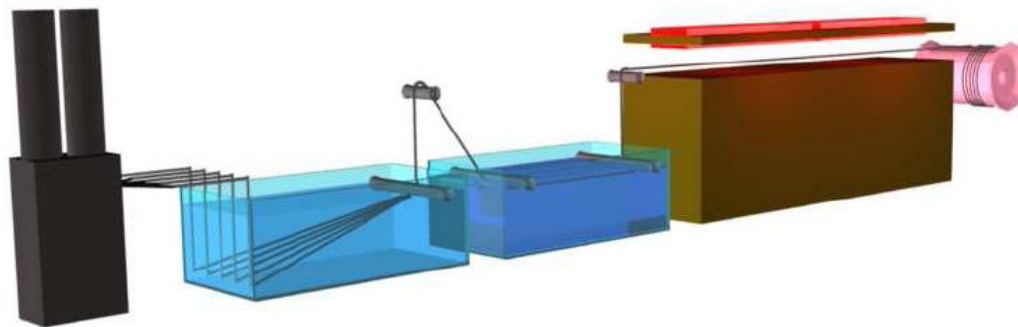


Figure 1: Scheme of the coagulation wet spinning process

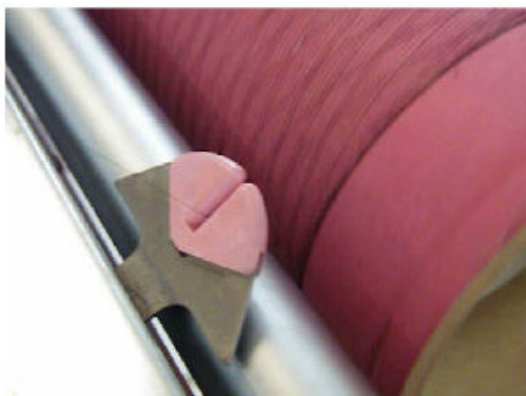


Figure 2: Collecting the composite CNT fiber on the winder

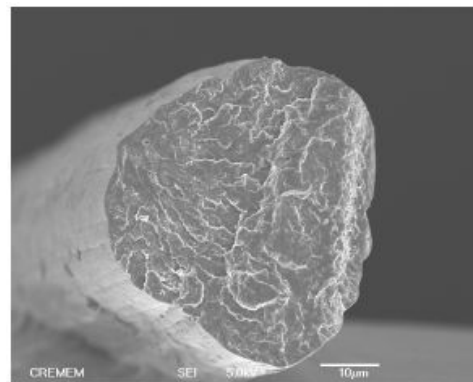


Figure 3: SEM picture o the cross section of the composite CNT fiber

W. I. Milne^{1,2}, D. Hasko¹, M. Cole¹, Chi Li¹, Ke Qu¹ and Y. Zhang¹

¹Electrical Engineering Division Building, University of Cambridge, 9 JJ Thomson Avenue, Cambridge CB3 0FA, UK

²Kyung Hee University, Dept. Information Display, Seoul 130701, South Korea

Semiconductor The aim of this paper is to describe the growth and optimization of carbon nanotube (CNT) based nanostructures to produce novel electron sources for use in a variety of applications including, Electron microscopy, e-beam lithography, travelling wave tubes (TWTs), backlighting and x-ray sources.

Because of their unique properties including their shape and current carrying capabilities Carbon Nanotubes are ideal as electron sources. The emitters studied in this project include spaghetti type layers of CNTs and regular array of vertically aligned CNTs. They will also include CNT/ZnO nanostructures as alternative sources. The objectives of this work are to develop a cathode that is able to deliver a stable current density of $> 1\text{A}/\text{cm}^2$ at DC and even higher in pulsed mode and to produce cheap, stable light emission sources for lighting applications such as backlighting which are able to run at comparatively high pressures to provide $1\text{mA}/\text{cm}^2$. In order to attain the large current densities with reasonable uniformities and long life time required for application to X-ray sources, it is necessary to prevent the best CNT emitters in the array from emitting too large a current by use of an integrated ballast resistor. In this paper we will also describe our recent work in this area.

Although we can get significant emission from the spaghetti type layers of CNTs, which are suitable for use in backlight structures in AMLCDs, as shown in Figure 1 (a), the CNTs we have investigated most frequently are in arrays which are vertically aligned, as previously described in reference [1]. Such a cathode design allows us to minimize the electric field shielding effects and lead to the higher current densities needed in TWTs and X-ray sources. A typical array is shown in Figure 1(b).

A smaller version of such an array consisting of a $22.5\ \mu\text{m} \times 22.5\ \mu\text{m}$ array of CNTs spaced $2.5\ \mu\text{m}$ apart providing 100 CNTs, produced a current density of $18\text{A}/\text{cm}^2$ at $9\text{V}/\mu\text{m}$. In order to attain such large current densities with reasonable uniformities and long lifetimes, however, it is necessary to prevent the best CNT emitters in the array from emitting a current larger than the current which induces their destruction (around $100\ \mu\text{A}$). To solve this problem, a ballast resistor must be integrated.

Our initial efforts to produce the ballast resistor structure was based on an SOI (undoped-Si/SiO₂/Si) substrate employing electron beam lithography and plasma enhanced chemical vapour deposition (PECVD) - see Figure 2. First, a catalyst dot array similar to that shown in Figure 1(b) was produced using e-beam lithography and Ni metal sputtering. Finally, a top-contact layer of tungsten was used to bias the CNTs, with the gap between the tungsten and CNTs of undoped Si acting as the ballast resistor.

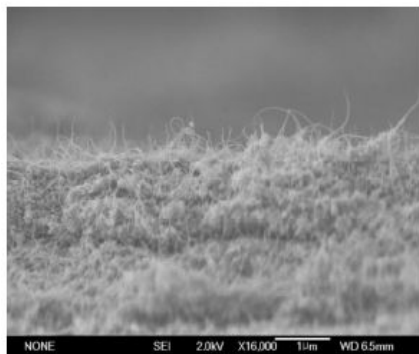
However, the fabrication process for this structure is very complex. This may be acceptable for expensive x-ray sources and Travelling Wave Tubes, but is undesirable for lighting applications and thus a novel, but simpler structure, incorporating a combination of Carbon Nanotubes and ZnO nanowires, has been produced for this application.

Firstly a CNT array such as the one shown above in Figure 1(b) was produced and then ZnO nanowires were grown onto these using a simple hydrothermal method to produce the arrays shown in Figure 3. A solution of zinc acetate dehydrate (98%, Aldrich) in 1-propanol (spectroscopic grade) was prepared. The solution was then spin coated onto the VACNF array at 2000 rpm for 30 s. The substrates were then annealed at 100°C for 2 minutes after each spin coating step to promote adhesion. A uniform seed layer was obtained after three layers of spin coating. The ZnO nanowires were then grown by dipping the substrates in an equimolar mixture of 25 nM zinc nitrate hexahydrate (Zn(NO₃)₂·6H₂O, Sigma Aldrich) and hexamethylenetetramine (HTMA, Sigma Aldrich) in deionized (DI) water heated in an oven at 80°C .

This presentation will therefore describe the growth and production of the CNT emitters, their optimisation and their use in electron microscope sources, parallel e-beam lithography, travelling wave tubes, portable X-ray sources and backlights.

Figures:

(a)



(b)

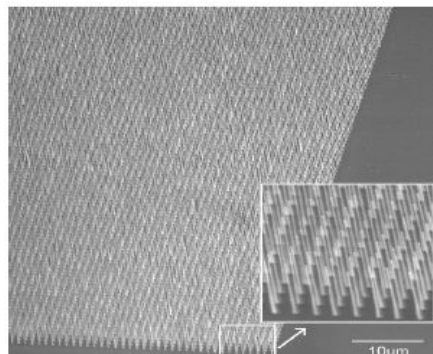


Figure 1: (a) Spaghetti type CNTs; (b) Vertical array of MWCNTs

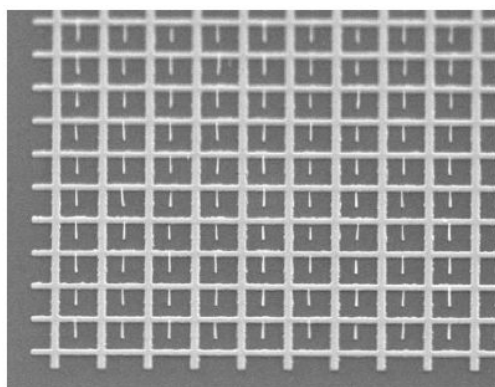


Figure 2: An array of CNTs grown on undoped SOI

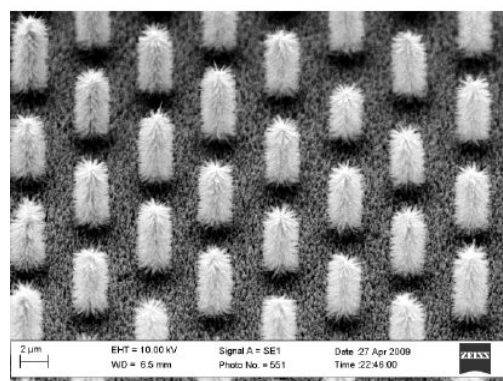


Figure 3: ZnO coated CNT array

TUNING WRITING MAGNETIC FIELDS IN MULTI-STATE STORAGE MEDIA

R. Morales^{1,2}, M. Kovylna³, Z.-P. Li⁴, M. Erekhinsky⁴, J. E. Villegas⁵, A. Labarta³, X. Batlle³, and Ivan K. Schuller⁴

¹Dpto. de Química-Física, Universidad del País Vasco, 48940 Leioa, Spain.

²IKERBASQUE, Basque Foundation for Science, 48011 Bilbao, Spain.

³Departament de Física Fonamental and Institut de Nanociència i Nanotecnologia, Universitat de Barcelona, 08028 Barcelona, Catalonia, Spain

⁴Physics Department, University of California San Diego, La Jolla 92093 CA, USA

⁵Unité Mixte de Physique CNRS/Thales, Université Paris Sud, 91405 Orsay, France

rafael_morales@ehu.es

Antiferromagnetic/ferromagnetic (AF/FM) bilayers exhibiting both negative and positive exchange bias have been proposed as multi-state storage media [1]. In such media the same magnetic region or element can store more than two digits. Thus, a track length comprising 8 magnetic elements stores up to $2^8 = 256$ bytes in regular media, whilst in a threefold multi-state system it could store up to $3^8 = 6561$ combinations, that could be called Tits (Ternary Digits). A multi-state digit is defined by the remanent magnetization (M_s) of the magnetic element. M_s is determined by the external field (H_{FC}) applied while cooling the AF/FM bilayer through the AF Néel temperature. A low H_{FC} yields a FM hysteresis loop with negative exchange bias providing a state with the highest M_s value (Fig. 1, $H_{FC} = 0.5$ kOe). High H_{FC} leads to a loop with positive exchange bias giving a digit with the lowest M_s (Fig. 1, $H_{FC} = 5.0$ kOe). States in-between can be defined either by a fractional value of M_s or even by a null remanence, by applying intermediate cooling fields (Fig. 1, $H_{FC} = 2.0$ kOe).

The minimum H_{FC} necessary to obtain positive exchange bias establishes the magnetic field required for multi-state storage writing. In continuous thin films it depends on structural parameters. However, we demonstrate in this work that this minimum H_{FC} yielding positive exchange bias can be tuned by patterning the continuous bilayer. It will be showed that both dots and antidots nanostructures reduce the writing magnetic field of all multi-states. The writing magnetic field decreases either as the dot size decreases or as the antidot density increases. [2,3] These findings are explained upon energy considerations of buried and bare pinned uncompensated spins in the AF.

Work supported by U.S. DOE, Spanish MICINN (MAT2009-08667 and FIS2008-06249), Catalan DURSÍ (2009SGR856), U.S. Air Force Office for Scientific Research, and IKERBASQUE Basque Foundation for Science.

References:

- [1] I. V. Roshchin, O. Petravic, R. Morales, Z.-P. Li, X. Batlle, I. K. Schuller, US Patent Number 7,764,454.
- [2] Z.-P. Li, R. Morales, and I. K. Schuller, Appl. Phys. Lett. 94 (2009) 142503
- [3] M. Kovylna, M. Erekhinsky, R. Morales, J. E. Villegas, I. K. Schuller, A. Labarta, and X. Batlle, Appl. Phys. Lett. 95 (2009) 152507

Figures:

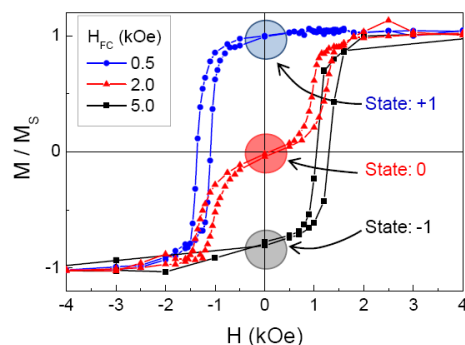


Figure 1: Three hysteresis loops of a continuous FeF_2/Ni bilayer for different cooling fields. These cooling fields defined a threefold multi-state.

EULER BUCKLING INSTABILITY AND ENHANCED CURRENT BLOCKADE IN SUSPENDED SINGLE-ELECTRON TRANSISTORS

F. Pistolesi, G. Weick, and F. von Oppen

Laboratoire d'Ondes et Matière d'Aquitaine, Université de Bordeaux 1 and CNRS,
Talence France

Fabio.Pistolesi@u-bordeaux1.fr

Single-electron transistors embedded in a suspended nanobeam or carbon nanotube may exhibit effects originating from the coupling of the electronic degrees of freedom to the mechanical oscillations of the suspended structure. Here, we investigate theoretically the consequences of a capacitive electromechanical interaction when the supporting beam is brought close to the Euler buckling instability by a lateral compressive strain (see Fig.1). Our central result is that the low-bias current blockade, originating from the electromechanical coupling for the classical resonator, is strongly enhanced near the Euler instability. We predict that the bias voltage below which transport is blocked increases by orders of magnitude for typical parameters (see Fig. 2). This mechanism may make the otherwise elusive classical current blockade experimentally observable.

References:

- [1] G. Weick, F. von Oppen, F. Pistolesi, Phys. Rev. B, in press (2011)
- [2] G. Weick, F. Pistolesi, E. Mariani, F. von Oppen, Phys. Rev. B 81, 121409 (R) (2010)
- [3] F. Pistolesi, Y. Blanter, and I. Martin, Phys. Rev. B 79 085127 (2008)
- [4] F. Pistolesi and S. Labarthe, Phys. Rev. B 76 165317 (2007)

Figures:

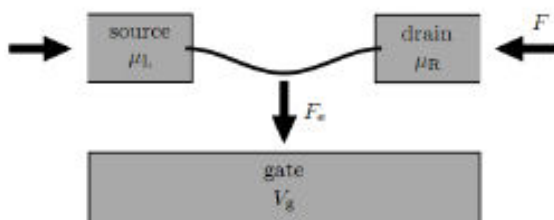


Figure 1: Sketch of the considered system: a suspended doubly-clamped beam forming a quantum dot electrically connected to source and drain electrodes. The beam is capacitively coupled to a metallic gate kept at a voltage V_g , which induces a force F_e that attracts the beam towards the gate electrode. An additional, externally controlled compressional force F acts on the beam and induces a buckling instability.

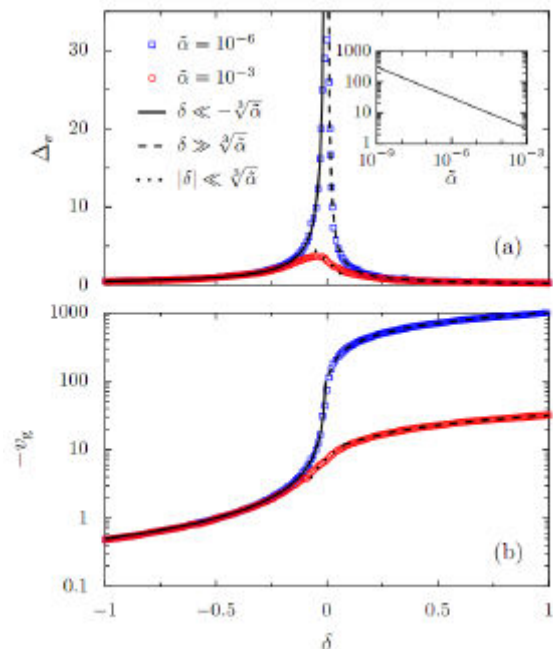


Figure 2: Gap (a) and gate voltage position of the minimum gap in dimensionless units (b) as a function of the dimensionless distance from the transition point: $\delta = F/F_{c-1}$, where F is the force acting on the rod, and F_c is the critical force. One can clearly see a great enhancement of the gap of the order of 30 times the original value at the transition point. The red and blue curves correspond to different values of the non-linear coupling.

A NOVEL DNA CHIP FOR SINGLE MOLECULE ANALYSIS

T.Plénat^{1,2}, C.Tardin^{1,2}, C.Vieu^{3,2}, C.Thibault^{3,2}, E.Trévisiol^{3,4} and L.Salomé^{1,2}

¹CNRS; IPBS (Institute of Pharmacology and Structural Biology); 205 route de Narbonne, F-31077 Toulouse, France

²University of Toulouse; UPS; IPBS; F-31077 Toulouse, France

³LAAS, Nanobiosystems, 7, Avenue du Colonel Roche, F-31077 Toulouse, France

⁴UMR 5504, UMR 792, Ingénierie des Systèmes Biologiques et des Procédés & Plate-forme Biopuces, CNRS, INRA, INSA, 135, avenue de Rangueil, 31077 Toulouse, France

plenat@ipbs.fr salome@ipbs.fr

The last two decades have seen the emergence of single-molecule experiments [1]. By avoiding the ensemble averaging inherent to traditional bulk-phase biochemistry, the study of molecular machineries at the single-molecule level permits a better understanding of the behavior of living systems. Indeed the dynamics of the machineries processes can be characterized and rare subpopulations can be identified [2].

One of the main shortcoming of single molecule experiments is that the acquisition of statistically solid data is very time consuming, which explains the fact that they are still not widely used in laboratories.

We will present the development of a new single DNA chip, allowing the simultaneous analysis of hundreds of single DNA molecules by the Tethered Particle Motion (TPM) technique. Our single DNA chip gives high-throughput capabilities to this approach of valuable interest for multiple applications.

The principle of a TPM experiment consists in tracking a bead tethered at the free end of a DNA molecule which is immobilized by the other end to a coverslip thanks to optical videomicroscopy. The amplitude of the Brownian motion of the bead is related to the effective length of the DNA molecule [3]. Any conformational change of the DNA molecule due to external factors (proteins, ions, temperature), that induces a variation of the effective length of the DNA tether, can be thus monitored by TPM [4].

References:

- [1] Cornish, P. V.; Ha, T., *Acs Chemical Biology* 1 (2007) 53
- [2] van Oijen, A. M., *Nature Chemical Biology*, 8 (2008) 440
- [3] Yin, H.; Landick, R.; Gelles, J., *Biophys J*, 6 (1994) 2468
- [4] Pouget, N. et al.; *Nucleic Acid Res.*, 9 (2004) e73

QUANTUM TRANSPORT AND HIGH MAGNETIC FIELD PHENOMENA IN CARBON NANOTUBES AND NANO-RIBBONS

Bertrand Raquet

Laboratoire National des Champs Magnétiques Intenses – Toulouse, LNCMI-T
UMR 3228, CNRS, UPS, INSA, Université de Toulouse, France

Over the last two decades, new forms of carbon, fullerenes, carbon nanotubes (CNT), isolated graphene flakes and more recently graphene nanoribbons (GNR) have been synthesized, manipulated and electrically connected. Their fundamental studies unravel remarkable electronic properties resulting from the electronic confinement at nano-scale and the electronic band structure of graphene. The feasibility of room temperature carbon based field effects transistors and inter-connexions have been demonstrated while their industrial integration as elementary bricks of new devices raises severe technological issues.

In this talk, after a brief comparative description of the electronic band structure of carbon nanotubes and graphene nano-ribbons, I will focus on (magneto)-transport experiments performed on individually connected CNTs and GNRs. I will show that magneto-transport in the high magnetic field regime along with an electrostatic control of the electronic doping is an outstanding probe of the 1-D electronic band structure and its unusual magnetic field dependence.

An applied magnetic field along the CNT axis induces giant quantum flux modulation of the conductance due to the periodic energy gap modulation at the charge neutrality point [1]. This so-called Aharonov-bohm effect is also an efficient tool to identify the metallicity of the external shell of a multi-walled carbon nanotube and to infer the locations of the different 1-D subbands [2]. By rotating the CNT perpendicular to the magnetic field, the energy gap of a semiconducting CNT is progressively reduced due to the onset of the first Landau level at zero energy and propagating Landau states develop at the flank of the tube [3]. Concerning (magneto)-transport experiments on GNR, I will present compelling evidences of the 1D transport character in the first generation of chemically derived GNRs with smooth edges and the possibility of tuning backscattering effects by means of an external magnetic field [4]. These experiments enlighten the richness of the electronic transport measurements on an individual nano-object in presence of a large magnetic confinement.

References:

- [1] M. Sagnes & al, Phys. Rev. Lett. 94, 066801 (2005); B. Lassagne & al, Phys. Rev. Lett. 98, 176802 (2007)
- [2] S. Nanot & al, C. R. Physique 10 (2009).
- [3] B. Raquet & al, Phys. Rev. Lett. 101, 046803 (2008); S. Nanot & al, Phys. Rev. Lett. 103, 256801 (2009)
- [4] J-M Poumirol et al, Phys. Rev. B 82, 041413(R) (2010)

ONE-STEP SYNTHESIS OF JANUS NANOPARTICLES BY SELF-ASSEMBLY MONOLAYERS

Javier Reguera^{1,2}, Miao Yu^{1,2}, Ines Pons-Siepermann³, Sharon C. Glotzer^{3,4}, Francesco Stellacci^{1,2}

¹SUNMAG, DMSE, Massachusetts Institute of Technology, 77 Mass. Av., Cambridge, MA (USA)

²SUNMIL, IMX, École Polytechnique Fédérale de Lausanne, Lausanne, Switzerland

³Department of Chemical Engineering, University of Michigan, Michigan, USA

⁴Department of Materials Science and Engineering, University of Michigan, Michigan, USA

jreguera@mit.edu

Described first by De Gennes[1] Janus Nanoparticles (Janus NPs) are called like the Roman God custodian of universe, God of gates and doors, beginnings and endings and hence represented with a double-faced head. Janus Nanoparticles are therefore particles with two distinct sides. The term Janus has been used to describe different particles such as dendritic macromolecules, block-copolymers micelles, or inorganic materials. The asymmetry generated in these particles is useful in wide range of applications. The most known is probably the one that uses the so-called Pickering effect, [2] that is, particles can be used to stabilize oil-in-water and water-in-oil emulsions. It has been demonstrated theoretically and experimentally that this stabilization is much higher when it is done by amphiphilic Janus nanoparticles instead of homogeneous particles, due to the higher adsorption energy of the particles at the liquid-liquid interface. These stabilized droplets could be used for diverse applications from water-based paints to heterogeneous nanocatalysis. The Janus nanoparticles can also be used in other important fields like electronic displays, nanomotors, drug or gene delivery or as building blocks for assembly of suprastructures. [3]

Up to now a few different strategies to obtain Janus nanoparticles have been described in the literature that can be included in one of these groups: toposelective surface modification that includes: 1. selective masking, use of reactive directional fluxes, microcontact printing or arrangement of the particle along an interface and partial contact with a reactive medium; 2. template-directed self-assembly; controlled phase separation phenomena; 3. and controlled surface nucleation. [3] There are several problems related to these strategies like the difficulty to obtain small nanoparticles (<10nm); the complexity of the synthesis methods that involves first the synthesis of symmetric particles (homogenous or core-shell) and then a posterior modification; and the low yield of this strategies due to the fact that most of them require the use of a surface where the particles are placed to avoid the reaction of one of the sides. To the best of our knowledge none of these strategies has the ability of producing truly large nanoparticle quantities in an easy way, as a direct synthesis can do. [3]

In our group it has been reported previously that when a metallic nanoparticle is synthesized with mixture of dislike ligands, there is a self-assembly with the formation of stripes on the topology of the nanoparticle.[4-7] However this is not the only possible topological conformation, depending on the parameters of the particle (ligand lengths, ligands functionality or surface curvature) other self-assembly structures such as Janus or random domains are also possible. [6] Here we report the synthesis of Janus Nanoparticles with the use of self-assembly monolayers (SAMs) composed of two types of ligand molecules of different length. The particles have been synthesized using a modification of the method described by Zheng et al. [8] extended to mixtures of ligands. This synthesis is an easy one-step, onephase synthesis for monodisperse metallic nanoparticles of small size (<10 nm) that can be scaled up to produce enough particles for useful applications and that can be extended to different functionalities. The two ligands used here were 1-hexanethiol (HT) and 1-dodecanethiol (DDT). TEM images were used to calculate the size and size distribution of the particle. [1] H NMR spectroscopy after particle decomposition was used to calculate the ligand ratio. Once synthesized the particles were deposited on gold-on-mica substrates using Langmuir-Blodgett deposition and then imaged using STM. The phase separation calculations were made using mesoscale simulations.

Figure 1 shows a representative STM image of a monolayer of nanoparticles made of 1:2 HT:DDT (ratio in solution). As we can see in the image the particles tend to order in a hexagonal lattice due to the monodispersity of the nanoparticles. The most interesting feature of these NPs is however the existence of two clear phases, a big one that corresponds to the DDT ligand and an small and circular one (on the left size of the particles) that correspond to the HT ligand. To be sure this was a real feature and not an artifact several images were taken in different areas and with different tips, in

In addition, these features were seen with two different STM microscopes: a Veeco Multimode in air and an Omicron in ultra high vacuum (UHV). We have also seen that the amount of Janus NPs depends on the ratio between ligands being bigger for mixtures far from the 1:1 ligands' ratio. Mesoscale simulations have shown the formation of Janus Nanoparticles for high values of the interaction parameter of the ligands. In our case the high difference in ligands length, and therefore high differences in the enthalpic component of the phase separation makes this parameter to be high enough to make a complete phase-separation of the two ligands.

This new way to obtain Janus nanoparticles has a really high potential to be used in several applications due to its simplicity, scalability and variability of ligands and therefore functionalities that can be used.

References:

- [1] de Gennes, P. G. *Reviews of Modern Physics*, 64, (1992), 645.
- [2] Pickering, S. U. *Journal of the Chemical Society*, 91, (1907), 2001-2021.
- [3] Perro, A.; Reculosa, S.; Ravaine, S.; Bourgeat-Lami, E. B.; Duguet, E. *Journal of Materials Chemistry*, 15, (2005), 3745-3760.
- [4] Jackson, A. M.; Myerson, J. W.; Stellacci, F. *Nature Materials*, 3, (2004), 330-336.
- [5] DeVries, G. A.; Brunnbauer, M.; Hu, Y.; Jackson, A. M.; Long, B.; Neltner, B. T.; Uzun, O.; Wunsch, B. H.; Stellacci, F. *Science*, 315, (2007), 358-361.
- [6] Singh, C.; Ghorai, P. K.; Horsch, M. A.; Jackson, A. M.; Larson, R. G.; Stellacci, F.; Glotzer, S. C. *Physical Review Letters*, 99, (2007), 226106.
- [7] Carney, R. P.; DeVries, G. A.; Dubois, C.; Kim, H.; Kim, J. Y.; Singh, C.; Ghorai, P. K.; Tracy, J. B.; Stiles, R. L.; Murray, R. W.; Glotzer, S. C.; Stellacci, F. *Journal of the American Chemical Society*, 130, (2008), 798-799.
- [8] Zheng, N.; Fan, J.; Stucky, G. D. *Journal of the American Chemical Society*, 128, (2006), 6550-6551.

Figures:

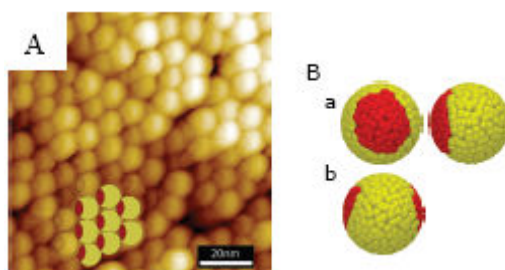


Figure 1: A) STM image of a monolayer of nanoparticles 1:2 HT:DDT Janus NPs (The cartoon has been drawn to help the reader to identify the Janus NPs). B) Mesoscale simulation of the same particles showing a phase separation in equilibrium with distributions in 2 or 3 domains (a and b respectively).

GAS SENSOR FOR FOOD INDUSTRY AND AGRICULTURE BASED ON ZnO NANOPARTICLES AND NANORODS

Andrey Ryzhikov, Pierre Fau, Myrtil Kahn, Katia Fajerweg, Bruno Chaudret, Philippe Ménini*, Chang-Hyun Shim*, Alain Gaudon**

Laboratoire de Chimie de Coordination, 205 route de Narbonne, Toulouse, France;

*LAAS-CNRS, UPS, Université de Toulouse; **Alpha MOS

andrey.ryzhikov@lcc-toulouse.fr

Semiconductor gas sensors can be widely used in food industry and agriculture. Measurements of ethylene concentration in vegetable stores and greenhouses allow the control of fruit ripening, whereas detection of H₂S, mercaptans, amines may be used to control of meat, fish and vegetable freshness. In this work we present a new generation of semiconductor gas sensors based on the combination of micromachined silicon substrates [1] and highly sensitive layer of ZnO nanoparticles. ZnO nanoparticles displaying 3 different morphologies (cloudy-like structures, size controlled isotropic particles and nanorods (Fig. 1)) were obtained through the controlled hydrolysis reaction of an organometallic precursor, namely the biscyclohexyl zinc, in the presence of various levels of long-chain amines surfactants [2]. ZnO nanopowders were deposited by a generic ink-jet method on low power consumption silicon substrates. High quality and micron thick layers have been obtained with a low defect level (no cracks, no delamination). The sensor responses to reducing gases (CO, propane, ammonia, ethylene, and acetaldehyde) have been studied in relation with the morphology of ZnO nanocrystals. Cloudy-like ZnO sensors showed a high response to ammonia vapors (20 ppm), whereas isotropic nanoparticles possessed the highest response to acetaldehyde gas (10ppm) and nanorods based layers displayed a higher sensitivity to ethylene (50ppm). These variations can be associated with the different ratios of crystalline faces exposed to reactive gases. These results open the route to the fabrication of a multisensor system based on pure ZnO nanoparticles with different shapes for the detection of reducing gases in complex mixtures.

References:

- [1] Ph. Ménini et al., Eurosensors XXII proceedings, 2008, 342
- [2] M. Monge et al., Angew. Chem. Int. Ed., 2003, 42, 5321

Figures:

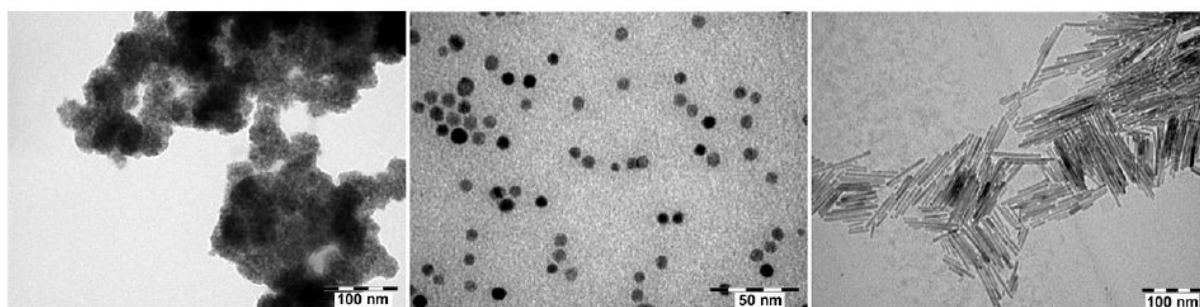


Figure 1: ZnO cloudy-like structures, isotropic nanoparticles and nanorods

NEW INSIGHTS INTO NANOMAGNETISM BY SPIN-POLARIZED SCANNING TUNNELING MICROSCOPY AND SPECTROSCOPY

Dirk Sander, Hirofumi Oka, Pavel Ignatiev, Safia Ouazi, Jérôme Borme **, Sebastian Wedekind, Guillemin Rodary*, Larissa Niebergall, Valeri Stepanyuk, and Jürgen Kirschner

Max-Planck-Institute of Microstructure Physics, Halle, Germany

*present address: LPN, CNRS UPR20, Marcoussis, France

**permanent address: Iberian Nanotechnology Laboratory, Braga, Portugal

sander@mpi-halle.de

Spin-polarized scanning tunneling microscopy (SP-STM) allows imaging and spectroscopic characterization of nanostructures with unsurpassed spatial resolution. Its working principle exploits the dependence of the tunnel current on the relative magnetization orientation of a sample and the magnetic STM tip. We present results by SP-STM, where we investigate the correlation between structural, electronic, and magnetic properties of individual nm small Co islands with several hundred to thousands of atoms. We use external magnetic fields of up to 4 T to tune the magnetic state of both tip and sample, and we extract the corresponding change of the differential conductance of the tunnel junction.

A recent example is our measurement of magnetic hysteresis loops of individual nm small Co islands on Cu(111) at 8 K by SP-STM in external magnetic fields. We find switching fields of up to 2.5 T for islands with roughly 8,000 atoms. The quantitative analysis of these results provides novel insights into the magnetization reversal on the nanoscale, and deviations from the venerable Stoner-Wohlfarth model are discussed.

We also exploit the high spatial resolution of SP-STM in magnetic fields to measure maps of the differential conductance within a single nm-small Co island for different magnetization states. In connection with density functional theory calculations we demonstrate that the spin polarization is not homogeneous but spatially modulated within the Co island, as indicated in Fig. 1. We ascribe the spatial modulation of the spin polarization to spin-dependent electron confinement within the Co island [1].

References:

- [1] Oka, Ignatiev, Wedekind, Rodary, Niebergall, Stepanyuk, Sander, Kirschner, Science 327(2010) 347

Figures:

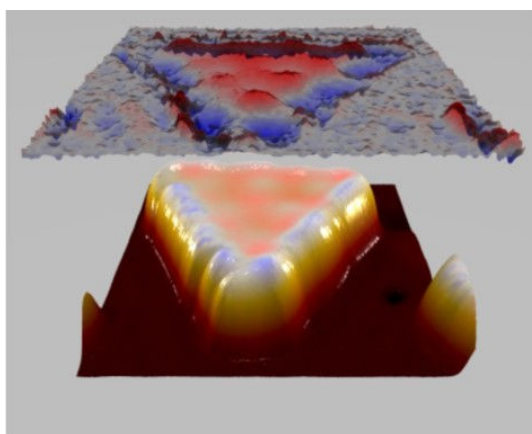


Figure 1: Superposition of a 3D-topographic representation of a bilayer high Co island with a base length of 12 nm from STM topography (bottom) with a map of the asymmetry of the differential conductance measured at the Fermi energy (top). Blue: negative; red: positive, gray: zero asymmetry. The top map reflects a spatial modulation of the spin-polarization, induced by spin-dependent electron confinement within the Co island [1].

DOXORUBICIN LOADED MAGNETIC POLYMERSOMES: THERANOSTIC NANOCARRIERS FOR MR IMAGING AND MAGNETO-CHEMOTHERAPY

Olivier Sandre, Charles Sanson, Odile Diou, Julie Thévenot, Emmanuel Ibarboure, Alain Soum, Annie Brûlet, Sylvain Miraux, Eric Thiaudière, Sisareuth Tan, Alain Brisson and Sébastien Lecommandoux

Laboratoire de Chimie des Polymères Organiques (LCPO)
UMR5629 Université de Bordeaux / CNRS / Institut Polytechnique de Bordeaux,
ENSCBP – 16 avenue Pey Berland, 33600 Pessac, France

olivier.sandre@ipb.fr

Hydrophobically modified maghemite ($\gamma\text{-Fe}_2\text{O}_3$) nanoparticles were encapsulated within the membrane of poly(trimethylene carbonate)-*b*-poly(L-glutamic acid) (PTMC-*b*-PGA) block copolymer vesicles using a nanoprecipitation process. This formation method gives a simple access to highly magnetic nanoparticles (MNPs) (loaded up to 70 wt %) together with a good control over the vesicles size (100 to 400 nm). The simultaneous loading of maghemite nanoparticles and doxorubicin was also achieved by nanoprecipitation. The deformation of the vesicle membrane under an applied magnetic field has been evidenced by small angle neutron scattering. These superparamagnetic hybrid self-assemblies display enhanced contrast properties that open potential applications for Magnetic Resonance Imaging. They can also be guided in a magnetic field gradient. The feasibility of controlled drug release by radio-frequency magnetic hyperthermia was demonstrated in the case of encapsulated doxorubicin molecules, showing the viability of the concept of magneto-chemotherapy. These magnetic polymersomes can be used as efficient multifunctional nano-carriers for combined therapy and imaging.

References:

- [1] S. Lecommandoux, O. Sandre, F. Chécot, J. Rodriguez-Hernandez, R. Perzynski, *Adv. Mat.*, 17 (2005), 712-718.
- [2] S. Lecommandoux, O. Sandre, F. Chécot, J. Rodriguez-Hernandez, R. Perzynski, *Journal of Magnetism and Magnetic Materials* 300 (2006), 71-74.
- [3] S. Lecommandoux, O. Sandre, F. Chécot, R. Perzynski, *Progress in Solid State Chemistry*, 34 (2006), 171-179.
- [4] C. Sanson, J-F. Le Meins, C. Schatz, A. Soum, S. Lecommandoux, *Soft Matter*, 6 (2010), 1722-1730
- [5] C. Sanson, C. Schatz, J-F. Le Meins, A. Brûlet, A. Soum, S. Lecommandoux, *Langmuir* 26 (2010), 2751-2760.
- [6] C. Sanson, C. Schatz, J-F. Meins, A. Soum, E. Garanger, J. Thévenot, S. Lecommandoux. *Journal of Controlled Release*, 147 (2010), 428-435.
- [7] C. Sanson, O. Diou, J. Thévenot, E. Ibarboure, A. Soum, A. Brûlet, S. Miraux, E. Thiaudière, S. Tan, A. Brisson, V. Dupuis, O. Sandre, S. Lecommandoux, *ACS Nano*, Published online (2011), doi: 10.1021/nn102762f.

Figures:

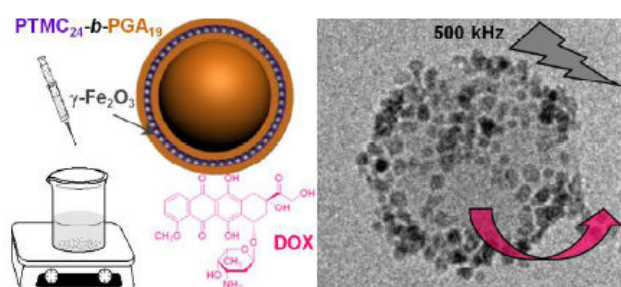


Figure 1: Left: Sketch of dually-loaded vesicles prepared by addition of an aqueous buffer into a mixture of PTMC-*b*-PGA copolymer, hydrophobically coated magnetic nanoparticles and doxorubicin drug. Right: Cryo-TEM image of vesicle showing the dense mantle of MNPs, which excitation by a radiofrequency magnetic field transmits heat locally to membrane and accelerates the DOX release.

ATOMIC-SCALE CONTROL OF MOLECULAR CONTACTS

Guillaume Schull¹, Thomas Frederiksen², Andrés Arnau^{2,3,4}, Daniel Sanchez-Portal^{2,3}, Mads Brandbyge⁵, Natalia Schneider⁶, Richard Berndt⁶

¹Institut de Physique et Chimie des Matériaux de Strasbourg, UMR 7504 (CNRS -- Université de Strasbourg), 67034 Strasbourg, France

²Donostia International Physics Center (DIPC), 20018 San Sebastian, Spain

³Centro de Física de Materiales CSIC-UPV/EHU, Materials Physics Center MPC, 20080 San Sebastian, Spain

⁴Depto. Física de Materiales UPV/EHU, Facultad de Química, 20080 San Sebastian, Spain

⁵DTU Nanotech, Technical University of Denmark, DK-2800 Kongens Lyngby, Denmark

⁶Inst für Experimentelle und Angewandte Physik, Christian-Albrechts-Universität, 24098 Kiel, Germany
guillaume.schull@ipcms.u-strasbg.fr

The transport of charge through a conducting material depends on the intrinsic ability of the material to conduct current and on the charge injection efficiency at the contacts between the conductor and the electrodes. Exploring the single molecule limit in experiments requires control of the junction geometry. Scanning tunneling microscopy (STM) provides here a way to probe this parameter with atomic scale precision.

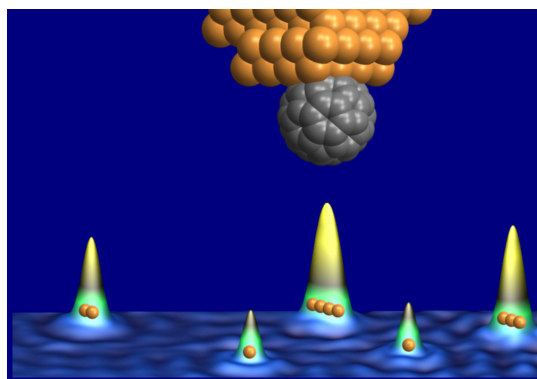
Using STM we will see that the current passing through a single molecule can be probed while changing, one by one, the number of atoms in the electrode that are in contact with a single molecule [1]. We show quantitatively that the contact geometry has a strong influence on the conductance. For C_{60} , this revealed a crossover from a regime in which the conductance is limited by charge injection at the contact to a regime in which the conductance is limited by scattering at the molecule. Thus, the concept of “good” and “bad” contacts, commonly used in macro-and mesoscopic physics, can also be applied at the molecular scale. In a second step, the transport properties of small chains made of two C_{60} trapped between the tip and the surface of a STM will be presented [2]. Here the orientation and electronic states of both molecules was characterized before connecting them with atomic-scale precision. The experimental results are complemented by first-principles transport calculations which give access to the distance-dependent nature of the inter-molecular electron transport and predict the evolution of the transport properties with molecular chain length. Finally, the properties of photons that are emitted at junctions bridged by a single metallic atoms [3,4] and the perspectives that it opens for molecular contacts will be evocated.

References:

- [1] Schull G, Frederiksen T, Arnau A, Sanchez-Portal D, Berndt R. Nature Nanotec. 6, (2011) 23
- [2] Schull G, Frederiksen T, Brandbyge M, Berndt R. Phys. Rev. Lett. 103, (2009) 206803
- [3] Schull G, Néel N, Johansson P, Berndt R. Phys. Rev. Lett. 102, (2009) 057401
- [4] Schneider N, Schull G Berndt R. Phys. Rev. Lett. 105, (2010) 026601

Figures:

Figure 1: Graphical representation of a scanning tunnelling microscope tip with a C_{60} molecule fixed to its apex, above a copper sample with five atomic scale electrodes engineered atom per atom.



EFFECT OF PHONON CONFINEMENT ON HEAT DISSIPATION IN RIDGES

Pierre-Olivier Chapuis^{(a),1,*}, Mika Prunnila^(b), Andrey Shchepetov^{(b),1}, Lars Schneider^(a), Sampo Laakso^(b), Jouni Ahopelto^(b), and Clivia M. Sotomayor Torres^(a, c, d)

^(a)Institut Català de Nanotecnologia (ICN), Centre d'Investigació en Nanociència e Nanotecnologia (CIN2), Campus UAB, 08193 Bellaterra (Barcelona), Spain

^(b)VTT Technical Research Center of Finland, PO Box 1000, 02044 VTT, Espoo, Finland

^(c)ICREA, Institució Catalana de Recerca i Estudis Avançats, 08010 Barcelona, Spain

^(d)Dept. of Physics, Universitat Autònoma de Barcelona, 08193 Bellaterra, Barcelona, Spain

¹These authors contributed equally

olivier.chapuis@cin2.es

We have investigated experimentally the effect of lateral confinement of acoustic phonons in ridges as a function of the temperature. Electrical methods are used to generate phonons in 100nm large nanostructures and to probe the nanostructure temperature in the same time, what allows tracking the heat flux generated and its possible deviation to Fourier diffusive heat conduction.

It is now well-established that Fourier's law of heat diffusion in solids breaks down when device sizes reaches the nanometer-scale [1]. Detailed studies of the characteristic lengths where the law has to be replaced or modified are required as these lengths might depend on the considered device geometries.

We have fabricated special devices made of nanostructured ridges on top of planar substrate as represented on Figure 1. The top of a ridge is a wire made either of metal or of doped silicon that acts as a heater and as a thermometer in the same time. The lower part that supports the wire is made of an etched part of the wafer substrate. This type of structure enables to generate phonons in the ridge and to measure the heat flux flowing to the substrate.

Different electrical methods such as the 3ω method [2] are used to heat the wire. The goal is then to measure a wire-voltage component (dc or ac) proportional to the wire temperature. A model enables then to link the wire temperature to the heat flux transmitted to the substrate. In addition to the localized heat source effect due to the sub-mean free path size of the source [3], we have investigated experimentally the consequences of the fact that the source cannot be considered as a proper heat bath at equilibrium.

We have quantified the effect as a function of the two characteristic numbers that can be associated with the problem, namely the constriction Knudsen number describing the transmission of the phonons and the nanostructure Knudsen number characterizing the nonequilibrium of the source. We compare our results with those of a recent theoretical paper [4] based on the ballistic-diffusive equations. The determination of the mean free paths of phonons as a function of the frequency remains a key point due to the consequences for heat transport and thermal management [1].

We observe a strong decrease of the thermal conductance through the ridge in comparison to a prediction based on the Fourier diffusive as expected. But, more strikingly, we also observe a decrease in comparison to the ballistic prediction. We aim at ascribing part of this decrease to an effect of phonon confinement in the ridge.

Acknowledgements:

We acknowledge the support of EU FP7 projects NANOPACK and NANOPOWER. We also acknowledge the support of Spanish MICINN project ACPHIN.

References:

- [1] D. G. Cahill, W. K. Ford, K. E. Goodson, G. D. Mahan, A. Majumdar, H. J. Maris, R. Merlin, S. R. Phillpot, *J. Applied Physics* 93, 793-818 (2003)
- [2] D. Cahill, *Rev. Scient. Instr.* 61, 802 (1990)
- [3] M.E. Siemens, Q. Li, R. Yang, K.A. Nelson, E.H. Anderson, M.M. Murnane, and H.C. Kapteyn, *Nature Materials* 9, 26 (2010)
- [4] S. Volz and P.O. Chapuis, *J. Applied Physics* 103, 34306 (2008)

Figures:

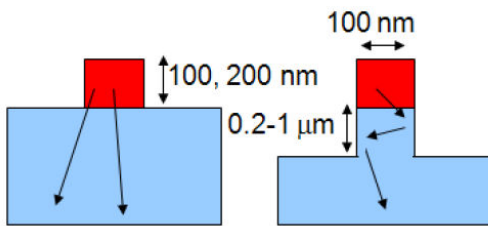


Figure 1: Schematic of the nanostructures

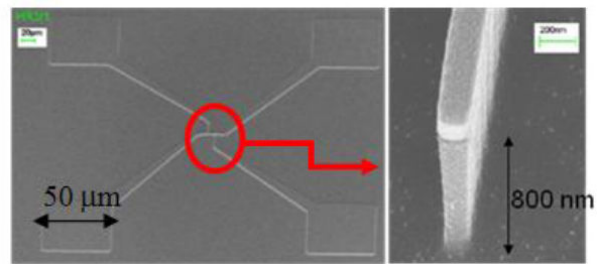


Figure 2: Electrical accesses and ridge before mask removal

ORIGIN AND EVOLUTION OF POSITIVE EXCHANGE BIAS IN EPITAXIAL (HCP)Co/CoO BI-LAYER STRUCTURES

A. K. Suszka, O. Idigoras and A. Berger

CIC nanoGUNE Consolider, Tolosa Hiribidea 76, E-20018 Donostia-San Sebastian, Spain
a.suszka@nanogune.eu

The phenomenon of unidirectional anisotropy of antiferromagnetic (AF)/ferromagnetic (FM) bi-layers, also referred to as exchange bias, is a prominent scientific and technological topic. Exchange biased magnetic thin films with uniaxial magnetic anisotropy (UA) are currently at the forefront of technology in magnetic recording and represent a challenge for scientific research. A relatively small number of experiments has been dedicated to study the exchange bias for systems with in-plane UA of the FM layer. Specifically, some recent studies focused on the competition of UA and exchange bias and revealed a distinct temperature dependence of uniaxial anisotropy at the interface of the FM layer that is in contact with the AF, for both out-of-plane [1] and in-plane magnetized thin films [2]. So far, however, very little work on the exchange bias has been done for Co/CoO structures in the presence of UA, even though Co/CoO-bilayers are the prototypical exchange bias system, and to our knowledge no previous work was dedicated to the study of (hcp) Co/CoO bi-layers with in-plane c-axis orientation [3].

Two types of multilayers with structure: Si-substrate/Ag(75nm)/Cr(50nm)/Co(12nm)/CoO(3nm) were grown by ultra high vacuum (UHV) sputtering. For one type of the multilayers, we modified the Co texture and consequently the UA by interrupting the epitaxial growth sequence in between the HFetched Si-substrate and Ag underlayer, specifically by exposing the substrate to an ultra-low power SiO₂ plasma for 30s prior to Ag deposition [4]. In this way, we fabricated samples with uniaxial (epitaxial structure) and isotropic (polycrystalline structure) magnetic characteristics as shown in figs. 1(a) and (b) respectively. X-ray diffraction studies confirm the Si(110)/Ag(110)/Cr(211)/Co(10 $\bar{1}$ 0) structure for samples without SiO₂ interlayer [4]. CoO was formed by natural oxidation in both types of multilayers. Samples were characterised using magneto-optical Kerr effect setup (MOKE), superconducting quantum interference device (SQUID), X-ray diffraction, ellipsometry and Kerr microscopy.

We measured hysteresis loops for epitaxial and polycrystalline samples as a function of temperature in the easy (EA) and hard axis (HA) magnetization direction. Epitaxial multilayer shows higher values of exchange bias (H_{ex}) and blocking temperature (T_B) in comparison with polycrystalline structures. In addition to that, a positive exchange bias is measured for the epitaxial structures in a certain temperature window while it is not observed in polycrystalline samples. Increasing the magnitude of the cooling field (FC) results in a decrease of the positive H_{ex} effect and causes a different transition temperature from positive to negative H_{ex} . We also find a direct relation between the asymmetry of the magnetization reversal process, and the enhancement of unidirectional anisotropy. Some previous reports suggested the existence of positive exchange bias due to anisotropic enhancement of the coercivity H_c [5]. This conclusion was originally supported by the existence of a peak in the coercivity around the positive H_{ex} . Here, we find a non-monotonous increase in the coercivity for the epitaxial sample. This is most pronounced in the hard axis magnetization direction (Figs. 2(a) and (b)). Changes in coercivity relate directly to the behavior of positive and negative switching fields as shown on figure 2 (c). Figure 2 (d) shows the extracted dm/dH of our hysteresis loops for different temperatures and reveals switching asymmetry near positive exchange bias. In current work we also analyze the magnetic characteristics of the EA for epitaxial structure and the exchange bias for polycrystalline sample. Each one of these cases shows different and unique evolution of exchange bias with varying temperature. The experimental results are analyzed in the framework of changes in magnetization states near interface of FM/AF and the influence of competition of uniaxial anisotropy and exchange bias on magnetization switching at various temperatures.

Acknowledgements:

We acknowledge funding from the ETORTEK Program, Project No. IE06-172, the Spanish Consolider-Ingenio 2010 Program, Project No. CSD2006-53 and the Basque Government fellowships No. BFI09.284.

References:

- [1] E. Sipton, K. Chan, T. Hauet, O. Hellwig, and E. E. Fullerton, Appl. Phys. Lett. 95, 132509 (2009)
- [2] M. Grimisditch, A. Hoffmann, P. Vavassori, H. Shi, and D. Lederman, Phys. Rev. Lett. 90, 257201 (2003)
- [3] F. Radu, M. Etzkorn, R. Siebrecht, T. Schmitte, K. Westerholt, and H. Zabel, Phys. Rev. B 67, 134409 (2003)
- [4] O. Idigoras, A. K. Suszka, J. M. Porro, P. Vavassori, and A. Berger, submitted to Phys. Rev. Lett.
- [5] T. Gredig, I. N. Krivorotov, P. Eames and E. D. Dahlberg, Appl. Phys. Lett. 81, 1270 (2002)
- [6] O. Idigoras, P. Vavassori, J. M. Porro, and A. Berger, J. Magn. Magn. Mater. 320, L57-L60 (2010)

Figures:

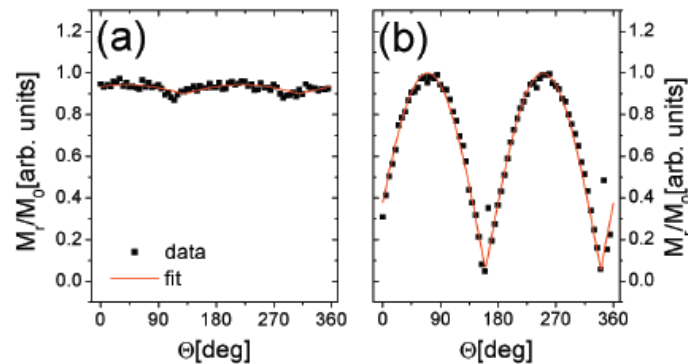


Figure 1: Normalized remanent magnetization (M_r/M_0) as a function of magnetic field orientation angle Θ for a polycrystalline (a) and an epitaxial (b) Co/CoO sample, measured at room temperature. Red line is a fit to the data ($M_r/M_0=a*\text{abs}(\cos(\Theta-\phi))+c$) following reference [6].

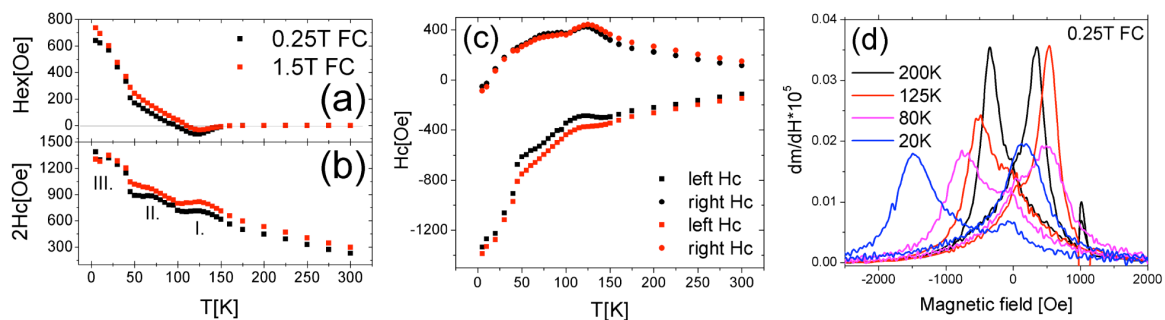


Figure 2: Exchange bias (a) and coercivity (b) as a function of temperature measured in the hard axis magnetization direction on an epitaxial sample for two cooling field values (0.25T and 1.5T), (c) left and right coercivity as a function of temperature for the same sample and orientation cooled at 0.25T (black) and 1.5T (red). (c) field derivative of hysteresis loops for an epitaxial sample cooled at 0.25T at different temperatures, revealing a substantial switching asymmetry in the region of positive exchange bias.

NOVEL PARADIGMS FOR BIOLOGICAL SENSING BASED ON NANOMECHANICAL SYSTEMS: FROM MICROCANTILEVERS TO NANOWIRES

Javier Tamayo, Eduardo Gil-Santos, Daniel Ramos, Priscila Kosaka, Valerio Pini, Johann Mertens, Sheila González and Montserrat Calleja

Instituto de Microelectrónica de Madrid (CSIC), Isaac Newton 8 (PTM), Tres Cantos, Spain

jtamayo@imm.cnm.csic.es

The development of ultrasensitive protein spectrometers and ultrasensitive biological sensors will speed up the identification of disease biomarkers and their rapid detection [1,2]. Nanomechanical resonators have emerged as promising candidates for ultrasensitive mass sensors [3,4]. The continuous advancements in top-down micro- and nanofabrication techniques has made possible increasingly smaller nanomechanical resonators with detection limits in the subattogram range. Moreover, resonant nanowires and nanotubes fabricated by bottom-up methods can weigh masses below a zeptogram ($1.66 \cdot 10^{-21}$ g). However, the implementation of these devices is hindered by several obstacles such as the need of operation in high vacuum, low specificity and low reproducibility and still little understanding of the effect of biomolecular adsorption on the mechanical properties of nanoresonators.

In this talk, I will present our recent developments oriented to apply nanomechanical systems for biological detection. In particular, I will present two novel paradigms for sensing that opens the door to develop ultrasensitive biological sensors. The first approach that is no longer depending on the extreme miniaturization of the devices is the use of coupled nanomechanical resonators fabricated by standard silicon technology [5,6] (Fig. 1). When the resonators are identical, the vibration of the eigenmodes is delocalized over the array. In a similar way to the Anderson's localization, the addition of the mass on one of the resonators leads to the spatial localization of the eigenmodes. Since vibration localization is insensitive to uniform adsorption, coupled nanomechanical resonators allows decoupling of unspecific and specific molecular adsorption in differentially sensitized resonators.

The second approach uses resonant nanowires/nanotubes and it is based on the fact that if a molecule alights on a perfectly axisymmetric resonant nanobeam, the frequency degeneration of the stochastic two-dimensional orbits is abruptly broken, and the vibration can be described as the superposition of two orthogonal vibrations with different frequency. The measurement of the frequency degeneration breakage enables the determination of the adsorbate's mass and stiffness, and the azimuthal direction from which the adsorbate arrives [7]. We experimentally demonstrate such sensing paradigm with resonant silicon nanowires, which serves to add kPa resolution in Young's modulus determination to their currently established zeptogram mass sensitivity. The proposed method provides a unique asset for ultrasensitive mass and stiffness spectrometry of biomolecules by using nanowire-like resonant structures.

References:

- [1] Naik, A., Hanay, M., Hiebert, W., Feng, X. & Roukes, M. Towards single-molecule nanomechanical mass spectrometry. *Nature Nanotechnology* 4, 445-450 (2009).
- [2] Mertens, J., Tamayo, J. et al. Label-free detection of DNA hybridization based on hydration-induced tension in nucleic acid films. *Nature Nanotechnology* 3, 301-307 (2008).
- [3] Tamayo, J. Nanomechanical systems: Inside track weighs in with solution. *Nature Nanotechnology* 2, 342-343 (2007).
- [4] Waggoner, P. & Craighead, H. Micro-and nanomechanical sensors for environmental, chemical, and biological detection. *Lab on a Chip* 7, 1238-1255 (2007).
- [5] Spletzer, M., Raman, A., Wu, A., Xu, X. & Reifenberger, R. Ultrasensitive mass sensing using mode localization in coupled microcantilevers. *Applied Physics Letters* 88, 254102 (2006).
- [6] Gil-Santos, E. et al. Mass sensing based on deterministic and stochastic responses of elastically coupled nanocantilevers. *Nano letters* 9, 4122-4127 (2009).
- [7] Gil-Santos, E., Tamayo, J. et al. Nanomechanical mass sensing and stiffness spectrometry based on two-dimensional vibrations of resonant nanowires. *Nature Nanotechnology* 5, 641-645 (2010).

Figures:

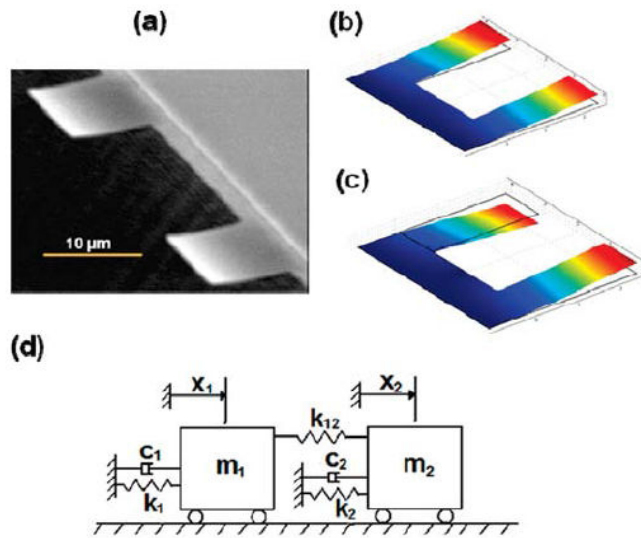


Figure 1: (a) Scanning electron micrograph of a system of coupled cantilevers. The cantilevers were fabricated in low stress silicon nitride. The length, width, and thickness of the cantilevers were 25, 10, and 0.1 μm , respectively. The gap between the cantilevers is 20 μm . The structural coupling between the cantilevers arises from the overhang connecting the cantilevers at the base, which is about 8 μm long. (b) Symmetric and (c) antisymmetric mode of vibration of this coupled array. (c) A lumped parameter model for this coupled array.

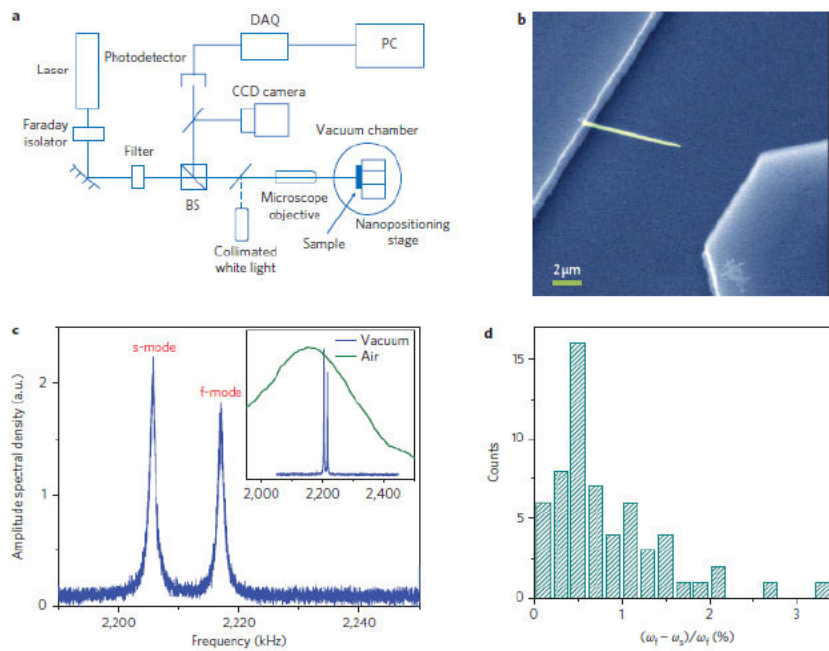


Figure 2: Thermal displacement fluctuations of silicon nanowires. a, Schematic of the optical interferometer used to detect the out-of-plane nanowire vibrations. The nanowire sample was placed in a vacuum chamber at approximately 1×10^{-6} torr and room temperature. The spot size was 0.7 μm and the incident power 0.5 mW. Picometre-scale modulation of the height of the nanowire above the substrate results in a measurable intensity modulation due to the interference between the light reflected from the nanowires and from the substrate. b, Scanning electron micrograph (SEM) of a typical nanowire used in this work. Nanowires anchored normal to the trench wall were selected, with lengths and diameters of 5–10 μm and 100–300 nm, respectively. c, A fast Fourier transform of the signal from the photodetector is dominated by the displacement thermal fluctuation of the nanowires. Only a single resonant peak can be seen in air (green line in inset), but two resonant peaks can be clearly seen in vacuum (blue lines). Depending on the nanowire dimensions, the resonance frequencies range from 2 to 6 MHz. s-mode and f-mode refers to the splitting of the resonance frequency into slower and faster vibration modes vibrating at orthogonal directions. d, Histogram of the relative frequency separation between the two close resonance peaks observed in vacuum.

Gerard Tobias^a, Belén Ballesteros^b, Malcolm L.H. Green^c

^aInstitut de Ciència de Materials de Barcelona (ICMAB-CSIC), Campus UAB, 08193 Bellaterra, Barcelona, Spain

^bCentre d'Investigació en Nanociència i Nanotecnologia (ICN-CSIC), Campus UAB, 08193 Bellaterra, Barcelona, Spain

^cInorganic Chemistry Laboratory, University of Oxford, South Parks Road, OX1 3QR Oxford, UK
gerard.tobias@icmab.es

Carbon nanotubes (CNTs) have been advocated as promising agents for biomedical applications including *in vivo* imaging, tumour targeting and drug delivery systems. One added advantage of using nanotubes is that their inner cavity can be filled with a chosen payload whilst the outer surface can be modified to improve their dispersability and biocompatibility.

A key step towards the characterisation and application of filled CNTs is the complete removal of the large amount of unwanted external material present after the filling step, whilst preserving the encapsulated payload (of the same nature). An absence of species outside the CNTs will reduce the side effects during targeting. We have developed two complementary methodologies for the containment of materials inside single-walled carbon nanotubes (SWCNTs), namely by closing their ends by thermal annealing[1] and by using fullerenes as corks[2]. These nanocapsules (filled and sealed SWNTs) can then be readily purified by stirring the sample in a suitable solvent.

In the context of drug delivery systems we have investigated methods that allow a controlled discharge of the encapsulated payload by lowering the pH of the media. Here, we demonstrate that removable “corking” of SWCNTs in aqueous media using pH sensitive “corks” is feasible [3]. As a test for the successful containment and release of the filling material, we chose copper and uranium salts as the cargo, not for medical or related reasons but because the presence of copper into washings can be detected with high sensitivity by UV–vis spectroscopy, and because the heavy atoms of uranium can be easily detected in filled SWCNTs by high resolution transmission electron microscopy (HRTEM). Thus, in this “proof-of-principle” study we demonstrate the use of acid-sensitive functionalized fullerenes as removable “corks” for the containment and controlled release of the cargo contained within SWCNTs by lowering of the pH in aqueous media (Figure 1). It is well known that the pH of primary tumours and regions of inflammation and infection is lower than physiological.

We will also present recent results on the development of “hot” filled SWCNTs for *in vivo* radioemitter localization and imaging [4]. The nanocapsules were prepared by first filling the SWCNTs with Na¹²⁵I, followed by their sidewall functionalisation with carbohydrates (Figure 2). Short SWCNTs were employed in this study to further improve the biocompatibility of the materials. Effectively, the nanocapsules (filled SWCNTs with closed ends) guaranteed essentially zero leakage of the radionuclide and remained stable *in vivo* for extended periods. The sealing of iodide within single-walled carbon nanotubes enabled its biodistribution to be completely redirected from tissue with innate affinity (thyroid) to lung. Surface functionalization of these nanocapsules offers versatility towards modulation of biodistribution of the radioemitting crystals in a manner determined by the capsule that delivers them.

Acknowledgements:

We acknowledge support by Thomas Swan Ltd. and by a Marie Curie ERG European Community FP7.

References:

- [1] L. Shao, G. Tobias, Y. Huh, M. L. H. Green, Carbon 44 (2006), 2855
- [2] L. Shao, T.-W. Lin, G. Tobias, M. L. H. Green, Chem. Commun. (2008), 2164
- [3] P. Luksirikul, B. Ballesteros, G. Tobias, M.G. Moloney, M.L.H. Green, Carbon 48 (2010) 1912
- [4] S.Y. Hong, G. Tobias, K. T. Al-Jamal, B. Ballesteros, et al. Nature Materials 9 (2010), 485 (highlighted in News and Views: Nature Materials 9 (2010) 467)

Figures:

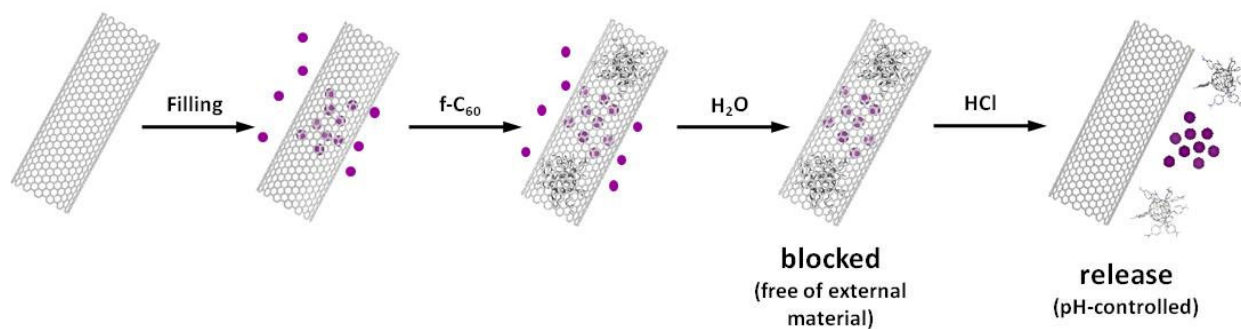


Figure 1: Schematic representation of the use of functionalized fullerenes as removable corks for SWCNTs [3].

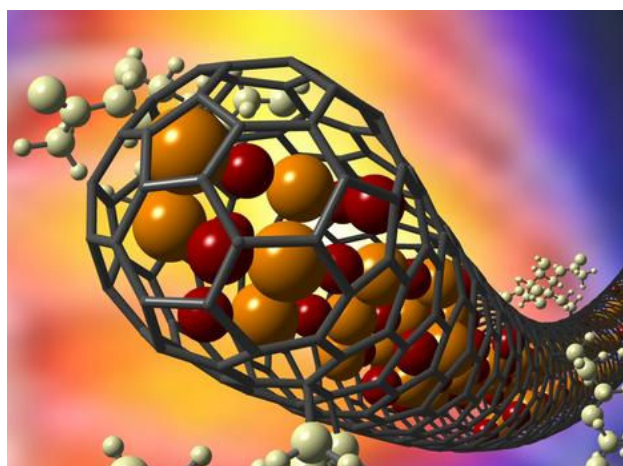


Figure 2: Schematic representation of the "hot" nanocapsules developed encapsulation Na¹²⁵I [4].

NON VOLATILE MOLECULAR MEMORY DEVICES BASED ON SWITCHABLE AND BISTABLE SELF-ASSEMBLED MONOLAYERS OF ELECTROACTIVE ORGANIC RADICALS

Jaume Veciana^a, Cláudia Simão^a, Marta Mas-Torrent^a, Núria Crivillers^a, Vega Lloveras^a
Juan Manuel Artés^b, Pau Gorostiza^b, Concepció Rovira^a

^aInstitut de Ciència de Materials de Barcelona (CSIC)-Networking Research Center on Bioengineering, Biomaterials and Nanomedicine (CIBER-BBN), Bellaterra, E-08193, Spain

^bInstitute for Bioengineering of Catalonia (IBEC), Institució Catalana de Recerca i Estudis Avançats (ICREA). Baldiri Reixac 15-21, E-08028 Barcelona, Spain, Networking Research Center on Bioengineering, Biomaterials and Nanomedicine (CIBER-BBN). Universitat de Barcelona. C/ Martí i Franquès, 1. Barcelona, E-08028 Barcelona, Spain.

vecianaj@icmab.es

The increasing interest in miniaturizing electronic devices to achieve denser circuits and memories will eventually entail the utilization of molecules as active components. In particular, self-assembled monolayers attached to substrates appear as suitable candidates in *Molecular Electronics* for the development of switchable and bistable memory devices based on electroactive molecules grafted on surfaces.[1] Polychlorinated triphenylmethyl (PTM) radicals are persistent electroactive organic radicals that can be easily reduced to the corresponding anionic species which also show a high stability in solution. Both species exhibit different optical and magnetic properties and can be reversibly interconverted in solution.[2] In addition such radicals can be covalently grafted on surfaces of different nature (Au, SiO₂) where they keep their bistability and switchability without degradation.[3-5]

Here, we describe the functionalization of transparent and conducting ITO surfaces with appropriately functionalized PTM radicals. Such hybrid organic/inorganic surfaces behave as chemical and electrochemical redox switches with bistable optical (absorption and fluorescence) and magnetic responses exhibiting an exceptionally high long-term stability and excellent reversibility and reproducibility. Moreover, such hybrid surfaces can be patterned as well as electrochemically locally addressed enabling to write-store-read information reversibly on the patterned clusters of electroactive molecules. One example of such a nonvolatile molecular memory device will be presented and discussed.[6]

References:

- [1] Liu, Z. et al., *Science* 302 (2003) 1543
- [2] Veciana, J., Ratera, I. in "Stable Radicals: Fundamentals and Applied Aspects of Odd-Electron Compounds", Ch. 2., Ed. by Hicks, R.G., John Wiley & Sons, Ltd, 2010
- [3] Mas-Torrent, M. et al., *J. Mater. Chem.* 19 (2009) 1691
- [4] Crivillers, N. et al. *J. Am. Chem. Soc.*, 130 (2008) 5499
- [5] Crivillers, N. et al. *Adv. Mater.* 21 (2009) 1177
- [6] Simão, C., et al. *Nature Chem.*, in press (2011)

Figures:

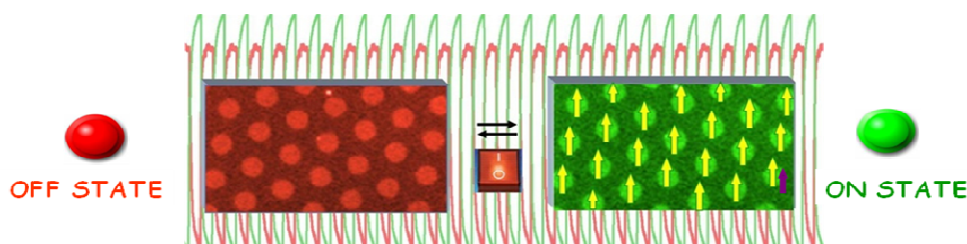


Figure 1: Schematic representation of the reversible switching between the two states of the hybrid organic/inorganic surfaces based on electroactive organic radicals

STM AND LEEM CHARACTERIZATION OF THE INTERACTION BETWEEN MAGNESIUM GROWN ON Ru(0001) AND HYDROGEN

L. Vergara¹, B. Santos¹, T. Herranz², M. Monti¹, K. F. McCarty³, J. de la Figuera¹

¹Instituto de Química-Física "Rocasolano", CSIC, C/ Serrano 119, 28006 Madrid, Spain

²Instituto de Catálisis y Petroleoquímica, CSIC, 28049 Madrid, Spain

³Sandia National Laboratories, 7011 East Avenue, Livermore, California 94550, USA

lvergara@iqfr.csic.es

Magnesium is a readily available non-toxic metal whose hydride (MgH_2) is being studied as a potential hydrogen storage medium, owing to its large content of 7.6% by weight of hydrogen. Magnesium is known to grow as almost perfect thin films on many substrates; in some instances, like in the case of refractory metals, with very sharp interfaces. Since a layer of $\text{MgO}/\text{Mg}(\text{OH})_2$ grows onto the magnesium surface when it is exposed to air, changing its reactivity, the understanding of the interaction between the surface of the magnesium layer and hydrogen is of the utmost importance. Most of the few works that have been devoted to the preparation of magnesium on refractory metals study its growth on W(110) substrates [1,2]. A study about the epitaxial growth of magnesium on Ru(0001) using low-energy electron diffraction (LEED) [3] reported that magnesium keeps its own in-plane spacing when growing on such substrate, owing to the large mismatch between their respective in-plane lattice spacings (around 18%). This results in a moiré pattern on the magnesium surface, and an overlayer film without significant strain. Additionally, not much has been published about scanning tunnel microscopy (STM) characterization of epitaxial growth of magnesium up to two monolayers at room temperature.

This work is a continuation of our recent studies about the growth and hydrogenation of magnesium on Ru(0001) substrates in ultra-high vacuum [4,5]. The characterization techniques we have employed are STM and low-energy electron microscopy (LEEM), an in-situ technique that provides real-time observations at different temperatures with spatial resolution of nanometres. Magnesium was grown to a thickness of one to ten atomic layers by evaporating a rod heated by electron bombardment at a pressure in the low 10^{-10} Torr range, with a typical deposition rate of about one monolayer per minute. Up to a temperature of 430 K, the films present a layer-by-layer growth with three levels exposed at the most. The submonolayers of magnesium, detected only by STM and only in the first two atomic layers, show a moiré pattern with a periodicity of 12 Å, as can be seen in figure 1. Dark-field LEEM experiments show that films with a higher number of monolayers present stacking faults and, on stepped areas, screw dislocations are observed by STM (see figure 2), owing to the mismatch of the step heights of magnesium and ruthenium in these areas. Electron reflectivity shows quantum size effects in the unoccupied bands, indicating an abrupt interface between magnesium and ruthenium for the thicker films. Additionally, we have studied the exposure to H and H_2 of the growing films by LEEM and STM. While growth in an H_2 atmosphere produces no significant change in the magnesium films, LEEM measurements have demonstrated the nucleation of dark islands as soon as H is fed into the vacuum chamber; further exposure to H leads to their almost covering completely the field of view. Using a mass spectrometer, we have performed thermal desorption experiments in these dark islands (see figure 3), which show that hydrogen is the only gas desorbed, with a sharp peak around 470 K coinciding with the disappearance of the islands in the LEEM images. At higher temperatures, only a faint trace of them remains on the surface.

References:

- [1] F. Schiller, M. Heber, V.D.P. Servedio and C. Laubschat, Phys. Rev. B 70 (2004), 125106.
- [2] L. Aballe, A. Barinov, A. Locatelli, T. Montes and M. Kiskinova, Phys. Rev. B 75 (2007), 115411.
- [3] H. Over, T. Hertel, H. Bludau, S. Pflanz and G. Ertl, Phys. Rev. B 48 (1993), 5572.
- [4] T. Herranz, K.F. McCarty, B. Santos, M. Monti and J. de la Figuera, Chem. Mat. 22 (2010), 1291.
- [5] T. Herranz, B. Santos, K. F. McCarty and J. de la Figuera, Surf. Sci., in press.

Figures:

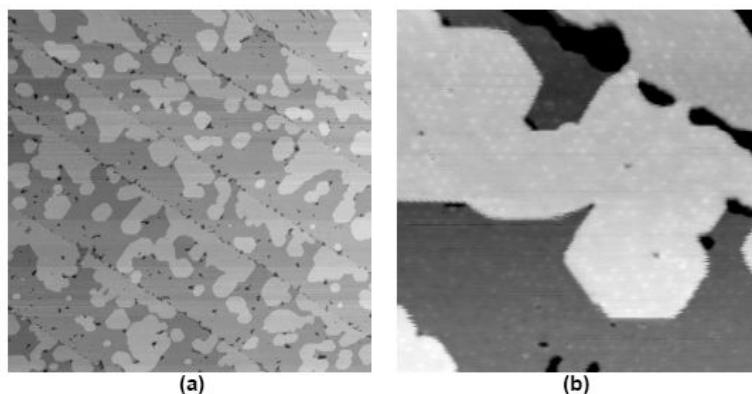


Figure 1: STM images of a magnesium film with an almost complete first monolayer and islands of the second monolayer. a) 4500-Å wide image, and b) 550-Å wide image, in which the moiré in the islands can be seen.

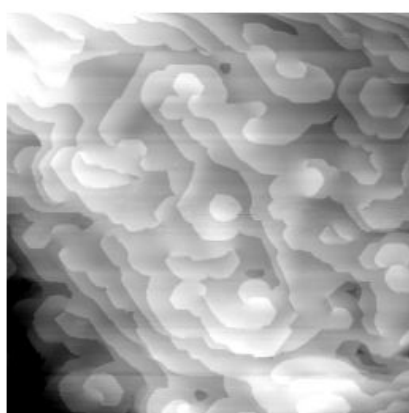


Figure 2: Screw dislocation in stepped areas seen by STM (image width and height: 3500 Å).

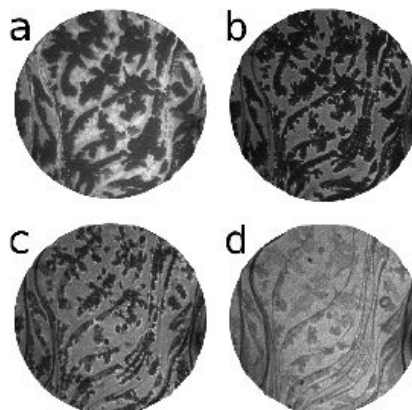
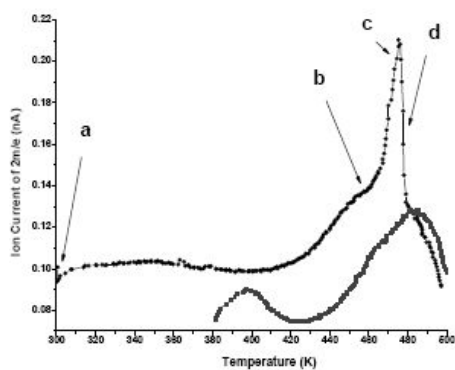


Figure 3: Thermal desorption measurements carried out in the dark islands of magnesium films with ten atomic layers grown under exposure to H₂ (lower curve) and H (upper curve). Labelled temperatures in the upper curve correspond to each of the LEEM images on the left (field of view is of 15 μm).